Final Project Report

Evaluating the Performance and Feasibility of Using Recovered Fly Ash and Fluidized Bed Combustion (FBC) Fly Ash as Concrete Pozzolan

By:
Farshad Rajabipour, Ph.D., F.ACI
Mona Zahedi, Ph.D.
Gopakumar Kaladharan

Department of Civil and Environmental Engineering
The Pennsylvania State University
University Park, Pennsylvania, USA

March 2020

Evaluating the Performance and Feasibility of Using Recovered Fly Ash and Fluidized Bed Combustion (FBC) Fly Ash as Concrete Pozzolan

CRC Grant Agreement # CRC 2017-49
ACI foundation
3880 Country Club Drive
Farmington Hills, MI 48331

Principal Investigator Dr. Farshad Rajabipour

Graduate Research Assistants Mona Zahedi
Gopakumar Kaladharan

Advisory Team: Patricia Baer, PennDOT
Jim Casilio, PACA
Paul Kish, First Energy
Randy Lindenmuth, Schuylkill Energy
Marty Mengel, Talen Energy
Jim Panaro, Robindale Energy
Mike Robinson, Boral
Barry Scheetz, Penn State
April Snyder, RJ Lee Group
Lawrence Sutter, Michigan Tech
Stephen Thomas, Boral

ABSTRACT

Supplementary cementitious materials (SCM) are a key ingredient of today's concrete and can vastly improve the durability (e.g., ASR mitigation) and sustainability of concrete mixtures. While the demand for fly ash (the highest used SCM) and other suitable pozzolans continues to grow, the supply of high-quality and specification-compliant fly ash has been shrinking. To maintain and expand the market share and ensure the durability of concrete products and structures, it is critical that a stable supply of high-quality and economical fly ash and other SCMs is available for foreseeable future. This study evaluates the feasibility, performance, and beneficiation of two alternative and abundant sources of fly ash: recovered landfilled fly ash and fluidized bed combustion (FBC) fly ash. Samples of both fly ashes were collected from an ash landfill in Pennsylvania and two FBC power utilities in Pennsylvania. These fly ashes were characterized against the composition, physical properties, and performance requirements of ASTM C618. A statistical sampling plan was also developed for characterizing the heterogeneity of fly ash in landfills.

The results show that the ash from the Pennsylvania landfill can be classified as ASTM C618 Class F ash and used in concrete after drying and particle size reduction (e.g., via sieving). Other ash landfilled should be evaluated on a case-by-case basis to determine (a) their heterogeneity, (b) their viability for use as concrete pozzolan, and (c) beneficiation measures that may be needed such as carbon reduction and separation of deleterious substances where possible.

The results also show that FBC fly ashes from the two Pennsylvania powder plants generally meet the chemical and physical requirements of ASTM C618, with exception of elevated SO_3 in one fly ash. Regardless, paving-grade concrete with good fresh and hardened performance could be prepared incorporation 20% of these fly ashes as a cement replacement. Further research

is recommended to evaluate other coal-based FBC fly ashes in the United States in terms of their properties, uniformity in time, and performance in concrete mixtures. Overall, it is determined that some FBC fly ashes have a very good potential for use as pozzolan. Specifications (prescriptive or performance) need to be developed to identify good quality FBC fly ashes and enable their use as concrete pozzolan.

ACKNOWLEDGEMENTS

Table of Contents

Chapter 1

Introduction

1.1. Motivation and Significance

Fly ash is the most commonly used supplementary cementitious material (SCM) in concrete production as it improves concrete durability and sustainability and potentially, its workability and long-term strength [1–3]. In recent years, the concrete industry in North America has witnessed significant uncertainty in the availability and quality of conventional fly ash for use in concrete. The AASHTO subcommittee on materials recently conducted a survey which included all State Departments of Transportation (DOTs), the Army Corps of Engineers, and the Federal Aviation Administration (FAA), and reported that over 80% of the participants faced challenges with fly ash availability within the surveyed period of 2012 to 2016 [4]. This is in part due to a more than 50% reduction in the production of pulverized coal (PC) fly ash over the last decade [5] (**Figure 1-1**) as a result of coal power plant retirements and conversions to natural gas fuel. Additionally, the consistency and quality of fly ash have been impacted by stricter air emission regulations, resulting in higher sulfur, alkali, and carbon contents (including contamination with activated carbon) [6] [2]. It is estimated (based on current practices) that by the year 2030, the demand for fly ash for use in concrete could exceed 35 million tons per year while the supply of ASTM C618-compliant fly ash would remain near or below current levels at 14 million tons [7].

Historically, less than 50% of the pulverized coal (PC) fly ash produced in the United States has been beneficially used, while the rest has been dry stockpiled (landfilled) or stored in surface impoundments (ponds). It is estimated that since 1980, over 1.3 billion tons of fly ash has been landfilled or ponded. This large quantity could potentially serve as a valuable source of fly ash for use in concrete. However, this resource requires beneficiation in the form of drying, particle size reduction (grinding and sieving), and removal of deleterious ingredients (e.g., excessive carbon, FGD materials, etc.). In addition, the performance of such beneficiated fly ashes in concrete must be evaluated and proven.
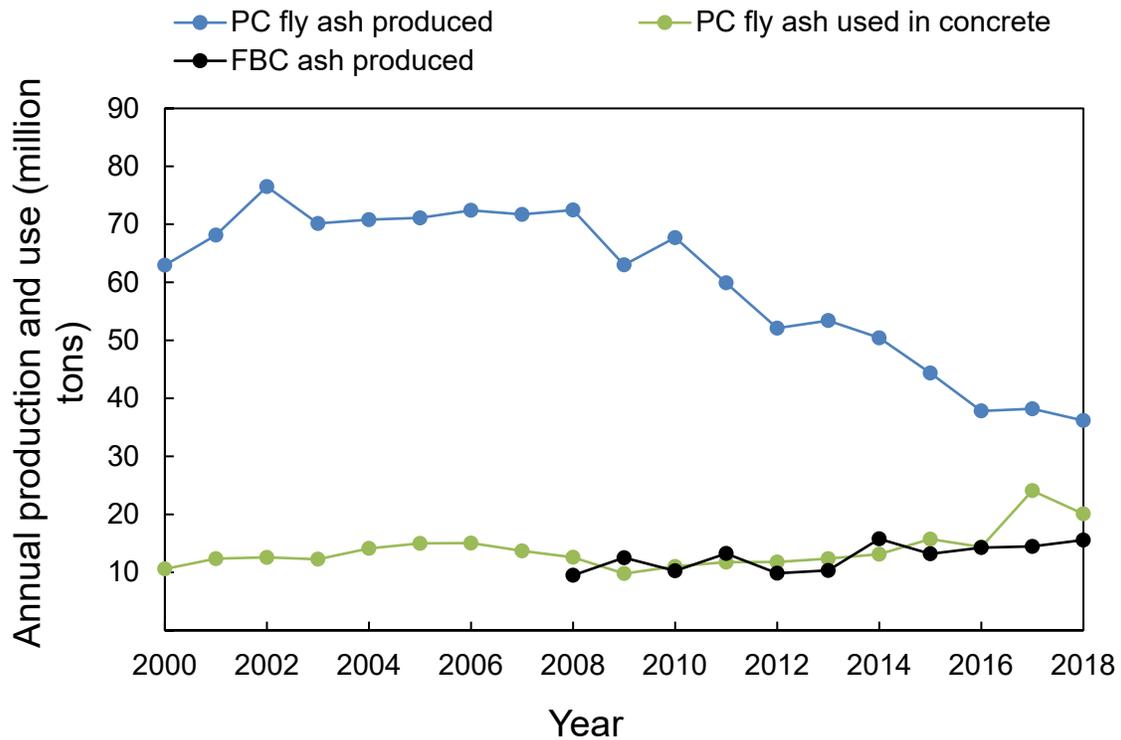
Figure 1-1. Statistics on the production and utilization of PC fly ash and FBC ash
(from the American Coal Ash Association [5])

Fluidized bed combustion (FBC) fly ash is an alternative source of fly ash that is widely available (annual U.S. production exceeding 14 million tons), but currently not used in concrete. The FBC process is a cheaper and more efficient way of burning low-grade coals compared to conventional pulverized coal (PC) combustion. It combusts coal at a significantly lower temperature (up to 850 °C) compared with typical PC combustion temperatures of up to 1700 °C. As a result, the mineral matter (e.g., clays) in coal do not melt but are dehydroxylated and form an ash that is similar to calcined clays. The SO_2 capture is also accomplished by injecting limestone powder into the combustion chamber, and this could result in elevated SO_3 content in the fly ash depending on the sulfur content of the coal. Overall, FBC fly ash may be a good SCM source; however, its performance as concrete pozzolan is not yet well established, and there is a significant need for research to identify usable sources of FBC ash and predict their performance in concrete.

1.2. Objectives and Scope

The main objective of this research is to determine if and how recovered landfilled class F fly ash and FBC fly ash can be used as viable and high-performance pozzolans for concrete. To achieve this objective, this study addresses the following questions:

- What are the potential problems with these fly ashes? What are the main technical obstacles that could mitigate the use of these ashes in concrete?
- How can these problems be fixed? What types of fly ash pre-conditioning and beneficiation processes would be needed?
- How would these fly ashes perform in concrete?
- How much would they cost? Would they be economically and practically feasible?
- What would specifications for use of these ashes look like? What are the prescriptive or performance criteria to distinguish good from bad recovered and FBC fly ashes?

Chapter 2 provides a background and literature review on coal combustion processes and products with a focus on PC and FBC fly ashes. The current state of understanding and practice with respect to FBC fly ash is summarized, and research needs to facilitate the use of FBC fly ash as a viable concrete pozzolan is highlighted.

For landfilled fly ash, a comprehensive literature review (Chapter 3) was performed to summarize (1) the potential issues and beneficiation strategies for this fly ash resource, and (2) its performance in standardized tests and in concrete. The key challenge identified was the lack of a sampling plan and protocol for reliable evaluation of fly ash landfills and their degree of heterogeneity, and for determining the necessary beneficiation steps. This research need was addressed and is detail in Chapter 6. In addition, the effectiveness of the sampling plan was demonstrated by applying it to characterize an ash landfill in Pennsylvania.

In Chapter 4, two sources of Circulating FBC (CFBC) fly ash are characterized for their bulk chemistry and mineralogy (using X-ray Florescence, batch leaching, and quantitative XRD); unburned carbon (using LOI, and Leco infrared analyzer); physical properties (moisture content, particle size, fineness, particle shape/agglomeration, density, soundness, and water requirement); and reactivity (strength activity index, compressive strength of lime-fly ash mortar according to ASTM C593-06, pozzolanic reactivity of lime-fly ash paste according to RILEM TC TRM267).

Chapter 5 explored the fresh (slump, air content, setting), mechanical (compressive strength, and durability properties (ion penetrability, formation factor, ASR, shrinkage, and sulfate

attack resistance) of concrete mixtures incorporating CFBC fly ashes. Additionally, mercury intrusion porosimetry (MIP) and pore fluid extraction tests were performed to relate concrete performance to microstructural features such as pore size distribution and pore solution conductivity.

Finally, the conclusions of the study are summarized in Chapter 7.

Chapter 2

Review on Coal Combustion Processes and the Performance of Raw or Beneficiated Fly Ash in Concrete

2.1. Coal Combustion Technologies

Power generation is the main consumer of energy in the United States, and coal is currently the second largest fuel source for this sector (i.e., accounting for 27.4% of the electricity generated in the United States in 2018) [8]. According to the U.S. Energy Information Administration's Annual Energy Outlook 2018 (AEO), coal usage is expected to remain relatively constant through 2050, despite recent wave of coal plant retirements [9] (**Figure 2-1**). Coal is a combustible sedimentary rock that primarily contains organic carbon, hydrogen, oxygen and lesser amounts of sulfur and nitrogen. Inorganic/non-combustible compounds in coal such as aluminum and silicon oxides (e.g., in the form of clay impurities in coal) constitute the combustion ash, but their concentration is no more than several percentage points of most coals (waste coals have significantly higher ash content as high as 70%). In fact, up to one tenth of the total mass of most coals is material with no fuel value.

There are two main theories for the formation of coal, based on the origin of vegetation that is later converted to coal. The autochthonous theory [10] is most accepted since it explains the origin of most coals. It states that plant debris accumulate in the bottom of nearby swamps and bogs, where oxygen content is low. The thick layer of partially decayed organic matter, also known as peat, is then covered by sedimentation (e.g., sand or mud) and coal seam is formed. Under gradual heat and pressure, biochemical reactions occur over thousands and millions of years and drive much of the water and other volatiles out of peat, resulting in the formation of various grades of coal (**Figure 2-2**). This coalification process constitutes three main reactions: microbiological degradation of plant cellulose; conversion of lignin within the plant to humic substances; and condensation of humic substances to larger coal molecules. Alternatively, the allochthonous theory [10] explains that vegetation is transported by water and the then deposited on the bottom of the sea or lake, and later compressed into solid rock. In general, the autochthonous theory refers to sediments that are native to its location, while the allochthonous theory refers to sediments originating from a place other than where it was found.
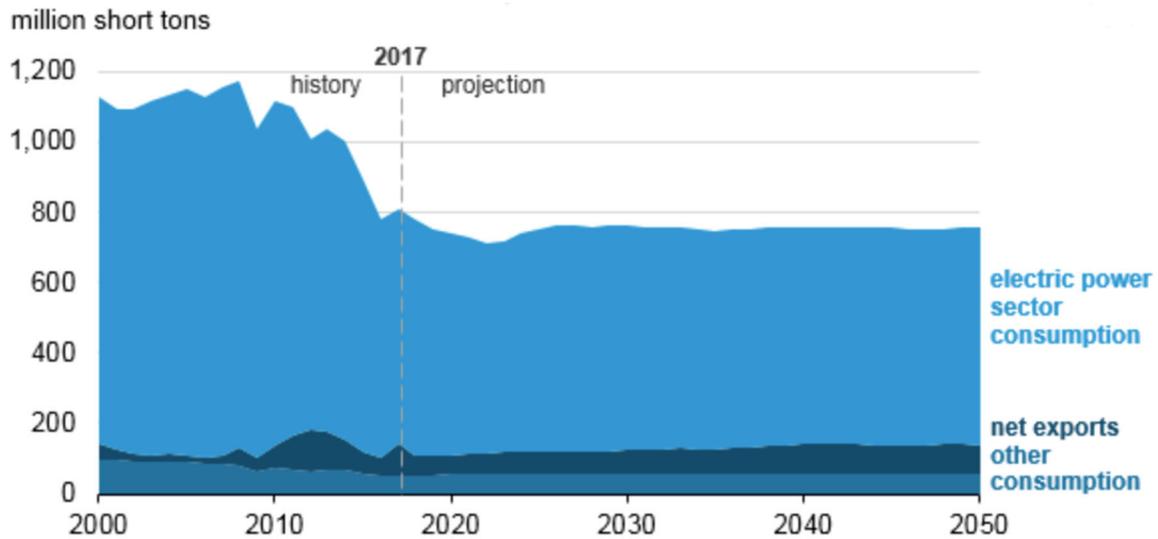
Figure 2-1. Prediction for U.S. coal consumption according to AEO2018 [11]
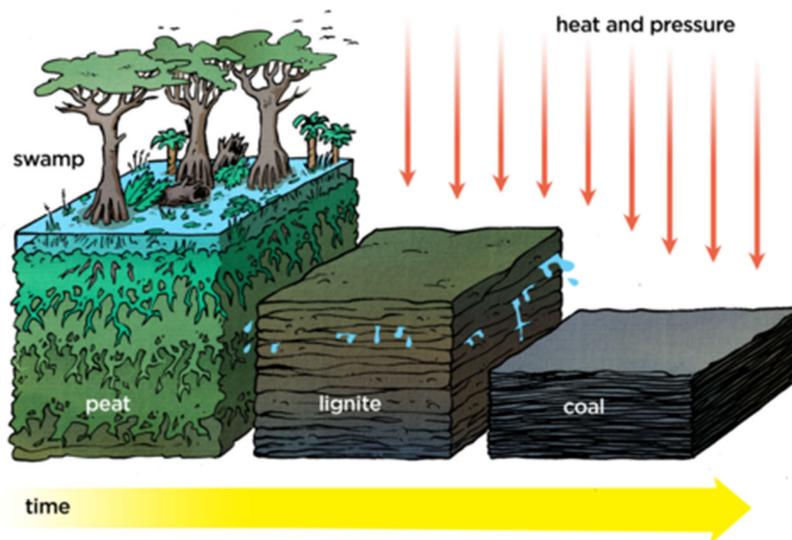
Figure 2-2. Coalification process to form coal under high temperature and pressure [12]

Different varieties of coal (i.e., coal types) arise because of differences in the types of plant material, degree of coalification (i.e., coal rank), and range of impurities (i.e., coal grade). The most common classification is that of coal rank, which refers to the degree of coalification (maturity) that has occurred [13]. The different forms of coal in the order of increasing age/maturity are lignite, sub-bituminous, bituminous, and anthracite coal (**Figure 2-3**).

Figure 2-3. From left to right: peat, lignite, sub-bituminous, bituminous, and anthracite coal [14]

A higher coal rank is accompanied by increases in the carbon content and calorific (heat) value, as well as decreases in the amount of moisture and volatile material (carbon oxides, hydrogen, and traces of sulfur and nitrogen compounds). As coal ages, the color changes from brown to jet black, and the coal becomes harder and more brittle, making it more difficult to burn [15]. In the United States, lignite and subbituminous coals are considered as low-rank, while bituminous coals and anthracite are classified as high-rank. As for European classifications, lignite is known as brown coal and anthracite and bituminous coals are hard coals. Subbituminous is in some cases considered as hard coal. The distribution of coal ranks within the United States and Pennsylvania, is provided in **Figure 2-4** and **Figure 2-5**, respectively. ASTM D388-17a (Standard Classification of Coals by Rank) defines four major classes of coals, but each are also subdivided into different groups. The higher rank coals are classified based on their fixed carbon and volatile matter content, whereas the low-rank coals are classified in terms of their heating value [10]. The different ranks of coal are described in detail below:

- Lignite is the lowest rank of coal. It is a peat that has been transformed into a rock, and that rock is a brown-black coal. Lignite has a heating value of less than 8300 Btu/lb (4614 kcal/kg) and is subdivided into Lignite A and Lignite B, on the basis of heating value (**Table 2-1**). Lignite constituted 9% of the total U.S. coal production in 2017 [16].

- Subbituminous coal is lignite that has been subjected to increased level of organic metamorphism. It has a heating value of 8300-11500 Btu/lb (4614-6393 kcal/kg) and is subdivided into Subbituminous A, Subbituminous B, and Subbituminous C groups

on the basis of heating value. Subbituminous coal constituted 45% of the total U.S. coal production in 2017 [16].
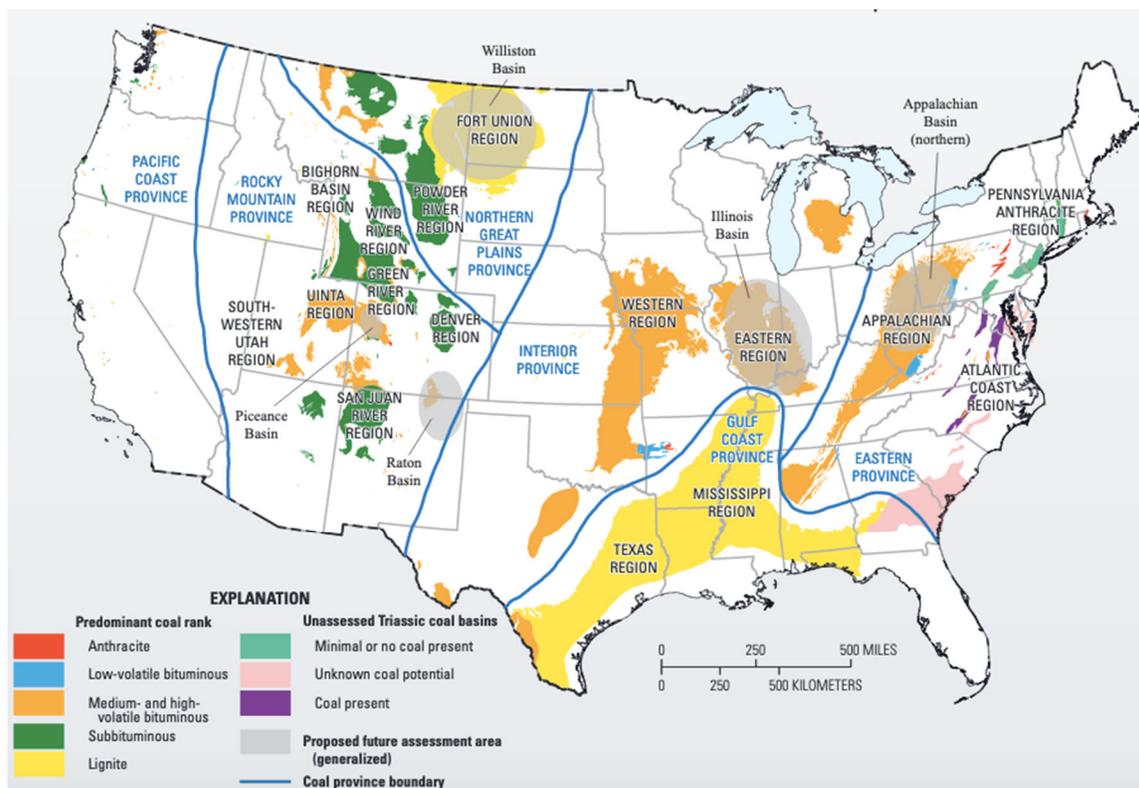
Figure 2-4. Distribution of coal ranks within the United States [17]
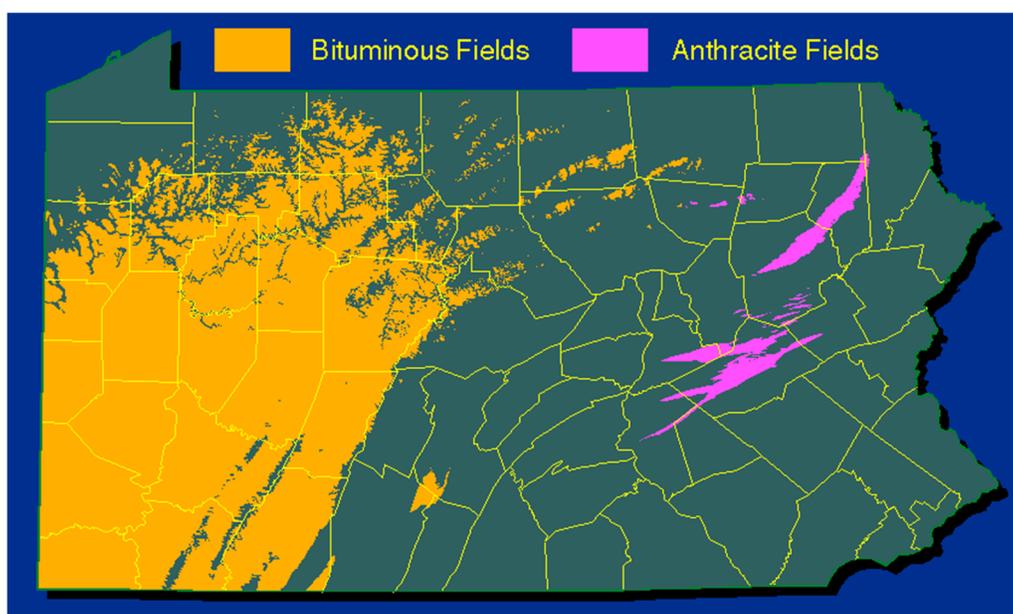
Figure 2-5. Distribution of coal ranks within Pennsylvania [18]

- Bituminous coal is the most abundant form of coal in the world that accounted for 46% of the total U.S. coal production in 2017. West Virginia, Illinois, Pennsylvania, Kentucky, and Indiana were the five main bituminous coal-producing states in 2017, contributing to 74% of total bituminous production [16]. There are five main classifications for bituminous coal: low volatile, medium volatile, high volatile A, high volatile B, and high volatile C. The low and medium volatile bituminous coals are classified based on fixed carbon content (69-86 wt%) and volatile matter (14-31 wt%), while high volatile A, high volatile B, and high volatile C bituminous coals are subdivided on the basis of heating value from 10500 to 14000 Btu/lb (5837 to 7783 kcal/kg).

- Anthracite is a hard, black coal that burns with little flame and smoke. It is the highest rank of coal, with fixed carbon content of 86-98 wt% and volatile matter of 2-14 wt%. Anthracite accounted for less than 1% of the coal mined in the United States in 2017 [16]. All of the anthracite mines in the United States are in northeastern Pennsylvania. It is subdivided into semi-anthracite, anthracite, and meta-anthracite on the basis of carbon content. In the U.S., anthracite is mainly used by the metals (e.g., steel) production industry.

Although coal reserves are estimated to last for the next 200 years, many challenges exist regarding efficient and environmentally-friendly use of coal combustion [13]. In conventional pulverized coal (PC) fired boilers, which currently dominate the electric power generation industry, the combustion of fuel takes place at temperatures ranging from 1150°C to 1750°C. This results in high sulfur (SO_x) and nitrogen oxides (NO_x) emissions. Removal of such pollutants from the flue gas requires expensive add-on scrubbing and desulfurization units [19], [20]. In an attempt to eliminate the need for external emission control units while fulfilling stricter environmental regulations and enabling the use of lower purity coals, the Fluidized Bed Combustion (FBC) process was developed and became commercially available in the 1970s. This rapidly maturing technology is widely used in Europe, North America, and China among other places [21]. Currently in the United States, there are 18 FBC power plants burning refuse coal (waste coal), 14 located in Pennsylvania, 2 in West Virginia, and one each in Montana and Utah [22]. Refuse coal

refers to any by-product of coal mining or coal cleaning operations with an ash content greater than 50 % (by weight) and a heating value less than 6000 Btu/lb (13900 kJ/kg) [23]. In addition to waste coal, the FBC technology is well suited for combustion of coke, petroleum coke, oil shale, biomass, and some types of municipal solid waste [24]. The PC and FBC combustion technologies, and their products are explained in detail in the following sections.

Table 2-1. Classification of coal by rank according to ASTM D388-19

Class/Group	$FC_{d,MMf}$ Limits, %		$VM_{d,MMf}$ Limits, %		$GCV_{im,MMf}$ Limits[B]				Agglomerating Character
					Btu/lb		MJ/kg[C]		
	Equal or Greater Than	Less Than	Greater Than	Equal or Less Than	Equal or Greater Than	Less Than	Equal or Greater Than	Less Than	
Anthracitic:									
Meta-anthracite	98	...	...	2	...	...	...	...	
Anthracite	92	98	2	8	...	...	...	...	non-agglomerating
Semianthracite[D]	86	92	8	14	...	...	...	...	
Bituminous:									
Low volatile bituminous coal	78	86	14	22	...	...	...	...	
Medium volatile bituminous coal	69	78	22	31	...	...	...	...	commonly agglomerating[E]
High volatile A bituminous coal	...	69	31	...	14 000	...	32.557	...	
High volatile B bituminous coal	...	...	...	...	13 000	14 000	30.232	32.557	
High volatile C bituminous coal	...	...	...	...	11 500	13 000	26.743	30.232	
					10 500	11 500	24.418	26.743	agglomerating
Subbituminous:									
Subbituminous A coal	...	...	...	...	10 500	11 500	24.418	26.743	
Subbituminous B coal	...	...	...	...	9 500	10 500	22.09	24.418	
Subbituminous C coal	...	...	...	...	8 300	9 500	19.30	22.09	non-agglomerating
Lignitic:									
Lignite A	...	...	...	...	6 300	8 300	14.65	19.30	
Lignite B	...	...	...	...	...	6 300	...	14.65	

[A] This classification does not apply to certain coals, as discussed in Section 1.
[B] Refers to coal containing its natural inherent moisture but not including visible water on the surface of the coal.
[C] Megajoules per kilogram. To convert British thermal units per pound to megajoules per kilogram, multiply by 0.0023255.
[D] If agglomerating, classify in low volatile group of the bituminous class.
[E] It is recognized that there may be nonagglomerating varieties in these groups of the bituminous class, and that there are notable exceptions in the high volatile C bituminous group.

2.2. Suspension Firing of Pulverized Coal (PC) and Its Products

Suspension firing is the most commonly used method for burning coal to generate electricity. In PC boilers, coal is ground in mills to a fine powder (e.g., 65% to 85% of the particles passing No. 200 sieve) and then pneumatically transported, with approximately 10% of the combustion air, through the burners into the furnace. There, the pulverized coal is combusted in suspension, with continuous mixing of fuel and air (**Figure 2-6**).

In PC boilers, pulverized coal is combusted at temperatures ranging from 1150°C to 1750°C, depending largely on the coal rank [19]. At such high temperatures, coal undergoes two main combustion mechanisms of devolatilization (i.e., release of volatile organic constituents in a matter of milliseconds), and char oxidation (i.e., a series of carbon-oxygen reactions). The latter reaction is relatively slower and in the order of several seconds. This results in melting of the majority of mineral impurities (e.g., clays) that are present in the coal. These molten droplets will subsequently solidify in the flue gas, primarily in the form of alumino-silica glass and iron oxide spheres, which make up the resulting fly ash. Other main combustion products in a PC boiler include bottom ash, boiler slag, and flue gas desulfurization (FGD) products. These are introduced in the following sections.
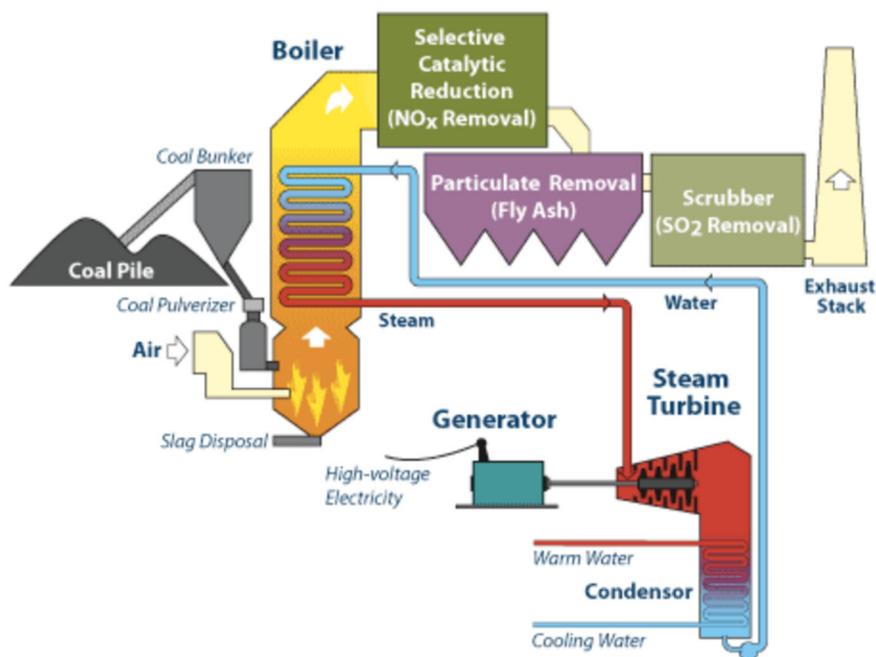
Figure 2-6. Suspension firing boiler to generate electricity and to produce PC fly ash [25]

2.2.1. Pulverized Coal (PC) Fly Ash

Fly ash is the particulate matter in the flue gas and is separated using bag house filters, electrostatic precipitators, or cyclones [10]. Electrostatic precipitators (ESP) are particle removal devices that use high voltage electrodes to create an electrical field and force charged particles out of the stream of flue gas and onto collector plates (**Figure 2-7**). Although the collection efficiency of ESP may be 99% or higher, its performance is affected by the flue gas properties, especially the electrical

resistivity of particles [26]. A more effective method of separating particles from flue gas, with guaranteed collection efficiency greater than 99%, is using baghouse filters. Most baghouses use an array of long and narrow cylindrical shaped fabric bags as a filter medium. As the flue gas is blown through the bags using fans, the solid particles get trapped inside, and clean air passes through. Once there is sufficient drop in pressure, the bag cleaning process begins, and the resulting fly ash is collected in hoppers (**Figure 2-8**). Cyclones are the third and a less efficient method of particulate removal compared to the previous techniques. They are typically used as pre-cleaners and are followed by electrostatic precipitators and/or baghouses. Cyclones create a vortex which causes larger particles within the flue gas to move outwards and hit the chamber wall, where they slide down into hopper at the bottom of the cyclone. The clean air continues to move upwards in a narrow spiral, and finally exits the outlet at the top (**Figure 2-9**).
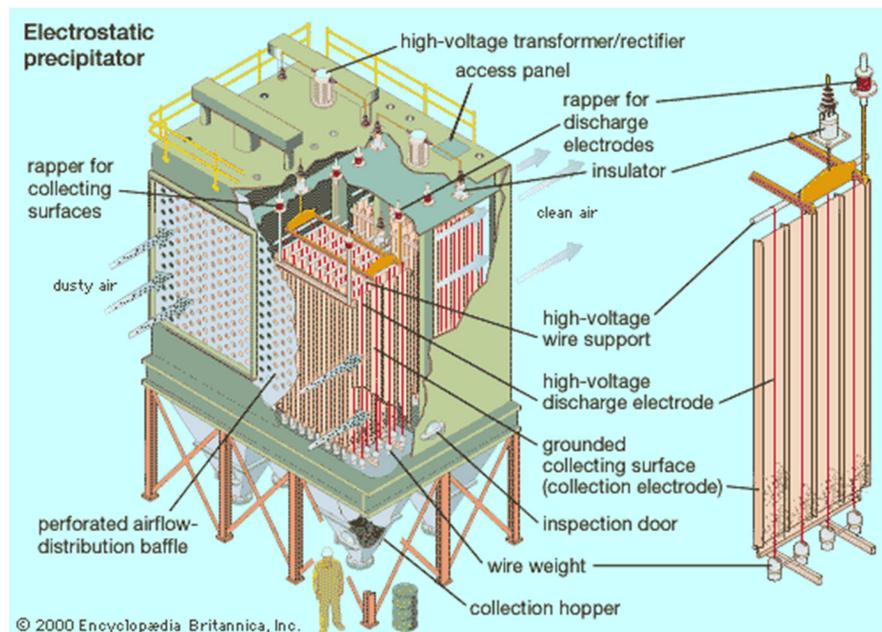
Figure 2-7. Electrostatic precipitators (ESP) used for separating fly ash from the flue gas [27]
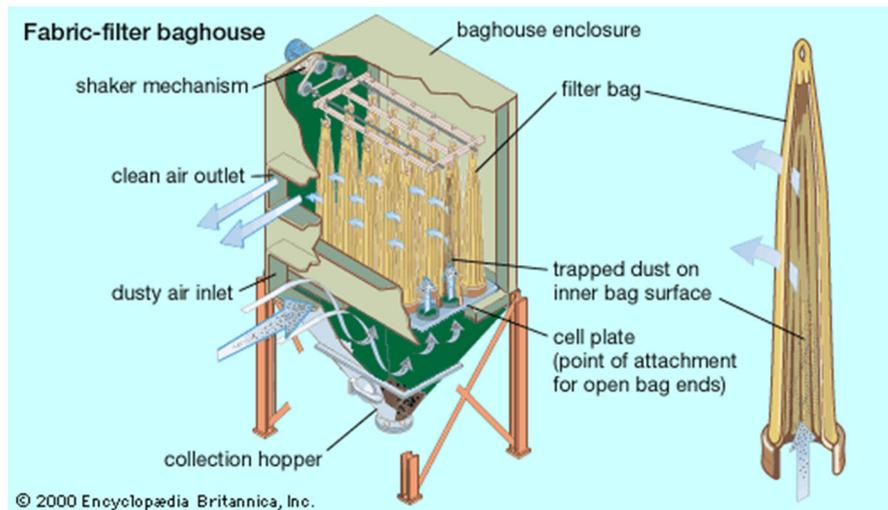
Figure 2-8. Baghouse filters used for separating fly ash from the flue gas [27]
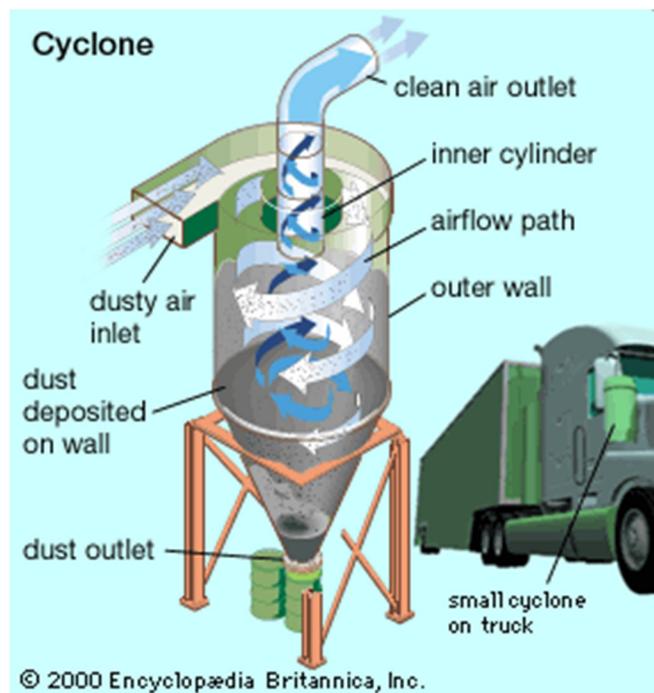
Figure 2-9. Cyclones used for separating fly ash from the flue gas [27]

Rapid cooling of fly ash within the flue gas results in the formation of solid spherical particles (0.5 to 300 μm in diameter) as well as hollow cenospheres (empty shells) and pleurospheres (shells containing smaller fly ash particles) as shown in **Figure 2-10**. The bulk chemistry of the PC fly ash is a function of feed coal (**Table 2-2**), the pulverizing process and combustion conditions. Its principal constituents include SiO_2 (35 to 60 percent), Al_2O_3 (10 to 30

percent), Fe_2O_3 (4 to 20 percent), and CaO (1 to 35 percent) (**Figure 2-11**) [2]. Coals that contain relatively small amounts of calcium, for example anthracite, bituminous, or some lignite coals, results in ASTM C618 Class F fly ash. This class of fly ash primarily contains amorphous aluminosilicate particles as well as spherical iron oxide particles (**Figure 2-12**). Subbituminous and some lignite coals contain larger amounts of calcium and produce calcium aluminosilicate glass phases in the fly ash [2].
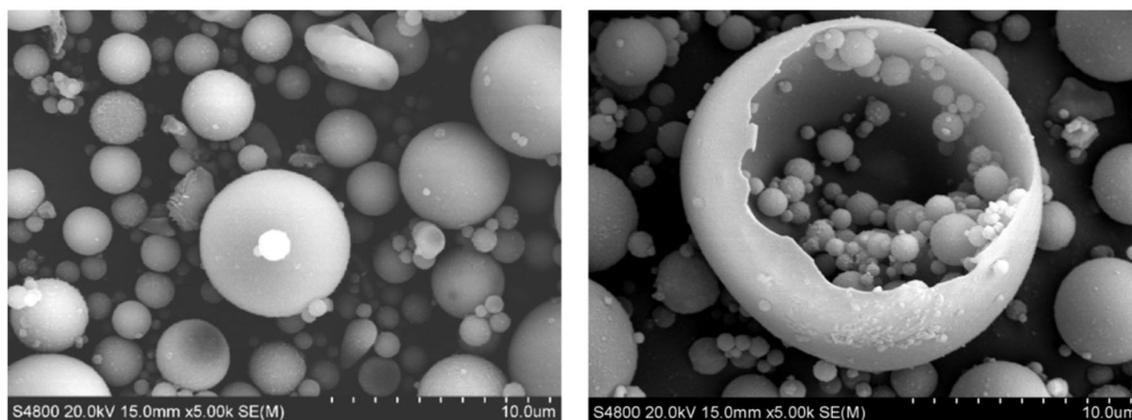
Figure 2-10. Left: hollow cenosphere fly ash,
right: pleurosphere fly ash containing smaller spheres [28]

Table 2-2. Normal range of chemical composition for fly ash produced from different coal types (expressed as percent by weight) [29]

Component	Bituminous	Subbituminous	Lignite
SiO_2	20-60	40-60	15-45
Al_2O_3	5-35	20-30	10-25
Fe_2O_3	10-40	4-10	4-15
CaO	1-12	5-30	15-40
MgO	0-5	1-6	3-10
SO_3	0-4	0-2	0-10
Na_2O	0-4	0-2	0-6
K_2O	0-3	0-4	0-4
LOI	0-15	0-3	0-5
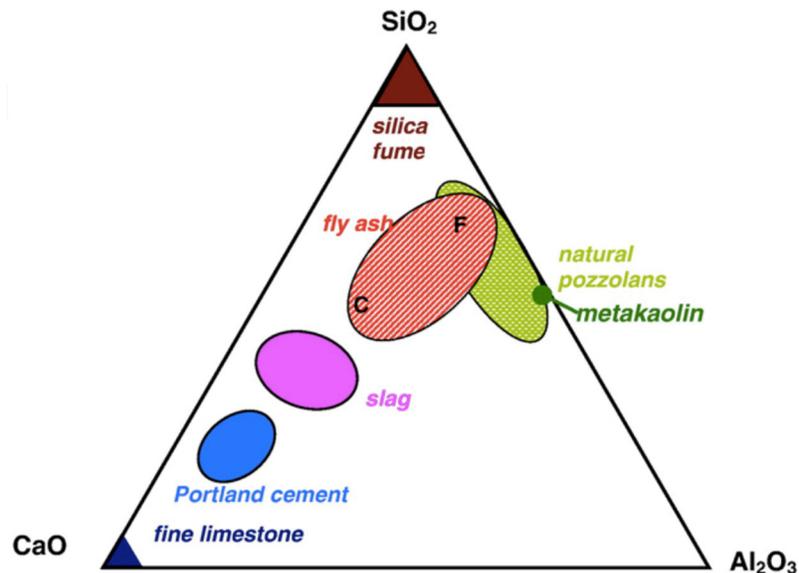
Figure 2-11. CaO–Al₂O₃–SiO₂ ternary diagram of cementitious materials, including class F and class C fly ash [1]
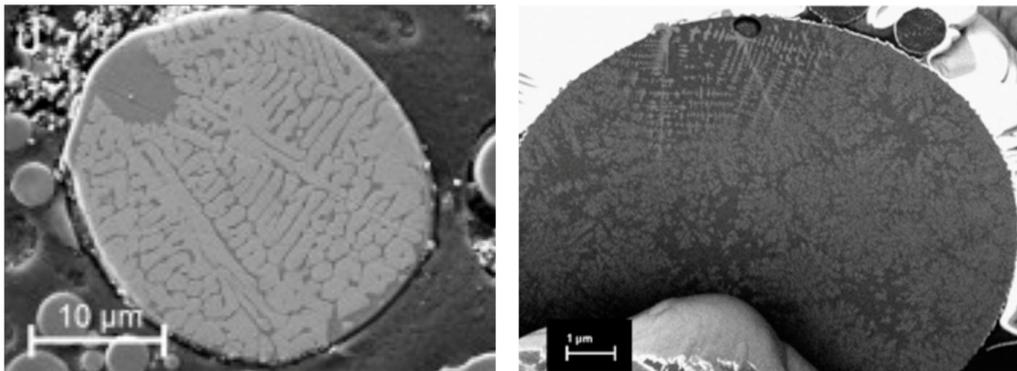
Figure 2-12. Cross section of aluminosilicate spheres with fine dispersion of dendritic mullite and iron oxide [30] [31].

For use in concrete and in the United States, PC fly ash must comply with the requirements of ASTM C618 (or equivalently, AASHTO M295). The chemical requirements stated by this standard are a maximum SO_3 content of 5%, maximum moisture content of 3%, maximum LOI value of 6%, as well as a minimum $SiO_2+Al_2O_3+Fe_2O_3$ content of 70% and 50% for class F and C fly ash, respectively. The use of Class F fly ash containing up to 12.0% LOI may be approved by the user if either acceptable performance records or laboratory test results are made available. With regards to physical requirements, maximum fineness of 34%, minimum strength activity index (at either 7 or 28 days) of 75%, maximum water requirement of 105%, and maximum autoclave

expansion of 0.8% are required. Some optional requirements such as the magnitude of drying shrinkage, uniformity requirements regarding the use of air-entraining admixtures, and sulfate resistance, may also be applied when specifically requested.

According to ASTM C618-19, PC fly ash is classified based on its bulk chemistry as class F (when mass fractions of $SiO_2+Al_2O_3+Fe_2O_3 >= 70\%$) or class C (when mass fractions of $SiO_2+Al_2O_3+Fe_2O_3 >= 50\%$). Class C fly ash has greater calcium oxide content than class F fly ash ($CaO > 18\%$). Generally, the higher the content of CaO, the lower $SiO_2+Al_2O_3+Fe_2O_3$, and the greater the amount of SO_3 and alkalis (Na_2O and K_2O) within the fly ash. Furthermore, LOI is higher for class F fly ashes than class C because of the presence of more unburnt carbon.

Low calcium fly ash (class F) primarily contains alumino-silicate glass, and lesser quantities of mineral phases, including quartz (SiO_2), mullite ($3Al_2O_3 \cdot 2SiO_2$) and iron oxides (Fe_2O_3, Fe_3O_4) [32]. Mullite is found in substantial quantities only in low calcium fly ashes and accounts for the majority of alumina in fly ash but is not normally chemically reactive in concrete [2]. High calcium fly ash (class C) contains the previously mentioned phases, and may also contain additional crystalline phases such as anhydrite, alkali sulfate, dicalcium silicate, tricalcium aluminate, free calcium oxide, and melilite [33]. When used in concrete, class F fly ash primary acts as a pozzolan (i.e., "siliceous or silico-aluminous material that in itself possesses little or no cementitious value, but that will, in finely divided form and in the presence of moisture, chemically reacts with calcium hydroxide at ordinary temperatures to form compounds having cementitious properties" [34]). Meanwhile, class C fly ash has both hydraulic (i.e., the ability to set, harden, and gain strength as a result of chemical reactions with water, in the absence of portland cement) and pozzolanic properties [35] [36] [37]. This is because the content of silica and alumina, which are the primary contributors to the pozzolanic reaction in concrete, are greater in class F fly ash while CaO, having hydraulic properties, are more abundant in class C fly ash. Silica and alumina combine with lime and water to form calcium silicate hydrate (C-S-H), calcium aluminum silicate hydrate (C-A-S-H) and alumino-ferrite hydrates (e.g., AFt and AFm phases) [2].

Partial replacement of portland cement with fly ash has been shown to increase the workability, water and chloride ion penetration resistance, and later-age strength of concrete, as well as, to reduce the heat of hydration, shrinkage and alkali silica reactivity. Other than its use in concrete, PC fly ash can be used in a range of other applications, including structural fill materials (e.g., embankments), soil and road base stabilization, and mine reclamation [36].

2.2.2. Other PC Combustion Products

The bottom ash and boiler slag are the un-combusted material that accumulate at the bottom of the boiler and are fairly similar in composition to fly ash (**Figure 2-13**). PC boiler units are classified as either dry bottom or wet bottom, depending on whether the bottom ash is removed in a solid or molten state. The majority of PC boilers operate with dry bottom units; i.e., they produce bottom ash. In the wet bottom units, the combustion temperature exceeds that of ash melting point; as such, they produce boiler slag [37]. Because of the higher content of fly ash in dry bottom furnaces, these boilers are larger and more expensive than wet bottom furnaces. However, they are simpler to operate and more flexible with regards to the fuel source [10].

Figure 2-13. PC bottom ash (left) and boiler slag (right) [38]

Bottom ash may be quite angular, with a large particle size (usually with 50 to 90 percent passing a 4.75 mm sieve and 0 to 10 percent passing a 0.075 mm sieve) and porous structure. Bottom ash can be used as fine aggregates in concrete, fill, anti-skid, and sand blasting applications. The porous structure of bottom ash makes it lighter and less durable than conventional aggregates [39]. If ground, bottom ash can also be used as a filler material to partially replace portland cement in concrete [36]. Research is ongoing to evaluate the use of ground bottom ash as concrete pozzolan. As for boiler slag, once the molten slag is quenched with water, it fractures, solidifies, and forms pellets. These hard, angular particles have a smooth glassy appearance and can be used as blasting grit and roofing granules, mineral filler in asphalt, fill

material for structural applications, and snow and ice traction control material. Recently, the supply of boiler slag has declined due to the shutdown of wet bottom boiler power plants [39].

In addition to particulate matter (i.e., fly ash), other harmful emissions must be prevented or separated from the flue gas before it is released to the atmosphere. Most importantly, SO_x, NO_x, ozone, mercury (Hg), and lead (Pb) emissions must be mitigated.

To control SOx emission, lower sulfur coals can be used, the fuel can be cleaned from sulfur-bearing compounds (e.g., pyrite) prior to combustion, or flue gas desulfurization (FGD) units can be used before or after particulate removal units to separate sulfur oxides from the flue gas (**Figure 2-6**). During combustion, most of the sulfur content in coal is converted to SO_2 and a small percentage is oxidized to SO_3 [37]. The Clean Air Act (1970) and its Amendments (1990) require major reductions in sulfur oxide (SO_2) and nitrogen oxides (NO_x) emissions, the pollutants that cause acid rain [10]. That is why most coal combustion facilities which use high-sulfur coals, decided to add flue-gas scrubbing systems [37]. The most widely used FGD units are the wet scrubbing systems. In these units, a limestone ($CaCO_3$) or lime ($Ca(OH)_2$) slurry is sprayed onto flue gas to transform SO_2 to sulfite hemi-hydrate ($CaSO_3.\frac{1}{2}H_2O$), which may be further forced oxidized to synthetic gypsum ($CaSO_4.2H_2O$) [37]. This process removes more than 90% of the SO_2 [37]. Also, CO_2 is produced as a by-product of the limestone calcination. The resulting scrubber sludge can be disposed of in slurry ponds or it is dewatered and landfilled. Where a higher quality synthetic gypsum is produced, it can be used in portland cement production or drywall manufacturing [10]. For dewatering, hydrocyclones and vacuum filters are employed to reduce the moisture content of the slurry to less than 10% [10].

A less common type of FGD units is the dry scrubbing systems, including spray dry scrubbers and sorbent injection processes [10]. These FGD units are placed before particulate removal units and produce dry FGD products that are collected together, and are as such comingled with, fly ash. As a consequence, the resulting fly ash has a high sulfur content and is usually unusable for concrete applications. A particular type of dry scrubber that has recently gained popularity is the dry sorbent injection (DSI) process. Here, dry hydrated lime or sodium-based sorbents (e.g., trona) are injected into humidified (~100% RH) flue gas to form sulfites and sulfates of calcium or sodium. The unused sorbent, FGD products, and fly ash are subsequently collected in the particulate control units. In this case, the resulting fly ash has high contents of sulfur, calcium, and/or sodium.

To reduce the amount of NO_x in the flue gas, two main approaches can be taken: furnace combustion modification, which includes the use of low-NO_x burners; and ammonia (or urea) injection with or without catalysts. In the first method, combustion is performed at different stages, meaning that at certain areas of the furnace, the oxygen level is kept low, and at later stages, air is added to complete combustion. One of the main challenges of this technique is ensuring complete fuel combustion whilst limiting the amount of NO_x formation [40]. Also, such low oxygen conditions may increase unburned carbon content and its reactivity in the resulting fly ash. The carbon (measured as LOI) associated with a low-NOx fly ash has a greater propensity to adsorb liquid chemical admixtures used in concrete, especially air entraining admixtures (AEA). This can lead to relatively large increases in the AEA dosage requirement in concrete [2].

The most common ammonia (or urea) injection technology is the selective catalytic reduction (SCR) method which reduces the amount of NO_x by oxidation/reduction reactions between ammonia and NO_x, in the presence of a catalyst. The main concern with this technique is the amount of unreacted ammonia (also known as ammonia slip) in fly ash, which may be released in the form of vapor when in contact with water, causing odor issues. Furthermore, ammonia can affect the leaching of trace elements in fly ash. However, since most modern SCR systems limit the ammonia slip content to less than 2 ppm, the effect of unreacted ammonia on fly ash performance in concrete is negligible [40].

The most common technologies for mercury capture, with the least negative impacts on coal combustion products are: sorbent injection and co-removal with fly ash; and mercury oxidation and co-removal with FGD solids. Powder activated carbon (PAC), referring to the product of heat- and steam treatment on carbon-based materials, is the most common sorbent for mercury removal. This highly porous powder can effectively absorb mercury and is later removed from the flue gas along with fly ash. The captured carbon may adversely affect the properties of fly ash in concrete, especially with regards to the increased AEA demand. Other sorbents such as specialty activated carbon and non-carbon are advantageous, since they preserve the quality of fly ash. As for the mercury oxidization technique, chemical addition (typically using halogen) or the catalysts from the SCR method are used to oxidize mercury so it can be removed with the FGD solids. Oxidized mercury is desired since it is soluble and can be removed from the downstream scrubber systems. This is not the case for elemental mercury, which is in fact the predominant form. Although some drawbacks of this method are increased mercury and halogen concentrations

in the resulting fly ash, these effects are insignificant compared to that of activated carbon injection [40].

2.3. Fluidized Bed Combustion (FBC) and Its Products

In an attempt to eliminate the need for external emission control units while fulfilling stricter environmental regulations and enabling the use of coals with low calorific and high sulfur contents, the fluidized bed combustion process was developed and commercialized in the 1970s. FBC is a combustion technology suitable for burning extremely low-grade coal (refuse coal) for power generation, with the environmental benefit of cleaning up acid mine drainage (AMD)-producing gob piles (piles built of accumulated waste rock, removed during coal mining, that can leach acid mine water and hazardous substances into water resources). In this method, sulfur-absorbing materials (e.g., limestone or dolomite) are added in a powder form to the fuel along with an inert material (e.g., sand or ash) inside the boiler. The mixture is fluidized using air jets and combusted at temperatures ranging from 750°C to 900°C. Fluidization refers to the dynamic fluid-like state of the solid-air mixture within the furnace, which is caused by the passage of upwards jets of air through the granular material. The main purpose of the inert material is to improve mixing and heat transfer among different components, while the sulfur-sorbent is used to minimize SO_x emissions in the flue gas. Depending on the sulfur content of the fuel, the sorbent may comprise up to 50% of the bed inventory [10]. The temperature of the furnace is high enough to allow calcination of limestone and combustion of coal [10], but does not result in melting of clays and other mineral matter. Temperatures are well below the threshold of nitrogen oxidization (i.e., 850 °C), and creation of thermal NO_x [19]'[20]'[41]. The temperature range is chosen to ensure that the reactions between SO_2 and sorbent are thermodynamically and kinetically balanced [10]. It is worth noting that the low combustion temperatures of FBC boilers affects their electricity generation capacity. While FBC powerplants are typically up to 300 MW in size, and can be as high as 400-600 MW, PC power plants can exceed size of 2000 MW [42].

During the FBC process, initially limestone is thermally decomposed (calcined per **Eq. 2-1**), and porous CaO particles are formed. A significant fraction (approximately 70%-80%) of this CaO combines with SO_2 emissions and $CaSO_3$ (calcium sulfite) is formed (**Eq. 2-2**) [43]. In the presence of abundant oxygen, anhydrite ($CaSO_4$) is produced from the oxidation of $CaSO_3$ (**Eq. 2-3**) [20]. As high as 95% of the sulfur in coal is captured during these reactions.

$$CaCO_3 + heat \rightarrow CaO + CO_2 \qquad \text{(Eq. 2-1)}$$

$$CaO + SO_2 \rightarrow CaSO_3(s) \qquad \text{(Eq. 2-2)}$$

$$CaSO_3(s) + 1/2 \ O_2 \rightarrow CaSO_4(s) \qquad \text{(Eq. 2-3)}$$
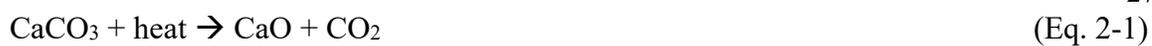
In addition to lower overall SO_x and NO_x emissions, FBC enables energy efficient combustion and the use of both high and low-grade coals, as well as partial replacement of coal with biomass. During the combustion, upwards jets of air cause the solids (pulverized fuel, limestone, and sand) to be suspended, ensuring the gas and solids to mix together turbulently for better heat transfer and chemical reactivity. In fluidized bed combustion, the solid concentration is significantly greater than that of PC boilers, and therefore convective heat transfer dominates over radiation [10]. This significantly reduces the size of FBC furnaces. Furthermore, the elutriation of particles (i.e., separation of particles based on their size using a stream of gas or fluid flowing in a direction usually opposite to the direction of sedimentation) at high velocities yields high amounts of fly ash (60-80 wt% of the total ash produced) versus bottom ash [44][45]. Similar to PC combustion, fly ash is collected using particulate removal systems such as electrostatic precipitators, cyclones, and bag filters.

To further increase the gas-solid contact time, the CFBC technology was developed in the late 1970s as a subcategory of FBC boilers. Its basic concept is using high gas velocities to entrain a considerable portion of the heavier particles and carry them out of the boiler. The solids are then separated from the flue gas in one or more recycling cyclones and returned to the combustion bed, thus preventing unburnt fuel from leaving the furnace (**Figure 2-14**). This creates a recycling loop through which fuel particles can pass 10 to 50 times until near-complete combustion is achieved [46]. The prolonged combustion time also ensures that lower combustion temperatures compared to conventional FBC and PC boilers can be used. In comparison with conventional FBC, the CFBC technology allows a better combustion efficiency, smaller combustor size, simpler fuel feed system, lower SO_x and NO_x emissions, lower limestone consumption and in turn, lower CaO content in the ash, and lower unburned carbon and loss-on-ignition (LOI) in the ash [19].

The Pressurized Fluidized Bed Combustion (PFBC) technology, which operates at elevated pressures (4 to 30 atmospheres) rather than atmospheric conditions, also provides similar benefits as CFBC. In the PFBC process, the CaO in the combustion residue tends to stay in the form of calcite, rather than in the form of free lime, due to the higher CO_2 partial pressure in the combustor

[20]. Therefore, the content of free lime in PFBC ash is significantly lower than that of FBC ash, and this results in low ettringite formation when the ash is used in concrete [45]. Finally, the pressurized circulating FBC (PCFBC) is the combination of CFBC and PFBC [10].
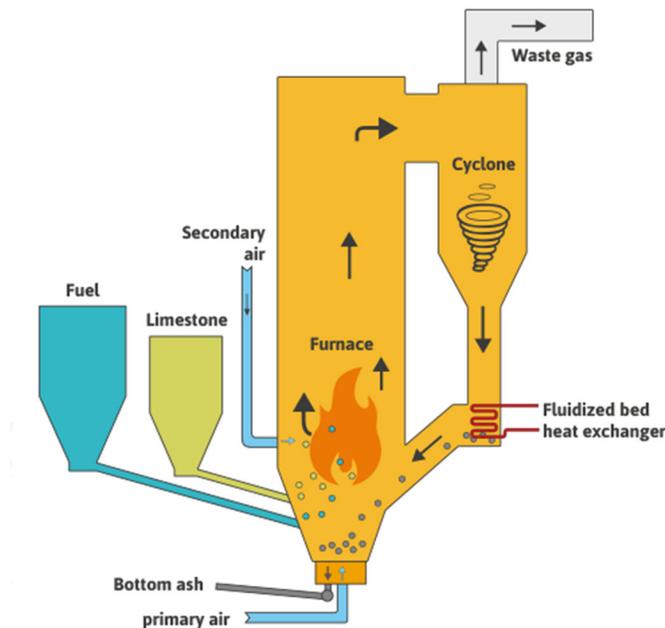
Figure 2-14. Schematic of circulating fluidized bed combustion (CFBC) unit [47]

FBC fly ash and bottom ash constitute approximately 13wt.% of the annual 111 million tons of coal combustion products (CCPs) produced in the United States [48]. Other main CCPs include PC fly ash (~34wt.%), FGD materials (~47wt.%), bottom ash (~9wt.%), and boiler slag (~2wt.%) [49]. Roughly 60 – 80 % of the total FBC ash is fly ash, the rest being bottom ash. FBC fly ash has a similar bulk chemistry (with respect to major elements) to conventional PC fly ash, except for the absence of mullite which is a product of coal combustion at 1500°C [50]. FBC fly ash primarily contains crystalline and amorphous alumina-silica phases (e.g., calcined clays), quartz, anhydrite, iron oxide, calcite, and free lime [50]. However, due to the lower combustion temperature of FBC boilers, the ash-forming minerals in coal are not melted but de-hydroxylated (e.g., calcined clays), resulting in a fly ash with sub-angular particles [51] (**Figure 2-15**). These particles also have internal porosity, resulting in up to 5× the surface area of PC fly ash, and this contributes to their reactively and also increased water demand [32].
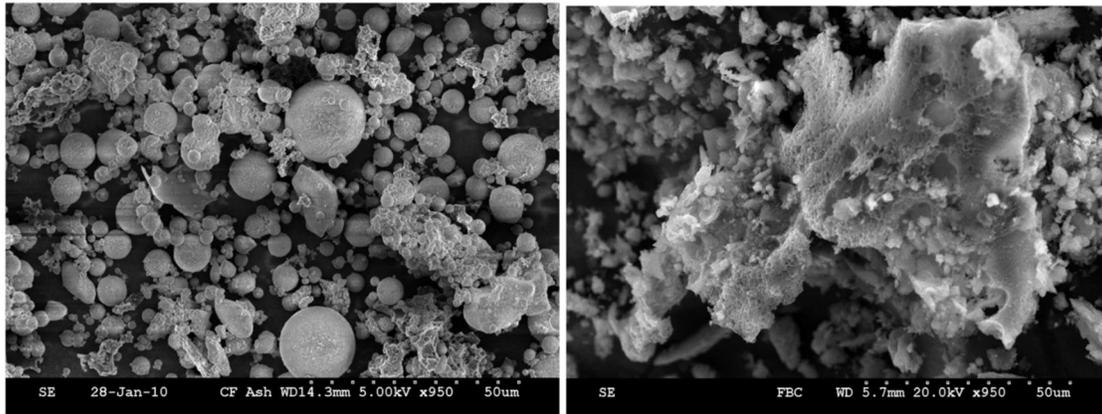
Figure 2-15. SEM/EDS images of (left) PC fly ash (right) FBC fly ash [52]

FBC bottom ash is coarser, with lower fixed carbon (i.e. solid combustible residue that remains after a coal particle is heated and the volatile matter is expelled), and hematite (Fe_2O_3) content [53] [54]. Anhydrite is the most abundant crystalline component in FBC ash and its amount in bottom ash is expected to be higher than that of FBC fly ash [54]. In most cases, the content of SO_3 and free lime is also greater in bottom FBC ash [55]. Some of the applications of FBC ash include surface and subsurface mine reclamation, soil stabilization, road base, structural fill, and synthetic aggregate [36] [35]. However, the majority of FBC ash is disposed in dedicated landfills [36].

2.3.2. Performance of FBC Fly Ash in Concrete

The use of FBC fly ash in concrete is not without potential challenges, as ASTM C618 [56] currently excludes FBC fly ash from its scope. Based on the available literature, FBC fly ash may have high sulfur (SO_3), free CaO, and unburned carbon (LOI) contents [57][58]. $SO_3 > 5$ wt% may cause rapid setting and abnormal expansion at early ages, due to ettringite formation. Similarly, hydration of free CaO can cause excessive heat and volume instability [36]. The LOI may vary from a few tenths of percent to more than 10%, and this impacts the workability and air entrainment performance of concrete mixtures [45],[59],[60],[61].

Studies on the use of FBC fly ash in concrete have been limited and reported contradictory results. Havlica et al. [20] showed that mortars containing pressurized FBC ash or conventional FBC ash can produce similar or better strength in comparison with ordinary Portland cement

(OPC) mortars after only 3 days of hydration. Nguyen et al. [62] studied a high volume fly ash (HVFA) cement paste and reported improved mechanical properties (compressive strength, dynamic Young's modulus, shear modulus, and ultrasonic wave velocity) when up to 5% of class F fly ash was replaced with CFBC fly ash. Glinicki et al. [63] showed that CFBC fly ash reacts pozzolanically with portlandite and also produces a slightly higher quantity of ettringite as a result of its SO_3 content. On the other hand, Gazdič et al. [50] compared the performance of FBC fly ash to PC fly ash at 15% and 30% cement replacement levels and reported a reduced strength in mixtures containing FBC fly ash compared to those with PC fly ash or straight OPC. Wu et al. [64] studied mortars containing class F and/or CFBC fly ash and reported a reduced 28-day strength, delayed setting, and length expansion in mortars with CFBC fly ash. The latter was attributed to the higher SO_3 content of the CFBC fly ash. Robl et al. [65] reported both an increase and a decrease in mortar strength with the partial replacement of cement with CFBC fly ash, depending on the source of cement.

Very few studies have evaluated the effects of FBC fly ash on concrete durability. Chi and Huang [66] examined a CFBC fly ash with very high contents of free lime and SO_3, making it unusable for use as a sole pozzolan in concrete. Instead, they evaluated blends of class F PC fly ash and the CFBC fly ash at mass ratios of 1.5 and 2.5 (PC to CFBC). They reported that the blended fly ashes reduced the water and chloride permeability of concrete and increased the resistance to sulfate attack, but also increased concrete susceptibility to carbonation. Jóźwiak-Niedźwiedzka [67] reported lower chloride diffusion coefficient and higher electrical resistivity for concretes containing 15% or 30% CFBC fly ash as cement replacement. She also observed an improved scaling resistance with 15% CFBC fly ash, but at 30%, the scaling resistance declined. Similarly, Glinicki and Zielinski [68] showed that using 20%, 30%, or 40% CFBC fly ash worsened the de-icing salt scaling of concrete, and the negative effects were proportional with the dosage of CFBC fly ash and its unburned carbon content.

Chapter 3

Literature Review on the Use of Recovered Pulverized Coal Fly Ash as Concrete Pozzolan

3.1. Introduction

Pulverized coal fly ash that has been stockpiled in landfills or ponded in lagoons over the years when fly ash supply exceeded demand, or when fly ash quality did not meet concrete specifications (as shown in **Figure 3-1**). For stockpiling, fly ash is moistened with 10~15% water and compacted in layers in a landfill. When fly ash is being ponded, it is first slurried with water and then pumped to the lagoons. The ash in lagoons may occasionally be drained or de-watered and sent to nearby landfills for stockpiling [69,70]. Fly ash recovered from landfills is termed as recovered or harvested fly ash. Literature study on using recovered fly ash in concrete is presented below.

Figure 3-1. Fly ash stockpile in the UK [70]

3.2. Recovered Fly Ash in Concrete – Potential Issues and Beneficiation

Potential challenges with respect to using recovered fly ash as concrete pozzolan are: (1) high moisture content [70], (2) high unburned carbon (LOI) content [71], (3) presence of lime (calcium oxide or calcium hydroxide), or excess alkalis or sulfur [69,70,72], (4) contamination of fly ash with salts, soil, and organic materials, or co-mingling with other coal combustion products (CCPs), (5) heterogeneity in fly ash properties within a landfill or pond [69], and (6) reduction in fly ash

reactivity due to agglomeration and partial reaction as a result of long-term exposure to moisture [72,73]. A few of these issues have simple solutions. For example, if the ash is moist (exceeding the 3% moisture content limit of ASTM C618-19), then it requires drying. Although it is possible to account for the moisture content of the fly ash as part of the mix water when producing concrete, it is not recommended as the fly ash reactivity reduces with prolonged exposure to moisture, and the transportation cost increases due to the added weight [72]. In addition, concrete production facilities are not equipped to handle damp or wet fly ash.

Other challenges may be more difficult to address. Significant heterogeneity and variability in the material properties of landfilled fly ash may exist because of changes in a power plant over time (e.g., coal type, burning conditions, emission control settings) [69]. This issue requires reliable statistical sampling and evaluation of the landfill to determine if the fly ash is of acceptable uniformity and quality for use in concrete. Fly ash heterogeneity may be partly addressed through homogenization of the recovered fly ash, but this may be costly.

If the stockpile is not a mono-fill and contains fly ash co-mingled with FGD or other CCPs, it may not be possible to recover high-quality fly ash from such a landfill. Contamination with bottom ash, soil, sand, and gravel may be handled through sieving. Presence of excess alkalis, chlorides, and sulfides/sulfates [70,71,75] may render the fly ash unusable or necessitate the disposal of certain sections of a landfill. Presence of active or hydrated lime (as part of, or co-mingled with fly ash) could be problematic as it undergoes a pozzolanic reaction with fly ash over the years, thus reducing the fly ash's reactivity [72]. Other significant issues, including high LOI and reduction in fly ash reactivity due to long-term storage, have a variety of solutions and are discussed below.

3.2.1. Unburned Carbon in Recovered Fly Ash

Fly ash produced in conventional pulverized coal suspension firing systems typically contain 2 to 12% of unburned carbon. In some unique cases, unburned carbon content greater than 20% have been observed [75]. There are many factors which may affect the quantity of unburned carbon present in fly ash including nature/rank of the coal used as fuel; efficiency and design of the combustion process [76] (as cited in [77]); [78–80], particle size distribution of pulverized coal [81]; and plant maintenance frequency [82] (as cited in [71]).

In order to use fly ash as a pozzolan in concrete, it is essential to measure its unburned carbon content. Unburned carbon can cause problems with air-entrainment, workability, compressive strength, and color of concrete [71]. Primarily, the organic carbon adsorbs air-entraining admixtures (AEA) and can cause inconsistency in the air content and strength of concrete. Standards and specifications indirectly measure unburned carbon content of fly ash through the loss on ignition (LOI) test. However, several recent studies suggest that the LOI test may yield biased results because it also captures the mass change due to loss of bound water (e.g., in clays), decomposition of carbonates, and oxidation of sulfur and iron compounds[59,71,83–85]. Also, LOI does not provide information about the surface area and adsorption capacity of the carbon (specifically the isotropic, amorphous forms, as well as high-surface-area carbon including activated carbon tend to be more harmful). Hence sometimes, fly ash with acceptable loss on ignition values may still cause problems with air-entrainment [59,84]. In addition or in lieu of LOI, the foam index test[86,87], iodine number test[85,87], or the direct adsorption isotherm test[87] of fly ash may be performed to more accurately predict its impact on concrete air entrainment.

There are various techniques available to remove or modify the unburned organic carbon from fly ash. These are summarized in Table 3-1. Some of the popular techniques include size separation, electrostatic separation, froth flotation, oil agglomeration, chemical passivation, and thermal processing [71]. Although these techniques are popular for freshly produced fly ash from a power plant, they are not always directly applicable to recovered fly ash stored under wet conditions. The effectiveness of these techniques with respect to recovered fly ash will be discussed as each technique is explained in detail below. While the recovered fly ash after carbon removal can be used in concrete (as long as it meets the specification requirements), the separated unburned carbon can also be of value and used in applications (e.g., water filtration) provided it has sufficient purity. Thus, a good separation technique will ensure the complete utilization of both fly ash and carbon and will increase its commercial value.

Table 3-1. Comparison of different methods for fly ash carbon removal or neutralization

Method	Benefits	Challenges
Sieving	Easy to use; Cheap	Not applicable in all cases
Electrostatic methods	Moderate cost; proven efficiency with fresh & dry fly ash; could be applicable for recovered fly ash; both fly ash and carbon can be extracted – complete utilization of raw material	Drying required; weathering may affect efficiency
Froth flotation & Oil agglomeration	Good separation efficiency; both fly ash and carbon can be extracted – complete utilization of raw material	Thermal drying required - costly
Chemical Passivation	Easy to use and effective	Not applicable at large UC content (could affect compressive strength as carbon is not removed); will not work unless the chemical is distributed evenly
Thermal processing	Very effective	Initial cost of setup is high; carbon is lost – therefore complete utilization of raw material not possible; emissions

Size Separation Techniques – Sieving, Cyclonic and Hydraulic Classifiers

Size separation involves discarding of the coarse fraction of fly ash, which may contain a higher carbon content. The efficiency of this technique depends on the particle size distribution of the individual components in the ash. In many cases, particularly in fly ash with high unburned carbon content, it has been observed that the carbon particles are coarser than fly ash particles. The greater than 150 μm size range often represents less than 10% of the total mass but may contain up to 50% by mass of the total unburned carbon present in the fly ash. When applicable, size separation provides the double benefit of removal of unburned carbon and improvement in the fineness and reactivity of the fly ash. But size separation will not be effective if the particle size distribution of unburned carbon is similar to that of the fly ash particles. Since this technique does not require a liquid medium and the subsequent drying, it is one of the cheapest techniques available [71]. One of the strategies used for sieving without liquid medium is ultrasonic sieving which has shown to provide good loss on ignition reduction [88].

Cyclonic classifiers are typically used for size classification of materials. It consists of a conical body with the raw material being fed from the top and an inner air vortex moving upwards. The finer particles get trapped in the vortex and move upwards while the coarser particles move down. Unfortunately, cyclonic classifiers cannot be used to separate fly ash from unburned carbon particles. This is because carbon particles (~ 1.8 g/cm^3) are less dense than ash particles (~2.5 g/cm^3) and hence they may remain in the inner vortex and get concentrated in the fine ash stream, while the coarse ash particles are rejected [89].

Similarly, hydraulic classification is another technique used for size separation. It consists of a tank wherein the solids (fly ash) mixed with a liquid medium (water) are introduced. Based on the differences in the settling properties of fine and coarse particles, size classification can be achieved. Hydraulic classification was also not found to be sufficient to separate carbon from the fly ash [69]. The authors used a lamella hydraulic classifier and found that the behavior of carbon particles was similar to that of fine fly ash particles and hence sufficient loss on ignition reduction could not be achieved.

Electrostatic Separation Method

Unburned carbon particles and fly ash particles have different electrical properties (specifically the work function) and this difference is used to separate them in the electrostatic separation method [71]. Unburned carbon particles (4 eV) have a lower work function when compared to ash particles (5eV-SiO2 & 4.7eV-Al2O3). As a result, electrons can be transferred from unburned carbon to ash particles, making the carbon particles positively charged and the ash particles negatively charged. This electron transfer is accomplished in a separator with turbulent flow through repeated interparticle contact or particle-container contact. Another way to charge the particles is through tribo-charging where a third material with a work function value that is in between that of carbon and fly ash particles (for example, copper (4.5 eV)) is used to charge the particles through repeated collisions with the intermediate material [90] (as cited in [91]), [92] (as cited in [91]), [88,93–96]. Following the charging of the particles, they are conveyed on a belt through two electrodes with a high voltage applied across them. Depending upon the charge, the carbon particles and the ash particles are drawn to opposite directions and are separated by the belt splitting into two, thus diverging from each other. The carbon particles are collected in the belt

coming out from near the negative electrode and the ash particles are collected from the positive electrode belt [70]. A diagram of the above process is shown in **Figure 3-2**.

It is essential that the ash must be dry before it is fed into an electrostatic separator [97]. This is because exposure to moisture and other weathering conditions have been shown to reduce the separation efficiency. The migration of water-soluble components between the various particles affects the extent of charging and polarities developed. It was found that the changes caused by wet storage were not necessarily reversible through drying. Wet storage may also lead to charge reversal wherein the carbon particles develop a negative charge instead of the usual positive charge or it may lead to no charge development depending on the extent of ion-migration [98]. In [99], it was noted that even though there was a charge reversal, it was still possible to separate the unburned carbon particles from fly ash effectively. In [100], it was observed that the charge reversal could be magnified by the use of sodium and calcium compounds of the borate ion which increases the separation efficiency. Another important factor that is to be controlled during the electrostatic separation process is the relative humidity of the surrounding air. For optimal separation, the relative humidity of the surrounding air should be less than 30%. Relative humidity values greater than 50% was found to cause the agglomeration of fly ash particles [91,101]. By optimizing relative humidity and other parameters like air flow and air temperature, the authors in [91] were able to achieve a recovery rate of 80%.
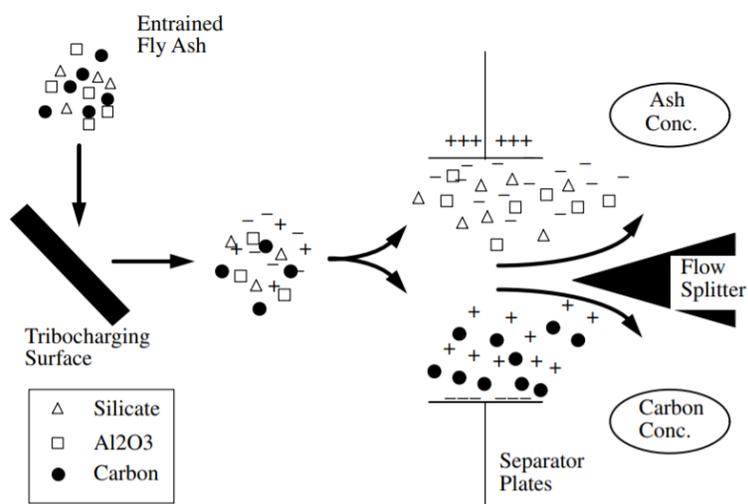
Figure 3-2. Principle of electrostatic separation [95]

In [88], the authors studied the combination of ultrasonic sieving and electrostatic separation in order to reduce the loss on ignition value. Although electrostatic separation by itself was able to reduce the loss on ignition value to less than 6% (ASTM C618 limit [102]) with fly ash recovery of 40 to 52%, the combination of ultrasonic sieving and electrostatic separation techniques was able to achieve loss on ignition values below 3% with recovery of roughly 25%. Electrostatic separation methods have been commercially adopted for separating unburned carbon from fly ash. One of the first applications was by Separation Technologies, Inc. [103].

Froth Flotation and Oil Agglomeration

There is a significant difference in the surface characteristics of unburned carbon and fly ash particles. While PC fly ash particles generally have a smooth spherical surface, unburned carbon particles have a highly irregular surface and high surface area, which is what enables them to absorb air-entraining agents. Froth flotation technique uses this difference in interface to separate the unburned carbon and fly ash particles. Froth flotation has been found to be highly effective in the case of fresh fly ash [71,104]. This method uses a chemical (called collector) to selectively coat the surface of the carbon particle which increase their hydrophobicity. Then, when air bubbles are introduced through agitation, the hydrophobic carbon particles attach themselves to the air bubbles and rise to the top as froth. The froth flows over a weir from which carbon particles are then recovered. The ash particles which are hydrophilic remain in suspension and can be collected from the agitation column [104]. A diagram representing the above process is shown in **Figure 3-3**. Various reagents used in this process are Orfom (collector), kerosene, methyl isobutyl carbinol or pine oil (for froth stabilization), sodium meta silicate (as dispersant) and butanol (used to improve the floating property of unburned carbon particles) [104–107].

An obvious disadvantage of this technique is that the ash needs to be dried before it can be used in concrete and this increases the processing cost [91,101]. It is difficult to maintain the optimum conditions in the flotation column since there is significant variability in the properties of unburned carbon [105]. Despite the disadvantages listed above, there are some advantages to this technique. It is applicable to fly ash stored in ponds (i.e., wet ash) and landfills. Another advantage is the potential for total utilization since all separate components are valuable products. Froth flotation can also reduce ammonia in fly ash when present due to the high solubility of the ammonium salts [97].
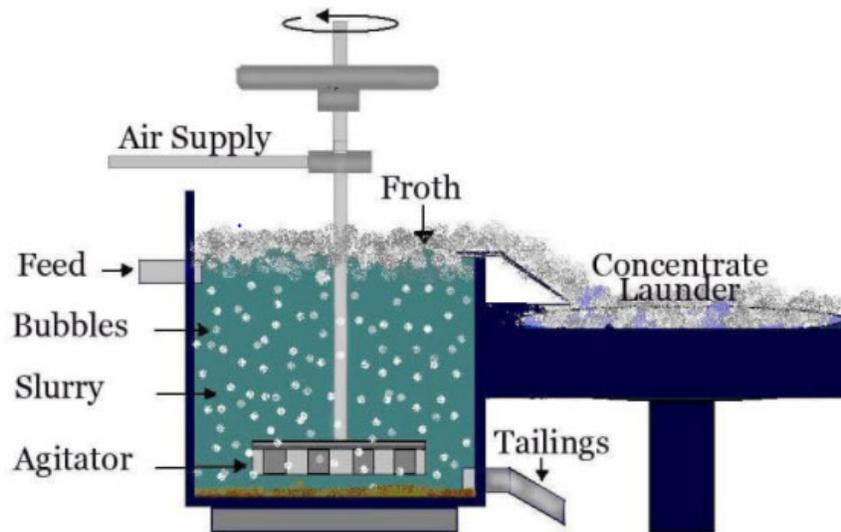
Figure 3-3. Froth flotation process [108]

Froth flotation has been combined with some of the techniques discussed before to achieve a good recovery. For example, In [104], the authors separated unburned carbon from ash efficiently by combining froth flotation with gravity separation and electrostatic separation. In [109], the authors combined size classification with froth flotation repeated twice (ash in suspension from first round used as raw material for the second round) to remove the unburned carbon from slurried stockpiled fly ash. The process was able to reduce loss on ignition to 4.2% (acceptable per ASTM C618 [102]) but the yield was only moderate (45.4%) for ash with fineness (measured based on amount retained when wet-sieved on 45 μm sieve) of 22%. In [110] a commercial application of the froth flotation principle using a cyclonic-static microbubble flotation column is described. The technique was able to reduce the loss on ignition value from 12.7% to 3.08%, but the final moisture content of the ash was roughly 20%.

Oil agglomeration uses the same principle as that of froth flotation but instead of using air bubbles to trap the hydrophobic carbon particles, oil is used. The setup is similar to that of froth flotation but instead of adding a collector and frothing agent, oil is added and the whole system is mechanically agitated. Oil preferentially wets the surface of the carbon particles and when these wetted particles collide due to the agitation, they agglomerate as a result of surface tension forces. The agglomerates are lighter than water and hence rise to the top where they can be skimmed off. The hydrophilic ash particles stay in the water and are subsequently recovered through drying. A

diagram representing the above process is shown in **Figure 3-4**. The most important part of the process on which the separation efficiency depends is the extent of mechanical agitation [111].
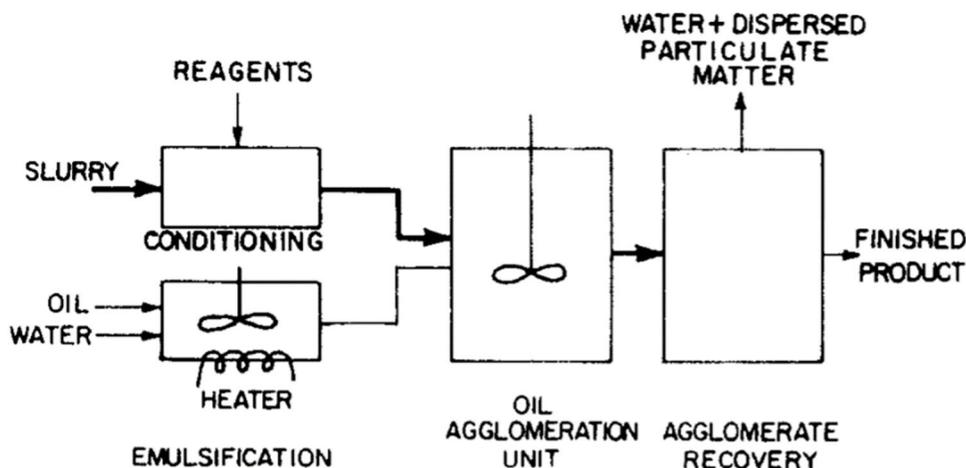
Figure 3-4. Typical oil agglomeration process [111]

The process used in [105] was able to reduce the unburned carbon content of fly ash to less than 3% under optimum conditions. The study used kerosene and optimized various parameters such as shaking time, pulp density, temperature, shaking speed and organic to suspension ratio. Other studies with oil agglomeration mostly focused on the carbon recovery rather than fly ash recovery and hence are not discussed in detail here.

Thermal Processing

Although reduction of loss on ignition of fly ash through burning of the unburned carbon may not always be cost effective, it can nevertheless be a very effective technique. While complete utilization of the 'as recovered' fly ash is not possible (because the carbon part of the material is lost) as in the case of the other techniques discussed above, this method is technologically suitable with respect to utilization of fly ash in concrete [71]. Also, thermal processing removes the ammonia present in the ash [97]. The main disadvantages of this technology are the initial cost of setup and environmental pollution as a result of CO_2, NO_x and SO_x emissions [70]. Conventional combustion techniques cannot be used for burning the carbon present in fly ash since the quantity of carbon is very low (4 to 10%) [71]. Modified reactor designs like the Carbon Burn-out (CBO – patented by PMI Ash technologies) technology and the Staged Turbulent Air Reactor (STAR – patented by SEFA group) technology are required to combust the carbon in fly ash [112].

CBO which uses a specific type of fluidized bed combustion process known as bubbling fluidized bed has been commercially applied for reducing the unburned carbon content of fly ash [112,113]. The process involves the initial heating of the fly ash to temperatures of 667-732 ºC. This temperature is greater than the auto-ignition temperature of the unburned carbon in fly ash. Once the carbon is burned off and the desired loss on ignition value is achieved, a portion of the ash is left behind and the rest of the ash is removed and allowed to cool. The ash that is left behind is used to maintain the bed temperature. Provided the system is balanced correctly and provided the fly ash has sufficient unburned carbon, it is possible for this process to sustain itself without additional fuel requirement. As such, fly ash with high loss on ignition value is suitable for this technique. This process could also potentially improve the fineness of the ash by releasing the fine ash particles entrained in the carbon particles [113]. PMI Ash Technologies has a patented design for processing recovered landfill fly ash using CBO [114]. CBO technology has been commercially applied in many places. Wateree station in Columbia, South Carolina can handle 180,000 tons of ash each year. The authors noted that the technology is quite robust to changes in the fly ash [113,115]. Another case is that of the Winyah station of Santee Cooper as reported in [113], where 200,000 tons of ash was processed each year using CBO process until it was partially demolished and replaced with STAR technology in 2015 [112].

Another patented thermal processing technique which has been commercially applied is the STAR (staged turbulent air reactor) technology developed and patented by SEFA group. Unlike the CBO process which is based on FBC system, STAR is a hybrid of circulating FBC and transport reactor process. This system also uses ash recycling to maintain the reactor temperature which enables the process to be self-sustaining. STAR system operates at a higher temperature than the CBO process (800-1000 ºC). The STAR process can also be designed to handle wet fly ash, thus making this process suitable for recovered fly ash beneficiation [112]. STAR technology has been commercially applied in many places. McMeekin station in Columbia, South Carolina has 140,000 tons per year facility owned by SEFA. As described previously, the Winyah station is currently operating a STAR system [112]. Morgantown station in Morgantown, Maryland also uses the second-generation STAR technology, which is claimed to be better than the original STAR technology [112,116].

It is important to note that these are proprietary technologies and most available information regarding their performance and efficiency are supplied by the technology owners, as opposed to a third-party verification.

Chemical Passivation

Chemical passivation (example shown in **Figure 3-5**) involves adding a sacrificial surfactant to the fly ash which adsorbs on the surface of carbon particles and thus prevents them from adsorbing the air-entraining admixtures (AEA) in concrete. Clearly, this technique does not reduce the loss on ignition value, as the carbon is not removed but neutralized. Yet, fly ash that is treated using this method can be used in concrete provided that it meets other specification requirements. The use of this technique depends on the applicable specifications; i.e., performance-based specifications may allow the use of chemically treated fly ash but prescriptive specifications with a limit on maximum LOI will not accept this technique as it does not reduce the LOI of fly ash [117]. Chemical passivation has been shown to reduce the AEA uptake based on the foam index test [118].

Chemical passivation can be especially effective in treating fly ash that contains power activated carbon (PAC, having very high surface area). To meet recent air pollution regulations regarding mercury (Hg) emission, many power utilities have started using PAC as Hg sorbent, which is removed together with fly ash in the particulate removal units. Even though the content of the activated carbon that ends up in fly ash maybe small (e.g., less than 1%, and as such, meeting LOI requirement of the specifications), due to its high surface area, PAC has a significant admixture binding capacity, which severely impacts the air-entrainment in concrete. It is difficult to remove activated carbon since it is present in such low concentrations [117]. Chemical passivation has been found to be effective for neutralizing PAC [119] (as cited in [117]).

Figure 3-5. RestoreAir setup (Boral) – a commercial chemical passivation technology[118]

The main challenges associated with the use of chemical passivation technique is identifying the correct dosage of sacrificial chemical required and the technique necessary to spray/distribute it evenly throughout the ash. Chemicals which were initially used for this purpose themselves could entrain additional air in concrete when the ash was overdosed [120] (as cited in [117]). The problem of even dispersion has to be addressed by carefully designing the spray nozzle and the distribution system (this has to be customized depending on the properties of the ash). The chemical used can also have an effect on distribution and needs to be addressed [117]. The issue of appropriate dosage of the sacrificial surfactant requires reliable testing of the carbon content in the ash. Once again, it is important to note that most available information on chemical passivation is from companies that own the patented technology.

Other Methods

Some other techniques for carbon separation, which have been used in literature but are not as popular, are density gradient centrifugation, incipient fluidization, and acid digestion [71]. Density gradient centrifugation involves the use of a liquid which will float the carbon particles and sink the ash particles given their density difference. It is primarily a laboratory technique useful for isolating the carbon particles for further study [96,121]. Incipient fluidization involves pulsing a non-reactive gas like helium through a vertical tube containing a small quantity of the sample so that the ash particles float to the top [122]. Acid digestion involves the removal of mineral

components of the fly ash by digesting it in acids like HF and HCl, leaving behind the carbon particles [80]. All of these techniques (especially acid digestion) are more suited for the recovery of unburned carbon rather than recovery of low carbon fly ash, and hence are not discussed in detail in this study.

3.2.2. Increasing Reactivity

Due to long-term wet storage of fly ash in landfills or ponds, some particle reaction and agglomeration may have occurred. The reaction products may deposit on the surface of aluminosilica glass particles in fly ash, thus reducing their dissolution and reactivity. The products also increase the surface roughness of fly ash particles, which result in an increased water demand and reduced strength activity index of fly ash[72,73]. Fly ash reactivity can be improved by grinding, thermal processing, and chemical activation, as described below.

Grinding (Mechanical Activation)

Various types of grinding or milling techniques are available for breaking down the particles of fly ash. These include ball mills, hammer mills, attrition mills, jet mills, and vibro-energy mills. Ball mills are the most common technique used for grinding of fly ash [123].

Many changes in the properties of fly ash subjected to grinding were observed in literature irrespective of the condition of the ash (fresh vs recovered). In both cases, the specific gravity of fly ash tends to increase and its fineness is improved with grinding. The strength activity index of ground fly ash tends to increase up to a certain optimum grinding time. The water requirement has been observed to be more or less the same for the fresh fly ash, but for the recovered fly ash, there was an improvement in the workability as indicated by the reduction in water requirement. This is probably due to the release of agglomerated spherical particles during grinding of recovered fly ash [124,125].

One important aspect to note about the recovered fly ash study [125] was that significant agglomeration was observed after storage in a landfill for 12 to 24 months. The as recovered fly ash did not meet the strength activity index requirements (minimum 75% of control at 7 or 28 days [102]). But after grinding, the water requirement was reduced and the strength activity index of the mechanically activated ash was improved to 81 to 97% at 7 days.

Chemical Activation

Chemical (e.g., alkali) activation of fresh fly ash has been extensively studied in portland cement and geopolymer mixtures[126–129]. Dissolution and reactivity of the aluminosilica glass in fly ash is enhanced by increasing the pH of the mix water in concrete. Heat curing can be further employed to facilitate fly ash reactivity and strength development. The most common chemicals used for chemical activation of fly ash are sodium sulfate and calcium chloride. It was observed that for mortars cast with fresh fly ash and sodium sulfate as an activator, there was a significant increase in the early age strength (mostly due to formation of ettringite) except when the fly ash contained a higher concentration of ferrous oxide [126]. Sodium sulfate and calcium chloride were also tested using the lime reactivity (pozzolanic activity) test of fly ash. It was observed that both calcium chloride and sodium sulfate increased the strength of the mixtures. Sodium chloride was also tested as part of this study and it did not have any effect on the strength [127]. Alkali activation of fly ash may also be considered to enhance its reactivity. However, a major issue with chemical activation is the use of sulfates, chlorides, and alkalis, which can cause problems in Portland cement concrete. As of now, it is not known whether this method can be used for the activation of recovered fly ash.

Thermal Activation

Thermal processing to combust the unburned carbon may release fine fly ash particles that are entrapped within the carbon. Since these finer particles are more reactive[130], they improve the overall reactivity of the fly ash. STAR treatment of fly ash has been reported to improve the strength activity index and the compressive strength of concrete mixtures [131,132].

3.2.3. Drying Technology

Water is typically mixed with fly ash before landfilling as it reduces volume (provides better compaction) and reduces air-borne dust. As mentioned earlier, the reactivity of fly ash reduces as the duration of wet storage increases. Hence it is necessary to dry the fly ash when it is excavated for beneficial use. Drying also has the added benefit of reducing the transportation cost by reducing the mass of the material.

Several commercial technologies are available for drying of powder-type materials including rotary dryers (direct and indirect), fluidized bed dryers, flash/pneumatic dryers, and tray

dryers [133]. A comparison of the methods is shown in **Table 3-2** below. Use of direct rotary dryers and fluidized bed dryers results in a loss of fine particles resulting in two disadvantages – 1) equipment necessary for cleaning the exhaust gas increases cost and 2) the fly ash reactivity is reduced with increase in loss of fines. Flash/pneumatic dryers are not suitable for landfilled fly ash as the presence of moisture produces lumps whereas tray dryers will significantly increase cost as the process is labor intensive. Based on the evaluation of the pros and cons of the various dryers, indirect rotary dryers seem to be optimum in terms of cost and quality of end product.

Table 3-2. Comparison of drying technologies for landfilled fly ash [133]

Technology	Characteristics
Direct rotary dryers	• Cheap and simple • Loss of fine particles – cleaning of exhaust gas required and fly ash reactivity reduces
Indirect rotary dryers	• Costlier than direct rotary dryer • Lower drying rate than direct rotary dryer • No loss of fine particles – clean exhaust gas and maximum reactivity retention
Fluidized bed dryers	• Loss of fines – not suitable for particles below 10 µm
Flash/pneumatic dryers	• Materials which form lumps cannot be dried
Tray dryers	• Labor intensive – increases cost

3.3. Performance of Recovered Fly Ash in Concrete and Mortar Tests

Fly ash recovered from landfills (built in 1970s and 80s) was compared against fresh fly ash from the same plant (2016) in one study[134]. The recovered fly ash was dried and screened to reduce the fineness to a level comparable to that of the silo-stored ash from the same power plant. The recovered fly ash was found to be superior in terms of the strength activity index, water requirement, sulfur content, and LOI, whereas both fly ashes were similarly effective in mitigating ASR.

Fly ash recovered form lagoons and stockpiles were evaluated for their performance in concrete in another study[130]. The recovered fly ash passing #30 (600µm) sieve was used as the reference/control material. A portion of the sieved recovered fly ash was further processed via either a 63µm sieve, air classification, or grinding, and considered as the test materials. This study gives us an insight into the effect of various beneficiation processes on the fresh properties of the

recovered fly ash concrete. Ground fly ash was found to have better slump than 63-µm sieved fly ash which was in turn better than the reference fly ash. Air-classified fly ash showed high variability in slump but it was still mostly better than the reference fly ash. Sieving and air classification could have improved the slump by removing the coarse agglomerated fly ash particles. Grinding can result in two opposing effect – breakdown of agglomerated particles to form rough spheres and breakdown of spheres to form angular particles. The effect of grinding on slump depends on which effect is predominant and, in this case, it seems to be the former effect (this is consistent with the results observed in the section on grinding). In general, fly ash that has been excessively ground can reduce the slump of concrete when used as a pozzolan. Ground fly ash also had the best performance in terms of compressive strength, air permeability, water absorption, 12-week accelerated carbonation, and chloride diffusion tests. The performance of sieved and air classified fly ash was slightly better or comparable to that of the reference fly ash in all these cases. It was observed that ashes that contained a significant proportion of particles smaller than 10µm performed better than other ashes with respect to durability.

Two fly ashes recovered from landfills and beneficiated through drying and grinding were investigated in one study[135]. The beneficiated ashes were compared with fresh fly ash across various properties. The beneficiated fly ashes (D50 = 22.2µm or 12.8µm) had mostly round particles despite grinding, and were finer than the fresh fly ash (D50 = 26.9µm). The flow, compressive strength of mortar, ASR mitigation capacity, and rapid chloride permeability results were comparable for the beneficiated and fresh fly ashes. The compressive strength of concrete cylinders was higher for the finer beneficiated fly ash at all ages, whereas the other beneficiated fly ash and the fresh fly ash had comparable strengths.

Fly ash co-mingled with bottom ash from a landfill was used as is without any beneficiation in another study [136]. The fly ash also had a high moisture content and unburned carbon content. Concrete mixtures were produced at a water to cement ratio of 0.42 with replacement levels ranging from 15-50%. The water content and sand content were adjusted according to the moisture content and bottom ash content of the ash. Further the dosage of air entraining admixture was also adjusted to obtain the necessary air content. At high replacement rates, the early age strength and setting was significantly. However, the later age strength was acceptable and the durability (RCPT, ASR mitigation) properties were very good when compared to OPC and fresh fly ash from the same plant.

In [116,131] recovered fly ash processed using the STAR technology is compared against a fresh fly ash which is representative of the average quality ash available today. Fly ash processed using STAR technology was found to have comparable [116] or better strength [131] than typical fresh fly ash mixes found in the marketplace. In [131], it was also noted that the recovered fly ash before beneficiation was not suitable for use in concrete but became much better post thermal processing. Beneficiated ponded fly ash in [137] was used to produce a blended mix at 25% and 35% cement replacement and was found to reach the same strength as Portland cement mix at 14 days and 28 days respectively. The mixes were compared at equal slump rather than equal water to cement ratio. Once again, it is to be noted that these are not a third-party analysis of the technology.

The four studies found in references[137–140] collected samples of fresh fly ash from a power plant and conditioned them with moisture for 18 months to simulate landfill conditions. The conditioned fly ash was compared to the fresh fly ash by studying various properties. The reduction of slump due to agglomeration of fly ash particles, when used without beneficiation in concrete, was investigated in one study. The slump of the concrete containing conditioned fly ash gradually decreased as the conditioning period increased from 1 to 18 months[138]. It was also observed that the compressive strength of concrete with fly ash decreased as the duration of conditioning increased. The largest drop was observed in the case of fly ash with the highest free lime content, indicating some loss in pozzolanic reactivity during the wet storage[138,139]. Fresh fly ash and conditioned fly ash mixtures had comparable flexural strength, elastic modulus, drying shrinkage, and creep coefficient – studied at 28 days at equal slump (75 mm) and compressive strength (35 MPa)[138,139]. The conditioned fly ash mixtures[137] performed better than fresh fly ash mixtures with respect to water absorption and air permeability, while similar performances were found in the case of other properties (carbonation, chloride diffusion, freeze-thaw scaling, abrasion[137], and ASR mitigation[140]).

Overall, studies evaluating the performance of recovered fly ash are limited and only report on promising landfills. There are no reported protocols on how to statistically sample and reliably evaluate the variability in fly ash and its properties within a landfill. This is addressed in the next section.

Chapter 4

Characterization of Circulating Fluidized Bed Combustion (CFBC) Fly Ash and Its Performance in Concrete[1]

4.1. Introduction

FBC fly ash is a potentially valuable pozzolan that is available at little cost and in large volumes. Given the recent shortage in the availability of conventional PC fly ash [4],[5],[141], it is logical to methodically research the composition, structure, and properties of FBC fly ash to determine which fly ash compositions may be usable as concrete pozzolan. Proper characterization of FBC fly ash and its performance in concrete can facilitate development of specifications and guidelines for evaluation, beneficiation, and use of this potentially valuable pozzolanic material.

To address this objective, two different CFBC coal fly ashes were evaluated for their compliance against ASTM C618-19 (equivalent to AASHTO M295) standard and their impact on the fresh and hardened properties of concrete. This is the first study in its kind to present a complete evaluation of the physical, chemical, and mineralogical properties of CFBC fly ashes produced in the United States and to link these properties with important characteristics of concrete beyond strength development. The fly ashes were sourced from two CFBC power plants in Pennsylvania that use anthracite or bituminous refuse coal as a fuel source. These power plants generate over 2.0 million tons of CFBC fly ash per year, the majority of which is currently landfilled.

4.2. Experimental Procedures

Two sources of CFBC fly ash, byproducts of anthracite and bituminous refuse coal combustion, were acquired, homogenized, and characterized for their physical properties, bulk chemistry, mineralogy, and pozzolanic reactivity. Areas of noncompliance with ASTM C618-19 were identified. Further, the performance of these fly ashes in mortar and concrete mixtures was evaluated by measuring the fresh properties (slump and fresh air content), and hardened properties (strength development, hardened air structure, autogenous expansion, and ASR mitigation

---

efficiency) of these mixtures.

4.2.1. Physical Properties and Unburned Carbon

Both CFBC fly ashes were characterized for their as-received moisture content (ASTM C311-17), particle size distribution (PSD using laser diffraction), fineness (ASTM C430-17), density (using helium pycnometer), particle shape/agglomeration (via SEM), water requirement (ASTM C311-17), soundness (ASTM C151-18), loss on ignition (ASTM C311-17), and carbon and sulfur contents (using infrared LECO analyzer). Two samples were tested per fly ash for each of the above tests (excluding the water requirement which was based on one sample). The results are reported as the average of the two samples. To achieve proper fineness, the anthracite CFBC fly ash passing #140 sieve was used in all tests. The bituminous CFBC fly ash was tested as received.

The SEM samples were prepared using a mixture of low-viscosity epoxy and fly ash (1-1 mass ratio) embedded in a molded epoxy disk, 25 mm diameter and 12.5 mm height, using a protocol similar to [142]. The samples were polished down to 0.25 μm, and carbon coated before imaging. Thermo Scientific™ Q250 Analytical SEM was used and operated at 10^{-4} mmHg, 15kV accelerating voltage, and ~10 mm working distance. Backscattered electron (BSE) images were obtained at 1000× magnification. Laser diffraction PSD testing was conducted by measuring the angular variation in the intensity of light scattered as a laser beam passed through a well dispersed sample of fly ash in water. A small amount (~0.03 g) of fly ash was added to distilled water and the sample was sonicated for 1 min before PSD testing. The particle size distribution was computed using a refractive index of 1.6 and absorption coefficient of 1.0, as reported by [143]. In addition to the standard LOI test, infrared spectroscopy using a Leco analyzer was used to measure the total carbon (organic and inorganic) and sulfur contents in each fly ash. In this technique, the sample was combusted in air up to 1450ºC inside the furnace, and the emitted CO_2 and SO_2 gases were measured separately using infrared detectors.

4.2.2. Bulk Chemistry and Mineralogy

X-ray fluorescence (XRF) analysis was conducted on fly ash samples to determine their bulk chemistry. Homogenous fused glass beads were prepared by heating a mixture of fly ash and lithium borate (flux) to 1000ºC. XRD with Rietveld refinement was performed to identify and quantify the mineral and amorphous phases present in each fly ash. Fly ash samples were ground

to less than #400 sieve, mixed with 15% internal standard (highly crystalline ZnO), and placed on spinner stage rotating at 4 rev/s. The incident X-ray beam was Cu Kα radiation (λ=1.5419 Å) produced using 45 kV and 40 mA. Incident settings were: 0.125° divergence slit, 0.25° anti-scatter slit, 0.04[rad.] Söller slits, and 15 mm beam mask. Diffracted settings were: 0.125° receiving slit, 0.04[rad.] Söller slits, and 0.02 mm nickel filter. Diffraction patterns were collected over the range 5-70° 2θ with step size of 0.02°, for a total scan time of ~30 min. A PIXcel detector in scanning line mode was used.

To monitor the dissolution rate of soluble species from CFBC fly ash into concrete pore solution, batch leaching tests were carried out. Of special interest was the solubility of sulfur compounds (e.g., anhydrite), which can lead to formation of ettringite and potential undesirable setting or expansion. In the leaching test, CFBC fly ash was exposed to synthetic concrete pore solution. The concentrations of S, Si, Al, Ca, Na, and K in the solution were measured at 1, 3, and 7 days of exposure. The results were compared with the concentrations obtained from the leaching test of a type I/II portland cement (composition reported in **Table 4-5**). The synthetic pore solution was prepared by mixing 0.2 mol/L NaOH and 0.5 mol/L KOH with saturated lime water to reach a pH=13.85. Next, fly ash or portland cement was added to the pore solution at a mass ratio of 1:20, and the resulting solution was tumbled for 100 h. Solution samples were taken at 1, 3, and 7 days of exposure, filtered (using 0.2μm polypropylene membrane) and tested using Inductively Coupled Plasma-Atomic Emission Spectroscopy (ICP-AES) to measure the concentrations of various elements. The chemistry and mineralogy experiments were not duplicated.

4.2.3. Pozzolanic Reactivity

The strength activity index (SAI) of the two fly ashes were measured according to ASTM C311-17 and after 7, 28, and 56 days of curing in a lime water bath. The control mortar mixture was prepared with w/c=0.484 and sand/cement=2.75 by mass, using type I/II Portland cement (**Table 4-5**) and standard sand with absorption capacity of 0.58%. In the test mixtures, 20% of the mass of cement was replaced with the anthracite or bituminous CFBC fly ash, and enough water was added to reach a flow ± 5% of the control mortar (measured according to ASTM C1437-15). This resulted in a net increase of the w/cm to 0.53 in mortars containing fly ash. To eliminate the effect of the increased w/cm on the compressive strength of mortars, a second series of mortar samples

were prepared, where the w/cm was kept constant between the test and control mixtures, and enough superplasticizer (Master Glenium 7620) was added to the test mixtures to maintain a flow of ± 5% of the control mixture. For both the SAI and mortar strength experiments, three cubes were tested at a given age.

In addition, two test methods were adopted for measuring the pozzolanic reactivity of fly ash; ASTM C593-06 (Standard Specification for Fly Ash and Other Pozzolans for Use with Lime for Soil Stabilization) and RILEM TC TRM267 (Tests for Reactivity of Supplementary Cementitious Materials). According to ASTM C593-06 (2011), lime-fly ash mortars were tested for their compressive strength. The mixture design is provided in **Table 4-1**, where sufficient water was added to produce an ASTM C1437 flow of 65 to 75 %, using 10 drops of the flow table in 6 seconds. Three 50 mm cube specimens were prepared for strength measurement at each age (7 and 28 days). After casting, the samples were steam cured at 54°C for 7 days, followed by demolding and storing at 23°C and 95%RH until the time of testing.

Table 4-1. Lime-fly ash mortar mixture design and properties (ASTM C593-06)

Sample	Fly ash (g)	Hydrated lime (g)	Standard Sand (g)	Water (g)	w/b	Flow (%)	Strength (MPa)	
							7 days	28 days
Anthracite CFBC	360	180	1480	421.5	0.78	65	6.73	6.13
Bituminous CFBC	360	180	1480	388.8	0.72	67.5	12.12	10.62

According to RILEM TC TRM267, lime-fly ash pastes were prepared with proportions provided in **Table 4-2**, using $Ca(OH)_2$/pozzolan mass ratio of 3.0, and a water/binder mass ratio of 1.2. Soluble alkalis were added to reproduce the cement pore solution pH and accelerate the pozzolanic reaction, while potassium sulfate and calcium carbonate were added to promote the formation of AFt (ettringite) and AFm phases. The pastes were hand mixed, poured into cylindrical molds (25.4 mm diameter and 20 mm height), sealed, and cured at 40°C to accelerate the pozzolanic reaction. After 1, 7, and 28 days, samples were demolded and ground using a mortar and pestle. To stop the hydration reactions, ground samples were immersed in 100 mL isopropanol for 15 min. The suspension was stirred and poured over a Büchner filter. The residue was dried in a ventilated oven at 40°C for 8 min. TGA testing was conducted by heating the resulting samples from 30°C to 950°C, at the rate of 10°C /min. The TGA chamber was purged with N_2. The

unreacted $Ca(OH)_2$ content of each sample was calculated by measuring the mass loss in the temperature range 375°C to 480°C using the tangent method proposed by Kim and Olek [144], and correcting the results based on an estimated mass of carbonated $Ca(OH)_2$. The reported results (**Figure 4-6**) correspond to the testing of one sample per fly ash at a given age. In addition, RILEM TC TRM267 suggests measuring the bound water of the paste at 7 days using the "oven method". According to this procedure, paste samples were ground using a mortar and pestle, and dried in an oven at 105°C to constant mass. Next, samples were calcined at 350°C for 2 hours, and the mass loss between 105°C and 350°C was measured and attributed to the loss of bound water. Two samples were tested per fly ash and the average of the two results are reported.

Table 4-2. Lime-fly ash paste mixture design according to RILEM TC TRM267

Components	Fly ash	$Ca(OH)_2$*	Deionized water	KOH[#]	K_2SO_4[#]	$CaCO_3$
Weight (g)	11.11	33.33	60	0.24	1.2	5.56

* Contained less than 5 wt.% $CaCO_3$
[#] The mixture of KOH and K_2SO_4 was equivalent to 0.3M K

4.2.4. Performance of CFBC Fly Ash in Mortar and Concrete

The performance of CFBC fly ashes in concrete mixtures was evaluated by measuring the fresh properties, including slump (ASTM C143-15a), and fresh air content (ASTM C231-17a). Also, the hardened properties were measured, including the compressive strength at 7, 28, and 56 days (ASTM C39-18), and hardened air structure (ASTM C457-16). In addition, setting time (ASTM C403-16), autogenous expansion/shrinkage (ASTM C1698-09), and ASR mitigation efficiency (ASTM C1567-13) was measured using equivalent mortar mixtures. These results were used along with the fly ash characterization results to identify the positive and negative effects of CFBC fly ashes on concrete properties, and to suggest appropriate fly ash beneficiation techniques.

Concrete mixtures were designed using proportions that are typically used for pavement applications in Pennsylvania. They were prepared with a w/cm=0.47 using type I/II Portland cement (**Table 4-5**), natural sand (SSD specific gravity of 2.62, absorption capacity of 1.66%, fineness modulus of 2.94), #57 crushed stone (SSD specific gravity of 2.70, absorption capacity of 0.44%, dry rodded unit weight of 1476.4 kg/m^3) and water reducing (Master Glenium 7620 by BASF) and air-entraining (MasterAir AE90 by BASF) admixtures. All aggregates met ASTM C33-18 requirements. The concrete mixtures were designed for a slump of 10±2.5 cm (4±1 in.)

and air content of 6±1% by volume. **Table 4-3** provides the concrete mixture proportions. In the test mixtures, 20% of the Portland cement was replaced with the anthracite or bituminous CFBC fly ash. Two sets of fly ash concrete mixtures were prepared. The first set contained the same AEA and water reducing admixture (WRA) dosage as that of the control mixture. Generally, these test mixtures resulted in lower slump and lower air content as described later. In the second set, the AEA and WRA dosages were varied to achieve the target slump (10±2.5 cm) and target air content (6±1%) in the fly ash mixtures. For each of the five mixtures, 10 concrete cylinders (diameter of 100 mm and height of 200 mm) were cast and moist cured at 23°C and 100% RH. For each mixture, after 28 days of hydration, a 100×120×10 mm section was cut (perpendicular to the finished surface) from the center of a concrete cylinder and analyzed for hardened air void distribution. The remaining nine samples per mixture were used for compressive strength testing at 7, 28, and 56 days of age. Three samples were tested at each given age.

Table 4-3. Mixture designs to evaluate the effect of CFBC fly ashes on concrete properties

Mixture	Cement (kg/m³)	Fly ash (kg/m³)	Water (kg/m³)	Coarse aggregate (kg/m³)	Fine aggregate (kg/m³)	AEA (kg/m³)	WRA (kg/m³)
Control	362	-	170	1098	643	0.47	0
Anthracite CFBC, set 1	290	72	170	1098	639	0.47	0
Bituminous CFBC, set 1	290	72	170	1098	640	0.47	0
Anthracite CFBC, set 2	290	72	170	1098	639	0.94	1.40
Bituminous CFBC, set 2	290	72	170	1098	640	0.47	0.88

Equivalent mortar mixtures were prepared with w/cm=0.47 and sand/cm=2.25. In the test mixtures, enough superplasticizer (Master Glenium 7620 by BASF) was added to achieve a flow of the control mix ± 5%. For autogenous shrinkage testing, the freshly made mortar was poured into sealable corrugated plastic tubes (length of 420 mm and outer diameter of 29 mm) and continuously rotated for the first 24 hours at 23°C and 50% RH. For each mixture, four samples were prepared. The length and mass of each sample were recorded at the time of final setting and at ages of 1, 3, 5, 7, 9, 11, 13, and 15 days. This test was conducted to capture both shrinkage and expansion strains that may occur in mixtures containing CFBC fly ash. To investigate the ASR

mitigation capacity of CFBC fly ashes, mortar bars were prepared and tested according to ASTM C1567-13. These mortars contained a borderline moderately-reactive/highly-reactive river sand (class R1/R2 according to ASTM C1778-16) with SSD specific gravity 2.52 and an absorption capacity of 1.49%. The control mixture was prepared with 100% Portland cement as binder. In the test mixtures, 20% or 40% of the cement was replaced with either CFBC fly ashes. A w/cm=0.47 was used and no superplacticizer was included in these mixtures. During the experiment, the mass and length change of each mortar bar was measured as a function of time and to the accuracy 0.01g and 0.0025mm. Four replicate prisms were measured.

4.3. Results and Discussion

4.3.1 Physical Properties and Unburned Carbon

The results (**Table 4-4**) show that both the anthracite and bituminous CFBC fly ashes satisfy ASTM C618-19 requirements of moisture content and soundness. The latter suggests that the fly ashes don't pose a risk of deleterious expansion caused by the hydration of free CaO and/or MgO. Similar results were also obtained by Wu et al. (2014) [64]. Although the fineness of the anthracite fly ash is greater than the maximum allowable limit of 34%, when passed through #140 sieve (105 μm), it complies with the ASTM fineness limit. Laser diffraction testing show that both fly ashes have a similar particle size distribution with a median particle size (D50) that is close to that of conventional PC fly ash (20-30 μm) [145].

Table 4-4. Physical properties and unburned carbon content of fly ash

Property	Anthracite CFBC	Bituminous CFBC	ASTM C618 limit
Moisture content (%wt)	0.12	0.18	3.0 max.
Density (g/cm^3)	2.61	2.63	-
Fineness (% >45μm)	40.0[1]	29.5	34 max.
LOI (%wt)	6.65	5.21	6.0 max.
Carbon (%wt) using Leco/IR	6.26	3.80	-
Sulfur (%wt) using Leco/IR	1.01	4.64	-
Particle size D10 (μm)	2.95	3.42	-
Particle size D50 (μm)	28.7	26.1	-
Particle size D90 (μm)	128.0	102.5	-
Soundness (AC exp. %)	-0.02	-0.03	±0.8 max.
Water requirement (%)	109.5	109.5	105 to 115 max.

[1] Fineness of Anthracite fly ash passed through No. 140 sieve is 27%

Furthermore, SEM imaging (**Figure 4-1**) show that contrary to the spherical shape of PC fly ash, CFBC fly ash particles have sub-angular shape and internal porosity, consistent with the lower combustion temperature of FBC boilers. These may result in higher water requirement and lower workability of concrete.
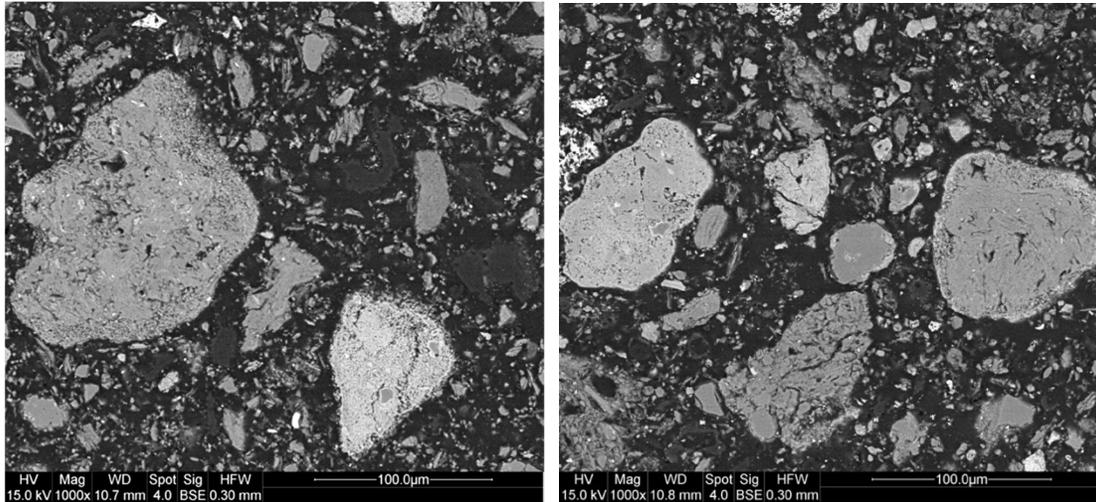
Figure 4-1. SEM images of the anthracite (left) and bituminous (right) CFBC fly ash

The main area of concern is the elevated LOI values for both fly ashes, which may cause problems for air entraining concrete. ASTM C618-19 allows a maximum 6.0% LOI for fly ash and 10% LOI for natural pozzolans. However, up to 12.0% LOI for class F fly ash is allowed if acceptable air entraining performance can be proven. LOI values >3% often increase the required dosage of AEA and may result in inconsistent air entrainment and strength of concrete. The fresh and hardened air properties of concrete mixtures containing CFBC fly ashes (results presented in **Table 4-6**) provide a more accurate insight into their effect on producing concrete with reliable air entrainment. The Leco/IR results show an elevated level of carbon in both fly ashes (higher in the anthracite CFBC) and an elevated sulfur content in the bituminous fly ash, which is in agreement with the high sulfur content of the bituminous coal. It should be noted that both the LOI and the Leco carbon results are indicative of total carbon contents of the fly ashes, which include both the organic (unburned) and inorganic (carbonates) fractions. Only the organic carbon has a significant impact on the adsorption of air entraining admixtures in concrete.

Table 4-5. Oxide composition of cement and fly ash

Compound	Portland cement	Anthracite CFBC	Bituminous CFBC
SiO_2	19.41	50.10	37.64
Al_2O_3	4.61	22.54	16.88
Fe_2O_3	3.82	7.66	9.91
S+A+F	*27.84*	*80.30*	*64.43*
CaO	60.78	5.06	15.39
SO_3	4.00	2.39	9.83
K_2O	n/a	2.90	2.09
Na_2O	n/a	0.35	0.24
Na_2O_{eq}	*0.90*	*2.26*	*1.62*
TiO_2	n/a	1.34	0.91
MgO	2.91	0.75	1.29
P_2O_5	n/a	0.14	0.13
CO_2	1.69	n/a	n/a

Table 4-6. Effect of CFBC fly ash on concrete properties

Properties	Control	Anthracite CFBC set 1	Bituminous CFBC set 1	Anthracite CFBC set 2	Bituminous CFBC set 2
Slump, cm (in)	8.5 (3¼)	2.0 (¾)	4.5 (1¾)	12.5 (5)	11.5 (4.5)
Fresh air content (vol %)	6.0	1.3	1.5	6.8	6.8
7-day strength* (MPa)	21.5	24.0	25.2	19.8	22.7
28-day strength* (MPa)	30.3	35.4	35.6	27.7	31.6
56-day strength* (MPa)	32.0	36.9	37.4	32.6	33.0
Hardened air content (vol %)	7.2	2.2	3.1	8.5	8.1
Air spacing factor (mm)	0.17	0.52	0.37	0.13	0.10

* The coefficient of variation of strength measurements was 4.0% based on three 100×200mm concrete cylinders tested for each mixture at a given age.

4.3.2. Bulk Chemistry and Mineralogy

The chemical requirements of ASTM C618, limit the sum of oxides SiO_2 + Al_2O_3 + Fe_2O_3 to 70% and 50% by mass for class F and class C fly ash, respectively. It can be seen from the XRF results (**Table 4-5**) that the anthracite fly ash satisfies the requirements for class F fly ash, while the bituminous fly ash is more similar to a class C fly ash. This is also reflected in the low CaO content of the anthracite vs. the bituminous fly ash. Since the bituminous coal has higher sulfur content, it requires a larger proportion of limestone to be added to CFBC boiler to capture SO_x emissions. This leads to a higher CaO content of the resulting fly ash.

Both fly ashes show CaO<18% and Na_2O_{eq}<3.0, suggesting that they may be suitable for mitigating ASR according to ASTM C1778-16. This is later verified using ASTM C1567 testing.

To ensure volumetric stability, and in addition to the soundness criteria, ASTM C618 limits the SO_3 content of fly ash to 5%. While the anthracite fly ash meets this criteria, the bituminous CFBC fly ash contains 9.83% SO_3 (per XRF) and 11.6% SO_3 (per Leco/IR); this may result in a deleterious expansion due to ettringite formation. This risk is further evaluated using the autogenous shrinkage/expansion results presented below.

The XRD patterns and Rietveld quantification results are presented in **Figure 4-2** and **Figure 4-3** Both fly ashes show amorphous contents close to ~50%; this is smaller than the typical glass content of PC fly ash (>75% [142]). This was anticipated given the lower combustion temperature of FBC boilers (<900ºC) versus the conventional PC boilers (<1750 ºC). Other reactive phases include anhydrite and free lime. Also, the clay phases (talc and muscovite) are potentially reactive, depending on their degree of calcination. As such, the sum of reactive and potentially reactive phases is 74.5% for the anthracite fly ash, and 78.5% for the bituminous fly ash. This is more in line with the reactive glass content of PC fly ash. Quartz and hematite phases are non-reactive. Another notable observation is the higher quantity of anhydrite and free lime in the bituminous fly ash, which agrees with its higher CaO and SO_3 contents (**Table 4-5**). Previous literature have also reported quartz, anhydrite, free lime or calcite as the main phases detected in FBC fly ash [20], [63], [146], [51], [147].

The batch leaching results are provided in **Figure 4-4**, and lead to the following observations: (1) Both fly ashes bind Ca out of the solution, as a result of pozzolanic reaction and possibly formation of AFt and AFm phases. The anthracite fly ash removes Ca faster, which agrees with its lower CaO content. (2) Both fly ashes remove a considerable quantity of alkalis from the solution, even in the absence of solid portlandite to allow a significant degree of pozzolanic reaction. This feature can be beneficial in mitigating ASR. (3) The anthracite fly ash is a significant source of Al, likely originating from the clay phases. The bituminous fly ash is also a source of Al, but to a lesser degree. The soluble Al content of the fly ashes can provide ASR mitigation benefits [148] and can also promote formation of C-A-S-H, AFt, and AFm phases. (4) Silicon concentrations (not shown) exhibited a similar trend as Al, with the anthracite fly ash releasing up to 185ppm Si by 7 days, followed by the bituminous fly ash and the Portland cement, showing [Si]=27ppm and 5.7ppm at 7 days, respectively. (5) The bituminous fly ash release a significant concentration of S into the solution, in agreement with its high SO_3 and anhydrite contents. This may increase the risk of volumetric instability as a result of ettringite formation. The sulfur

58

contents in **Figure 4-4d** decline over time, potentially due to precipitation of sulfur-bearing AFt and AFm phases.

1 Zincite [ZnO]		6 Anhydrite [$CaSO_4$]	2.9%
2 Quartz [SiO_2]	22.5%	7 Lime [CaO]	1.0%
3 Muscovite [$K_{0.8}Na_{0.2}Fe_{0.05}Al_{2.95}Si_{3.1}O_{10}(OH)_2$]	14.5%	Amorphous + others	50%
4 Talc [$Mg_3Si_4O_{10}(OH)_2$]	6.1%		
5 Hematite [Fe_2O_3]	3.0%		
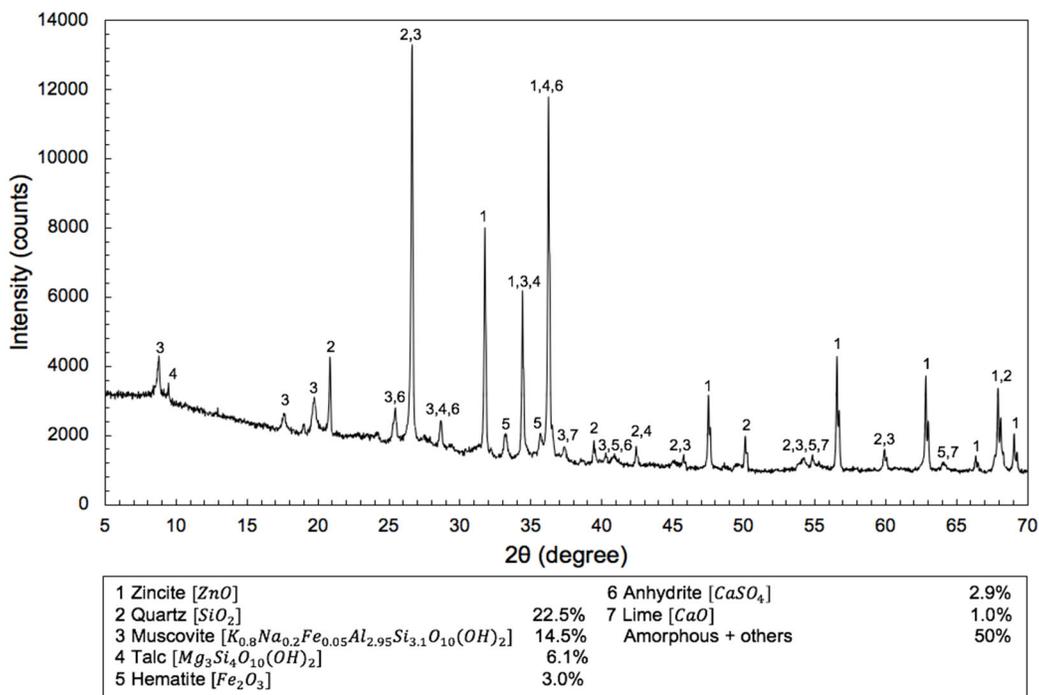
Figure 4-2. Quantitative XRD of the anthracite fly ash

1 Zincite [ZnO]		6 Lime [CaO]	2.7%
2 Quartz [SiO_2]	16.4%	Amorphous + others	48.8%
3 Muscovite [$K_{0.8}Na_{0.2}Fe_{0.05}Al_{2.95}Si_{3.1}O_{10}(OH)_2$]	15.3%		
4 Anhydrite [$CaSO_4$]	11.7%		
5 Hematite [Fe_2O_3]	4.3%		
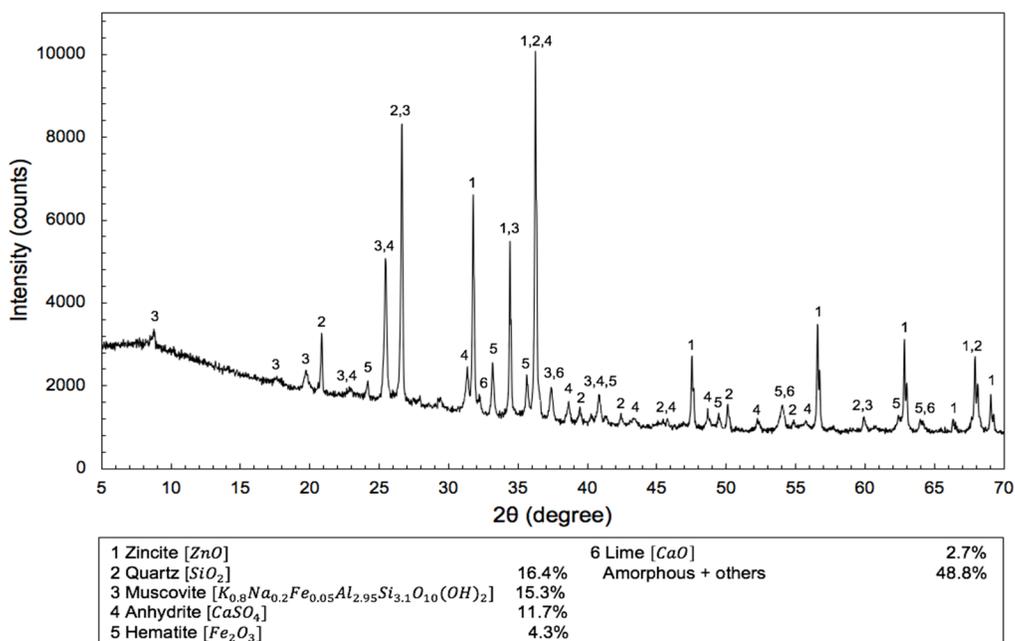
Figure 4-3. Quantitative XRD of the bituminous fly ash
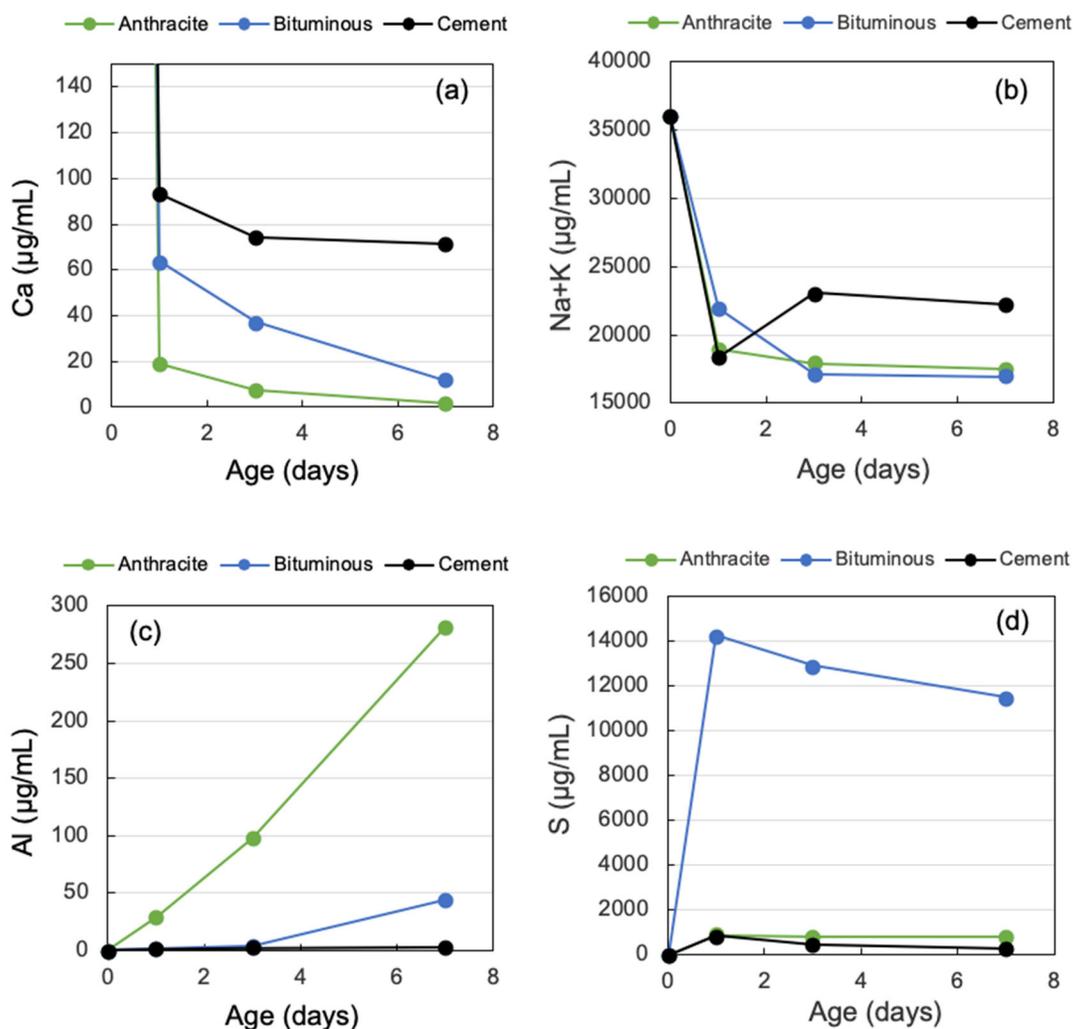
Figure 4-4. The batch leaching results showing the concentrations of major elements in synthetic concrete pore solution

4.3.3. Pozzolanic Reactivity

The water requirement of both fly ashes was measured as 109.5% (**Table 4-4**). This is larger than ASTM C618-19 limit for PC fly ash (105%), but smaller than the limit for natural pozzolans (115%). The elevated water requirement is in agreement with the sub-angular shape and the internal porosity of CFBC fly ashes (**Figure 4-1**).

The strength activity index (SAI) of the two fly ashes are shown in **Figure 4-5**. The results at 7, 28, and 56 days of age are within the range 86% to 104%, which meet the ASTM C618 minimum requirement of 75%. The anthracite fly ash shows a slightly higher SAI than the bituminous fly ash. It is interesting to note a declining trend in the SAI results with age. It should

also be noted that due to their 109.5% water requirement, the fly ash SAI mortars had a higher w/cm (=0.53) in comparison with the control mortar (100% cement) having w/cm=0.484. This higher w/cm puts the fly ash mortars at a disadvantage with respect to strength development and results in lowering their SAI values. Literature on SAI confirms that FBC fly ash can comply with the requirements of class F fly ash [20] [65], and that the higher dosage of water required for FBC mixes adversely affects their strength [50].
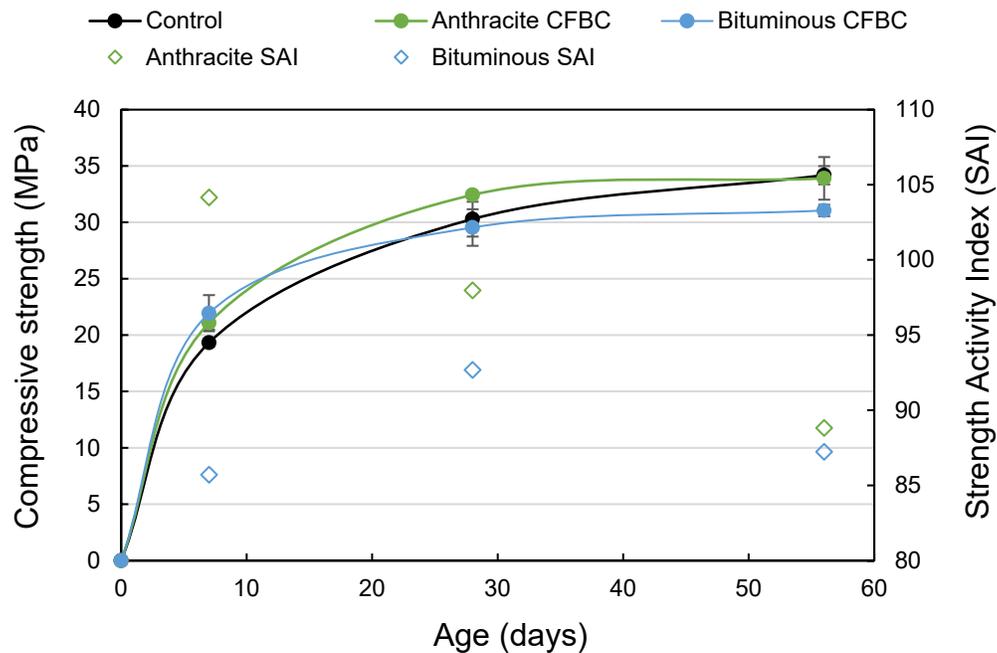
Figure 4-5. The strength activity index of CFBC fly ashes and the compressive strength of mortars containing 20% CFBC fly ash as a function of age

To exclude the effect of variable w/cm, a second set of test mortars were prepared at the same w/cm=0.484 of the control mortar and with addition of superplasticizer to maintain a similar flow in the control and test mortars (~88%). The cube compressive strength results of these mortars are also presented in **Figure 4-5**. The three mixtures generally showed similar strength values at 7, 28, and 56 days. However, mortars containing 20% CFBC fly ash had a slightly better strength than the control at 7 days, but this advantage diminished with age as the control mortar gained better strength over time. This may be due to the use of superplasticizer in the test mortars that gave them a head-start in strength development versus the control mortar that did not contain a superplasticizer.

The results of the lime-pozzolan mortar strength (ASTM C593-06) are reported in **Table 4-1**. They show a substantially better strength for the mortar containing the bituminous fly ash, and this may be due to a lower w/b or higher reactivity of the bituminous fly ash; e.g., a higher amount of ettringite may form due to a substantially higher anhydrite content in the bituminous CFBC fly ash. It is interesting to note a slight strength reduction between 7 and 28 days in both mortars, which may indicate that some porosity-forming reactions occur after 7 days. But, it should also be born in mind that the samples were steam cured for the first 7 days at 54°C and afterwards, they were moist cured at 23°C and 95% RH. As such, possible changes in the moisture content of the samples may be responsible for the observed strength retrogression.

The 7-day bound water content of the lime-fly ash pastes per RILEM TC TRM267 method was measured as 0.0234g (2.34%) and 0.0336g (3.36%) per gram of dried paste for the anthracite and bituminous fly ashes, respectively. The higher bound water content in the bituminous fly ash may indicate a greater reactivity, but this may be primarily a result of ettringite formation due to the larger SO_3 content of this fly ash. The portlandite consumption over time in these pastes was measured by TGA and the results are presented in **Figure 4-6**. Both fly ashes show similar degree of pozzolanic reactivity at 28 days, with slightly higher $Ca(OH)_2$ consumption by the anthracite fly ash at 1 and 7 days. At 28 days, each fly ash consumed 0.74g $Ca(OH)_2$ per gram fly ash. Increasing the amount of FBC fly ash has been shown in the literature to increase the $Ca(OH)_2$ consumption due to a pozzolanic reaction. Glinicki et al. [63] reported a reduction in $Ca(OH)_2$ content from 1.2% to 0.4% by mass after increasing the FBC fly ash replacement level from 20% to 40%.

4.3.4. Performance of CFBC Fly Ash in Mortar and Concrete

Table 4-6 shows the fresh and hardened properties of concretes containing 20% CFBC fly ash and compares these with the properties of the control (100% cement) mixture. Set 1 fly ash mixtures had the same AEA dosage as the control and had no WRA. In these mixtures, the replacement of Portland cement with CFBC fly ash resulted in a reduction of slump and fresh and hardened air content of concrete. The air content reduction can be linked to the elevated LOI of the fly ashes; the anthracite fly ash had a higher LOI and resulted in a lower air content. This indicates that LOI reduction of these fly ashes may be beneficial for their practical application. The slump reduction is likely due to joint effects of elevated LOI and water demand of CFBC fly ashes. On the other

hand, the 7, 28, and 56-day compressive strengths of set 1 mixtures containing CFBC fly ash were greater than the control by approximately 18%. Most of this strength improvement is likely attributed to the lower air content of the fly ash mixtures. According to the literature, each percentage point of additional air content results on average in approximately 5.5% loss of compressive strength [149][150].
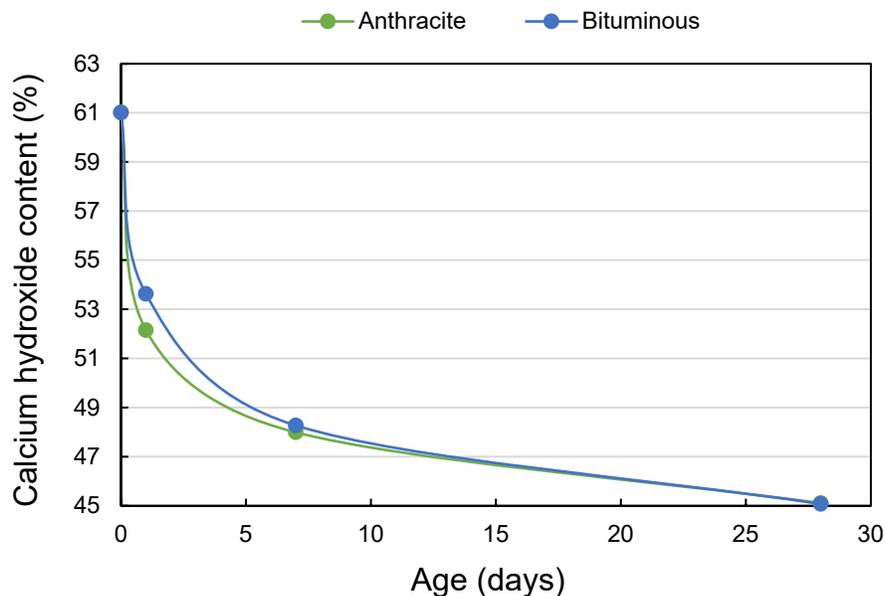
Figure 4-6. Calcium hydroxide content of lime-fly ash pastes per RILEM TC TRM 267 method

Set 2 concrete mixtures containing 20% CFBC fly ash were prepared by adding sufficient dosages of WRA and AEA to achieve a similar/target slump and air content to those of the control mixture. These mixtures produced compressive strength values comparable to those of the control (100% cement) mixture at 7, 28, and 56 days of age, despite having a slightly (~1%) air content in the fly ash mixtures. The hardened air void spacing factor for the control and set 2 fly ash concretes was less than 0.203 mm which is maximum allowable limit by ASTM C457-16 to provide acceptable freeze-thaw durability. Both fly ash concretes showed a smaller spacing factor than the control, and this is advantageous.

The autogenous shrinkage/expansion results (**Figure 4-7**) show a small (<60µε) initial expansion at 1 day for the control and the anthracite fly ash mortars. The mortar containing the bituminous fly ash, however, exhibits a larger expansion, up to 247 µε at 3 days. This is likely due

to early-age ettringite formation in this mixture. All three mortars subsequently shrank as a result of chemical shrinkage. This autogenous shrinkage was slightly larger in mortars containing CFBC fly ash. Throughout this test, the magnitude of expansion and contraction remained below the tensile strain capacity of concrete (~400 $\mu\varepsilon$). This may suggest that the higher SO_3 content in the bituminous CFBC fly ash does not pose a serious risk of volumetric instability. If anything, the bituminous fly ash acts as a shrinkage compensating additive. Although these results are promising, it is advisable to monitor the volume stability of mortar or concrete containing CFBC fly ash over a long term and in exposure to moisture, e.g., via ASTM C1038 test, to more confidently rule out the risk of volume instability.

The accelerated mortar bar test (ASTM C1567) ASR results are shown in **Figure 4-8**. All mortars contained a borderline moderately/highly reactive aggregate (R1/R2). Replacement of 20% cement with CFBC fly ash reduced the 14-day ASR expansion from 0.30% in the control mixture, to 0.21% and 0.26% in mortars containing the anthracite and bituminous fly ashes, respectively. However, these expansions are still above the ASTM failure threshold of 0.1%. The use of 30% anthracite fly ash and 40% bituminous fly ash was successful in mitigating the ASR. A higher efficiency of the anthracite fly ash is in agreement with its lower CaO and higher $SiO_2+Al_2O_3$ contents in comparison with the bituminous fly ash. Longer term ASR testing (e.g., ASTM C1293) is recommended.
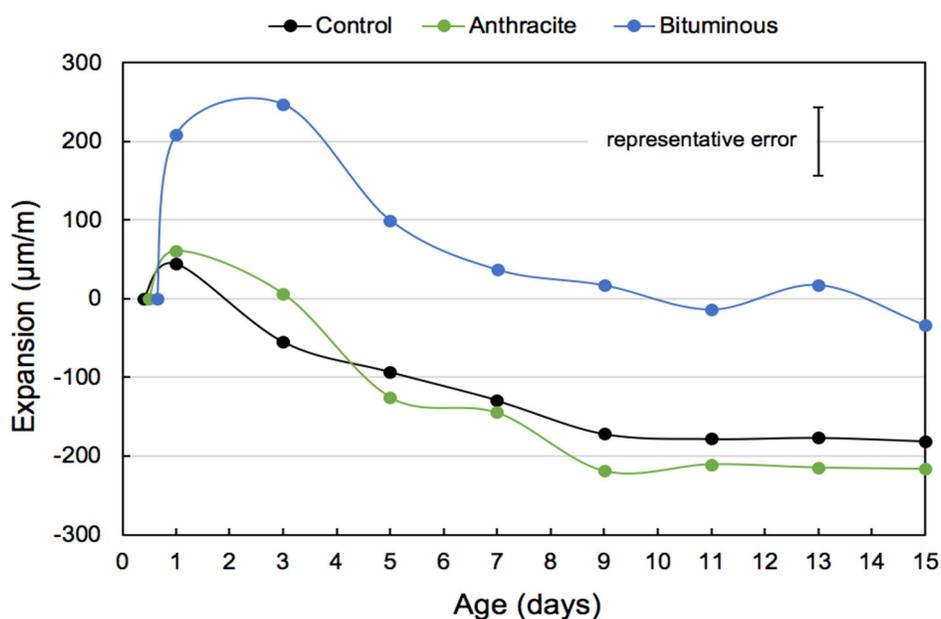
Figure 4-7. Autogenous shrinkage of mortar samples (zeroed at the time of final setting)
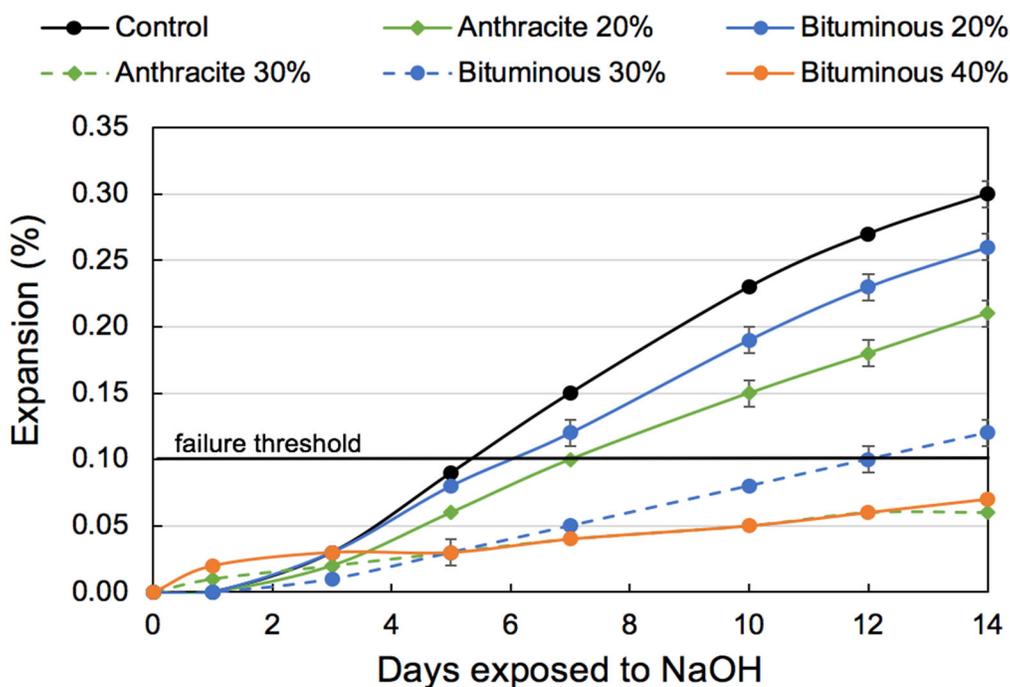
Figure 4-8. ASR induced expansion of mortar samples in ASTM C1567 test

4.4. Conclusions

Based on the experimental results reported in this chapter, the following conclusions are drawn:

- FBC fly ash results from burning coal at 750 to 900 ºC. This lower combustion temperature, in comparison with conventional PC boilers, results in an FBC fly ash with similar chemistry but different mineralogy than the conventional PC fly ash. In addition, FBC fly ash particles are sub-angular in shape and contain internal porosity as they don't melt during the combustion process.

- According to X-ray diffraction, the two CFBC fly ashes studied contained reactive phases (thermally-altered clays, anhydrite, free lime) and inert phases (quartz and hematite). The reactive phases made up 74.5% and 78.5% of the mass of the fly ashes. The presence of anhydrite is a notable difference with conventional fly ashes and is a result of internal SO_x scrubbing in FBC boilers via injection of pulverized limestone.

- Both CFBC fly ashes met the physical and chemical requirements of ASTM C618-19, except for a borderline high LOI in both fly ashes and high SO_3% in the bituminous fly ash. The high SO_3 content did not produce a deleterious volume instability during an autogenous expansion test.

- The CFBC fly ashes exhibited good reactivity and strength development in mortar and concrete with a strength activity index of 86% or better at 7 days and 93% or better at 28 days. The compressive strength of mortars and concrete containing 20% CFBC fly ash was similar to the control mixtures at 7, 28, and 56 days.

- Concrete mixtures containing 20% CFBC fly ash and with proper dosing of water reducing and air entraining admixtures could achieve desirable slump and fresh and hardened air contents. These mixtures produced a similar compressive strength to that of the control mixture as early as 7 days of age.

- Both fly ashes could mitigate ASR, with the anthracite fly ash being more effective due to its lower CaO and higher Al_2O_3 and SiO_2 contents.

- Overall, these fly ashes may be used as a beneficial pozzolan in concrete mixtures in their present form. LOI reduction may be considered as a worthwhile beneficiation. Further research is needed to evaluate the consistency of the FBC fly ash properties from a given resource, to identify the reaction products of FBC fly ash in concrete, and to assess the impact of such fly ashes on other properties and durability of concrete mixtures. This latter item is studied in Chapter 5.

Chapter 5

Performance and Durability of Concrete Containing
Fluidized Bed Combustion (FBC) Fly Ash

5.1. Introduction

Earlier studies on the use of FBC fly ash as concrete pozzolan have been mainly limited to its effect on the mechanical properties of concrete. Very little is known with regards to the durability performance of concrete mixtures containing FBC fly ash. To supplement the existing literature, in this chapter, two CFBC fly ashes are examined for their impact on concrete performance. These fly ashes were a byproduct of combustion of anthracite or bituminous waste coals. These fly ashes were used as partial replacement of portland cement in a typical pavement-grade concrete mixture, and their impact on the concrete performance was investigated. Concrete mixtures were evaluated for their fresh properties (slump, fresh air content, and setting time), and hardened properties (compressive strength, hardened air structure, rapid chloride ion penetration, and water sorptivity). In addition, equivalent mortar mixtures were prepared and tested for their resistance to sulfate attack and drying shrinkage. Concrete performance was later related to microstructural features such as pore size distribution and the formation factor.

5.2. Materials and Methods

5.2.1. Materials

Two CFBC fly ashes were acquired from power plants in Pennsylvania, USA. One power plant burns an anthracite refuse coal (low CaO and SO_3) while the other burns a bituminous refuse coal (higher CaO and SO_3). A complete ASTM C618 characterization of the fly ashes was performed in an earlier study [151]. The bulk chemistry (using X-ray fluorescence analysis of fused glass beads), fineness (ASTM C430-17), density (using helium pycnometry), particle size distribution (using laser diffraction), loss on ignition (ASTM C311-17), carbon content (using infrared LECO analyzer), water requirement (ASTM C311-17), strength activity index at 7 and 28 days (ASTM C311-17), and soundness (ASTM C151-18) of the two fly ashes were measured and are reported in **Table 5-1.** The relevant properties of a type I/II Portland cement that was used in this work are also provided. To achieve proper fineness, the anthracite CFBC fly ash was screened through a

#140 sieve (0.105 mm) and the passing portion was used in all tests. The bituminous CFBC fly ash was tested as received.

Table 5-1–Chemical composition and physical properties of the Portland cement and the fly ashes

Parameter	Unit	Portland cement	Anthracite CFBC fly ash	Bituminous CFBC fly ash
Bulk Chemistry				
SiO_2	%wt	19.12	50.10	37.64
Al_2O_3		5.11	22.54	16.88
Fe_2O_3		3.98	7.66	9.91
$SiO_2 + Al_2O_3 + Fe_2O_3$		28.21	80.30	64.43
CaO		60.58	5.06	15.39
SO_3		3.21	2.39	9.83
K_2O		0.89	2.90	2.09
Na_2O		0.35	0.35	0.24
Na_2O_{eq}		0.94	2.26	1.62
TiO_2		<detection	1.34	0.91
MgO		2.89	0.75	1.29
P_2O_5		<detection	0.14	0.13
CO_2		1.25	not measured	not measured
LOI @ 750ºC		2.13	6.65	5.21
Carbon using Leco/IR		not measured	6.26	3.80
Physical Properties				
Density	g/cm^3	3.17	2.61	2.63
Particle size, D10	μm	not measured	2.95	3.42
Particle size, D50			28.7	26.1
Particle size, D90			128.0	102.5
Fineness (>#325 sieve)	%wt	not measured	25.5	27.5
Blaine fineness	m^2/kg	400	not measured	not measured
Water requirement	%	100.0	109.0	108.9
SAI at 7 days	%	100.0	103.6	85.0
SAI at 28 days	%	100.0	99.2	91.2
Soundness	%	0.07	-0.02	-0.03

In terms of mineralogy, quantitative X-ray diffraction (XRD) was performed, whose results are provided in **Figure 4-2** and **Figure 4-3**. Both fly ashes contained approximately 50% amorphous fraction. Other reactive phases included anhydrite, free lime, and partially-calcined clays (talc and muscovite). The sum of all reactive phases was 74.5% and 78.5% of the mass of the anthracite and bituminous CFBC fly ashes, respectively. The non-reactive phases were quartz and hematite.

Concrete mixtures were designed using proportions that are typically used for formed pavement applications in Pennsylvania. They were prepared with w/cm=0.47 using a type I/II Portland cement, natural sand (SSD specific gravity of 2.62, absorption capacity of 1.66%, fineness modulus of 2.94), and ASTM C33-18 #57 crushed stone (SSD specific gravity of 2.70, absorption capacity of 0.44%, dry rodded unit weight of 1476.4 kg/m^3). In the test mixtures, 20% of the Portland cement was replaced with either the anthracite or the bituminous CFBC fly ash. Sufficient dosages of an air-entraining admixture (AEA MasterAir AE90 by BASF) and a water-reducing admixture (WRA Master Glenium 7620 by BASF) were added to obtain a slump of 10±2.5cm and air content of 6±1%. Concrete mixture proportions are provided in **Table 5-2**. It is observed that mixtures containing CFBC fly ash needed WRA to achieve the target slump and air.

Table 5-2. Mixture designs to evaluate the effect of CFBC fly ashes on concrete properties

Mixture	Cement	Fly ash	Water	Coarse agg.	Fine agg.	AEA	WRA
	Kg/m^3 of concrete						
Control (100% PC)	362	-	170	1098	643	0.47	0
20% Ant. CFBC	290	72	170	1098	639	0.94	1.40
20% Bit. CFBC	290	72	170	1098	640	0.47	0.88

5.2.2. Test Methods

The performance of CFBC fly ashes in the above concrete mixtures was evaluated by measuring the concretes' fresh, hardened, and durability properties. These included slump (ASTM C143-15a), fresh air content (ASTM C231-17a), setting time (ASTM C403-16), compressive strength (ASTM C39-18), hardened air structure (ASTM C457-16), rapid chloride ion penetration (ASTM C1202-18), and water sorptivity (ASTM C1585-13). In addition, the drying shrinkage (ASTM C157-17), volume expansion under water (ASTM C1038−14b), and resistance to sulfate attack (ASTM C1012-18a) of equivalent mortar mixtures was evaluated.

For each concrete mixture, 12 cylinders (diameter of 100 mm and height of 200 mm) were cast and moist cured at 23ºC and 100% RH. These were used for compressive strength testing at 7, 28, and 56 days of age, rapid chloride penetrability (RCPT) at 56 days, water sorptivity at 74 days, and hardened air analysis at 28 days. The remaining fresh concrete was wet sieved through No. 4 sieve, poured into capped plastic molds (diameter of 150 mm and height of 150 mm), and used for measuring the initial and final setting time of concrete at various curing temperatures (14ºC, 23ºC, and 36ºC) according to ASTM C403-16 method. Three duplicate samples were

measured for the setting time test. The setting time test was of interest to determine if the elevated SO_3 in the bituminous CFBC fly ash causes set irregularities. Additionally, the setting time of paste mixtures with normal consistency and 20% replacement of cement with CFBC fly ash was measured using the Vicat method (ASTM C191-19).

After 28 days of hydration, a 100×120×10 mm section was cut from each concrete cylinder (perpendicular to the finished surface) and lapped using 75, 35, 17.5 and 12.5 μm grit sizes (No.220, 320, 600, and 800, respectively). Black marker and $BaSO_4$ powder were used to enhance surface contrast, resulting in a black surface with white air voids. The RapidAir 457 automated imaging system was used to analyze the air void distribution of the hardened concrete (ASTM C457-16). The volume fraction of air voids (vol%) and their spacing factor (mm), among other parameters, were determined in the hardened concrete. This analysis was conducted on one sample per concrete mixture.

The rapid chloride penetrability test (RCPT) was used to monitor the quantity of electrical charge passed through 50 mm thick concrete slices, during a 6-hour period. For this purpose, three disk samples (diameter of 100 mm and height of 50 mm) were cut from each 56-day concrete cylinder, coated on the sides with epoxy and vacuum-saturated according to the procedure described in ASTM C1202-18. During testing, a potential difference of 60 V was maintained across the two ends of the disks, one side in contact with 3% NaCl and the other with a 0.3N NaOH solution. The total charge passed in coulombs was measured as an indicator of the sample resistance to chloride ion penetration. The electrical resistivity of concrete was also calculated using Ohm's law, based on the current passed through each sample after 1 min of initiating the RCPT testing. These resistivity values were used in combination with the pore solution resistivity values (obtained by extraction the pore solutions as described below) to determine the formation factor (F) of each concrete. Formation factor is a measure of concrete's transport properties and is calculated as the ratio of the electrical resistivity of concrete to the electrical resistivity of the pore solution [152]. The formation factor for each mixture was measured using three duplicate samples and the average values are reported.

Similarly, three disk samples (diameter of 100 mm and height of 50 mm) were cut from each 56-day concrete cylinder and used to measure the rate of water absorption by capillary suction (ASTM C1585-13). Prior to testing, the samples were vacuum-saturated, maintained at 50°C and 80% RH for 3 days, and subsequently stored in separate sealable containers at 23°C for 15 days.

All surfaces except that exposed to water were sealed and the samples were placed over water (water level was 1-3 mm above the bottom of the sample), to measure the amount of mass gain after 1, 5, 10, 20, 30, and 60 min and at specified intervals up to 7 days.

To relate concrete properties to its microstructural features such as pore size distribution and pore fluid conductivity, equivalent paste samples with w/cm=0.47 (diameter of 20 mm and height of 40 mm) were cast and moist cured (at 23°C and 100% RH) for 56 days. Two replicates were tested for each mixture. Pore size distribution was measured using mercury intrusion porosimetry (MIP). For this purpose, two small pieces (approximately 1.5 cm diameter and 1.5 cm length) were cut from the center of one paste cylinder, solvent exchanged in 99.8% isopropanol for 14 days (with specimen to solvent volume ratio of 1:100), air dried in a desiccator for 24 hours, and then vacuumed dried for another 24 hours. This method has been recommended to preserve the pore structure of the hydrated cement paste [153].

The remaining paste samples were used for pore fluid extraction and analysis. The pore fluid extraction setup was used to apply an axial force (rate of 133 to 178 kN/min) to the paste sample inside a confined space, creating high tri-axial pressures that squeezed out the pore fluid. The fluid was filtered through a 0.45-μm polypropylene filter. Inductively coupled plasma - atomic emission spectroscopy (ICP-AES) was conducted on the extracted pore fluids to measure their concentrations of Na, K, Ca, and S ion species. Stoichiometry was used to calculate the concentration of sulfates (SO_4^{2-}), while titration with hydrochloric acid was applied to measure the concentration of OH^-. The model developed by Snyder et al. [154] and the step wise procedure provided by Chang et. al [152] were used to calculate the electrical resistivity (or conductivity) of the pore solution and subsequently the formation factor of concrete as described above.

Finally, a set of mortar mixtures were prepared and tested to evaluate the impact of CFBC fly ashes on volume stability and sulfate resistance of concrete. These performance parameters were of interest especially in light of the elevated SO_3 content in the bituminous fly ash. The mortars were prepared with sand/cm=2.75. A w/c=0.485 was used for the control mixture while w/cm=0.53 was needed for the mortars containing fly ash to achieve a flow of within ±5% of the control as required by the pertinent ASTM standards referenced below. To monitor the early expansion of mortars as a result of ettringite formation, four mortar prisms (285×25×25 mm) were prepared and tested in accordance with ASTM C1038−14b. The prisms were demolded after 23 h of moist curing, initial gauge readings were taken, and they were subsequently placed in a saturated

lime water bath at 23°C. The length change of each prism was measured after 14 days of storage in the lime bath. The measured expansion was compared against ASTM C1157-17 limit of 0.020%.

Mortar samples were also tested for expansion when exposed to a sulfate solution according to ASTM C1012-18a. Six mortar prims and nine cubes were cast and stored over water in a tightly secured container at 35°C. After 24 h, the samples were demolded and cured in lime water until reaching a cube compressive strength of 20 MPa. Once the required strength was obtained, initial comparator readings were taken from the prisms, and they were stored in a 50 g/L Na_2SO_4 solution. Prisms were removed from the solution for length measurements at 1, 2, 3, 4, 8, 13, 16, and 24 weeks, after which the solution was exchanged to maintain a pH level of 7±1. The volume expansion at 6 months was compared to the optional physical requirements set by ASTM C618-19 Procedure A.

Similar mortar samples were prepared and used for drying shrinkage measurements according to ASTM C157-17. For each mortar, four prims were cast and moist cured for 24 h, after which they were demolded and placed in a saturated lime water bath for 6 days. At the age of 7 days, initial comparator readings were taken, and the samples were moved to a 50%RH and 23°C environmental chamber for drying. Mass and length measurements were taken up to 150 days. The 28-day drying shrinkage of samples was compared to the optional physical requirements of ASTM C618-19. In all measurements, a comparator with accuracy of 0.0025mm and a balance with accuracy of 0.1g were used.

5.3. Results and Discussion

Table 5-3 shows selected fresh and hardened properties of concretes containing 20% CFBC fly ash and compares these with the properties of the control (100% Portland cement) mixture. Fly ash mixtures produced comparable slump and fresh and hardened air content, although they needed the water reducing admixture (WRA), and in one case, a higher dosage of the air entraining admixture (AEA) to achieve these properties. It is noted that both fly ashes had elevated loss-on-ignition (**Table 5-1**). The hardened air spacing factor for all three mixtures was in the range 0.1 to 0.2 mm, which complies with recommendations of ASTM C457-16 for acceptable freeze-thaw durability. Both fly ash concretes showed a smaller spacing factor than the control concrete, and this is advantageous.

Table 5-3. Effect of CFBC fly ash on selected properties of concrete

Properties	Control (100% PC)	20% Ant. CFBC	20% Bit. CFBC
Slump (mm)	83 (3¼ in)	127 (5 in)	114 (4.5 in)
Fresh air content (vol %)	6.0	6.8	6.8
Hardened air content (vol %)	7.2	8.5	8.1
Air spacing factor (mm)	0.17	0.13	0.10
Chloride ion penetration at 56-days (coulombs)	3024	1291	1679
Concrete resistivity at 56-days (Ωm)	83	178	134
Formation factor at 56-days	446	620	466
Initial sorptivity at 56-days (mm/s$^{0.5}$)	15.3	15.8	9.2
Secondary sorptivity at 56-days (mm/s$^{0.5}$)	7.4	9.1	5.8

The compressive strength versus age of the three concrete mixtures is depicted in **Figure 5-1**. The fly ash mixtures produced compressive strength values that were comparable to those of the control mixture at 7, 28, and 56 days, despite having a slightly higher (~1%) air content. Interestingly, the strength of the concrete containing the anthracite fly ash shows an upward trend at 56 days while the other mixtures have plateaued. It is possible that the use of WRA in the fly ash mixtures have contributed to their desirable strength development. It is also worth noting that the strength activity index for the anthracite fly ash was in the neighborhood of 100% while that for the bituminous fly ash was closer to 90%.
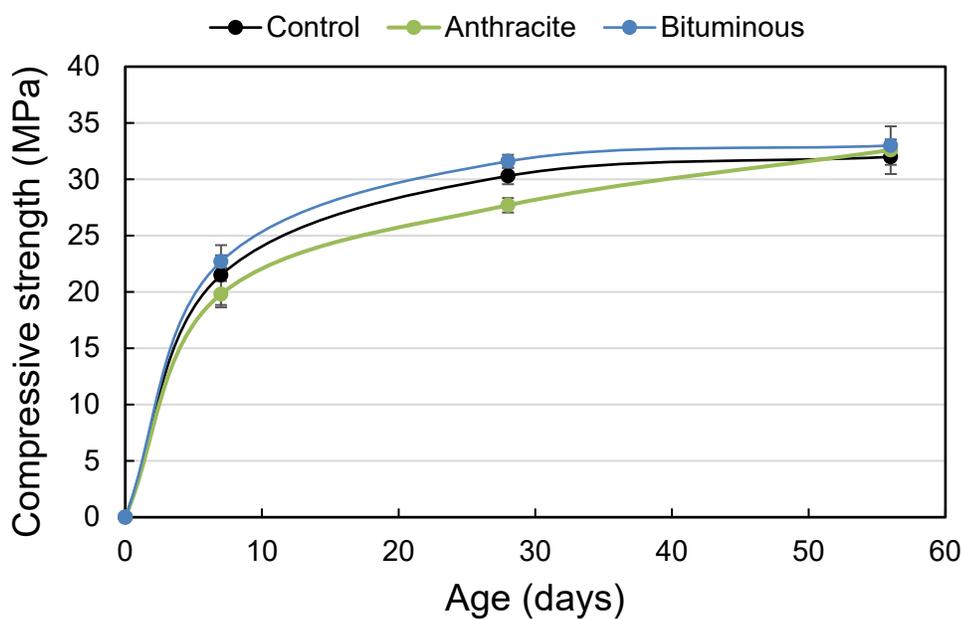
Figure 5-1. Compressive strength of concrete cylinders after 7, 28, and 56 days of hydration

Results for the setting time of concrete (ASTM C403) is provided in **Table 5-4**. As anticipated, the setting times increased with reducing the curing temperature. Replacement of cement with CFBC fly ash also delayed the setting time compared to the control mixture at all curing temperatures. This is likely associated with the slower reactivity of the fly ashes compared to Portland cement, and is common even in concretes containing conventional fly ash [155]. Between the CFBC fly ashes, the bituminous fly ash showed further delays in setting, in agreement with its smaller strength activity index (**Table 5-1**). In addition, the high content of anhydrite (11.7%wt. per QXRD) in this fly ash may have affected its setting performance. Similar to gypsum, anhydrate can retard the hydration of C_3A by supplying sulfate ions to the pore solution [156]. In a previous study [157], the initial setting time of cement pastes incorporating 30% CFBC fly ash was reported to double as the SO_3 content of the fly ash increased from 1.26% to 10.67%. At the same time, gypsum (and likely anhydrite) is known to accelerate the hydration of C_3S [158], and as such, sulfate optimization of concretes containing CFBC fly ash may be necessary given that these fly ashes also contribute soluble alumina to the system. This is recommended as a future study. A similar setting behavior was observed for paste samples with normal consistency (**Table 5-5**); i.e., pastes with CFBC fly ash set later than the control, with the bituminous CFBC fly ash showing the latest setting time.

Table 5-4. Initial and final setting time of concrete as a function of curing temperature

Curing temperature	14°C	23°C	36°C	14°C	23°C	36°C
Mixture	Initial setting (min)			Final setting (min)		
Control (100% PC)	420	355	250	560	480	315
20% Ant. CFBC	560	450	290	785	620	370
20% Bit. CFBC	670	545	340	905	700	425

Table 5-5. Initial and final setting time of pastes at normal consistency

Mixture	Normal consistency		
	w/cm	Initial setting (min)	Final setting (min)
Control (100% PC)	0.265	160	300
20% Ant. CFBC	0.310	200	340
20% Bit. CFBC	0.285	240	380

The rapid chloride penetrability test (RCPT) results can be found in **Table 5-3**, which show a significant reduction in the total charge passed through 56-day concrete samples, by substitution of 20%wt. of Portland cement with CFBC fly ash. Similarly, the bulk resistivity of concrete

improved from 83 Ωm for the control mixture to 178 and 134 Ωm for concretes with the anthracite and bituminous fly ash, respectively. Based on the measured coulomb and concrete resistivity values, and according to ASTM C1202-18 and AASHTO PP 84-19 guidelines, the control mixture demonstrated 'moderate' chloride ion penetrability (2000~4000 col. or 50~100 Ωm), whilst mixtures with CFBC fly ash can be classified with 'low' permeability (1000~2000 col. or 100~200 Ωm). The increased concrete resistivity and the reduced charge passed (coulombs) in concretes containing fly ash are partly due to tightening of the pore structure of concrete and partly due to reduction of the pore solution ionic strength and conductivity as a result of the pozzolanic reaction of the fly ash. The resistivity of concrete has been shown to be proportional to the resistivity of the pore solution, the total porosity, and the pore connectivity [159] [160].

To decouple these effects, the resistivity of pore solution was determined by extracting the pore solution of equivalent cement pastes at the same age and w/cm. The extracted solutions were analyzed using ICP-AES and the results were used in combination with the model by Snyder et al. [154] and Chang et. al [152] to calculate the pore solution resistivity. The results are provided in **Table 5-6**, suggesting a reduction in the ionic strength and increase in the resistivity of pore solution in mixtures containing fly ash. These results were further used to calculate the saturated formation factor (F), which is inversely related to the product of the porosity and the connectivity of the pore network for each concrete. The reported 56-day formation factors (**Table 5-3**) suggest a considerable improvement of the transport properties of concrete containing the anthracite fly ash while the concrete containing the bituminous fly ash showed a modest improvement compared to the control mixture.

Table 5-6. Calculation of pore solution resistivity using model developed by Snyder et al. [154]

Mixture	K^+ (mol/L)	Na^+ (mol/L)	Ca^{2+} (mol/L)	SO_4^{2-} (mol/L)	$Al(OH)_4^-$ (mmol/L)	OH^- (mol/L)	pH	Resistivity (Ωm)
Control (100% PC)	0.151	0.090	0.002	0.004	0.029	0.252	13.40	0.187
20% Ant. CFBC	0.096	0.059	0.001	0.003	0.062	0.157	13.20	0.287
20% Bit. CFBC	0.098	0.057	0.002	0.002	0.054	0.157	13.20	0.287

The improvements in the formation factor of the concrete containing fly ash are corroborated with pore structure refinement as evaluate by mercury porosimetry (MIP) testing of equivalent paste samples at the same age (56 days). These results are provided in **Figure 5-2** and

Table 5-7, which also report the critical pore diameter (i.e., the inflection point of each pore size distribution curve), the threshold diameter (i.e., the minimum diameter of pores that form a continuous network of chennels throughout the cement paste), and the total porosity [161]. The results show that although the total porosity of the cement paste remained unchanged, a significant reduction of both the critical and the threshold pore diameters are observed as a result of partial replacement of cement with fly ash. Such pore refinements reduce mass transport within fly ash concretes and improves their durability.
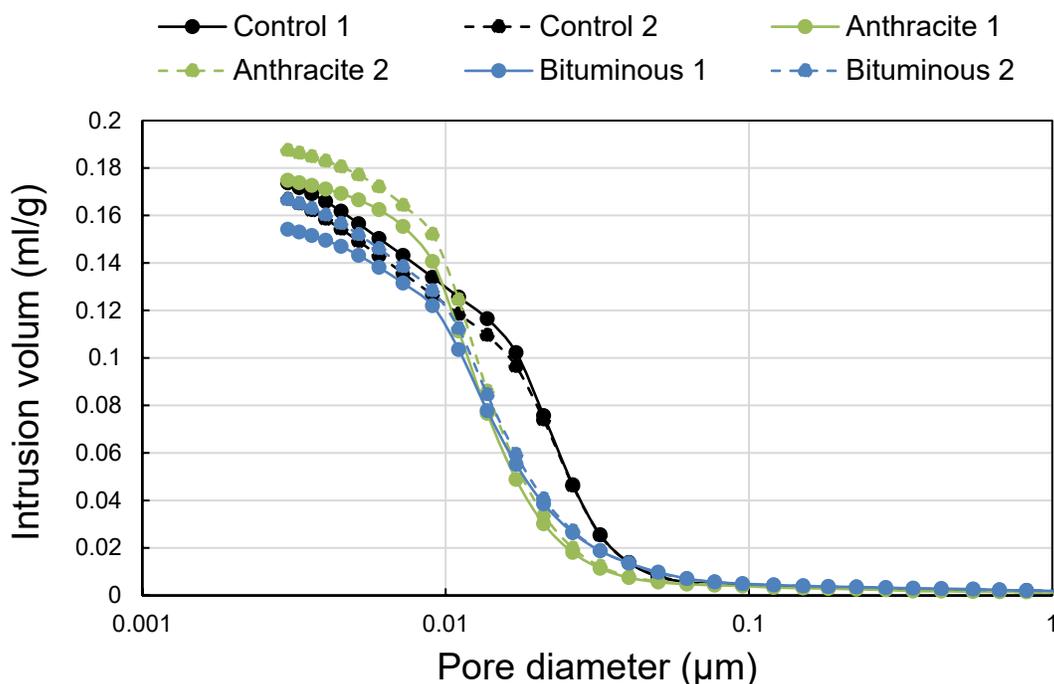
Figure 5-2. Pore size distribution of paste samples measured using MIP

In addition to reduction in the ion transport (diffusion) in concrete, the higher amounts of alumina in CFBC fly ash can help mitigate corrosion of reinforcing steel by binding chloride ions out of the pore solution. Chloride ions can be bound by reaction with C_3A to form calcium chloroaluminate ($3CaO.Al_2O_3.CaCl_2.10H_2O$), also known as the Friedel's salt. A similar reaction with C_4AF results in calcium chloroferrite ($3CaO.Fe_2O_3.CaCl_2.10H_2O$) [149]. In such conditions, a greater amount of chloride binding is expected for anthracite fly ash, as it contains greater amounts of Al_2O_3 and less SO_3. It has been found that increased sulfate ion concentrations result in slightly lower chloride binding, since sulfate ions react with C_3A to form AFm and AFt phases

[162]. Overall, the use of CFBC fly ash is anticipated to improve the corrosion service life of concrete by reducing the diffusivity and binding of chloride ions. And the anthracite fly ash is predicted to have a superior performance over the bituminous fly ash.

It is interesting to also note the reduction in the pH of the pore solution as a result of using CFBC fly ashes (**Table 5-6**). This reduction helps with mitigating the alkali silica reaction (ASR) in mixtures containing reactive aggregates. ASR evaluation is beyond the scope of the present paper. However, in our recent study, we reported on the beneficial effects of the two CFBC fly ashes in mitigating ASR and observed that the anthracite fly ash (despite having a higher alkali content) is more effective against ASR, due to its higher SiO_2 and Al_2O_3 and reduced CaO contents.

The results for the water sorptivity test (ASTM C1585) in 56-day old concrete samples is provided in **Figure 5-3**. The reported absorption (*I*) represents the change in mass of each test sample (in g) divided by the product of the cross-sectional area (mm^2) of the sample and the density of water ($0.001 \ g/mm^3$). Each data point represents an average of the measurements performed on three duplicate samples. Absorption follows a linear relationship with the square root of time elapsed and the constant of proportionality is the rate of water absorption, also known as "sorptivity". According to ASTM C1585, the initial rate of water absorption is the slope of the line that best fits (a correlation coefficient of greater than 0.98) the data from 1 min to 6 h. The secondary rate of water absorption is calculated in a similar manner based on the results of 1 to 7 days. These values are provided in **Table 5-3**. The error bars representative of the initial and secondary absorption portions of the graphs in **Figure 5-3** were measured by averaging the standard deviation of all data points from 1 min to 6 h and from 1 to 7 days, respectively.

The results show that the initial sorptivity of concrete containing the anthracite fly ash is similar to that of the control, while the use of the bituminous fly ash has reduced both the initial and the secondary rate of water absorption into concrete. However, since the standard error for secondary sorptivity is on the same order as the variation among the results, one cannot claim that the secondary sorptivity values among the three mixtures are statistically different. Sorptivity is directly related to pore structure features such as porosity, pore diameter, and pore connectivity. Of special interest are pores greater than 24 nm (calculated using Kelvin's equation [163]), as they dry when the samples are preconditioned at 50 °C and 80% RH, as prescribed by ASTM C1585. The MIP results (**Figure 5-2**) show that for the control sample, approximately 0.060ml of pore space is emptied at 50 °C and 80% RH per gram of solid paste. For the pastes containing the

anthracite or bituminous fly ash, this value is 0.027 ml/g and 0.034 ml/g, respectively. Clearly, the pore refinement in case of the bituminous fly ash agrees with its reduced in initial sorptivity. The same cannot be said for the anthracite fly ash; it is unclear why concrete containing this fly ash shows similar sorptivity as the control mixture despite having a larger formation factor (**Table 5-3**) and smaller threshold and critical pore diameters (**Table 5-7**).
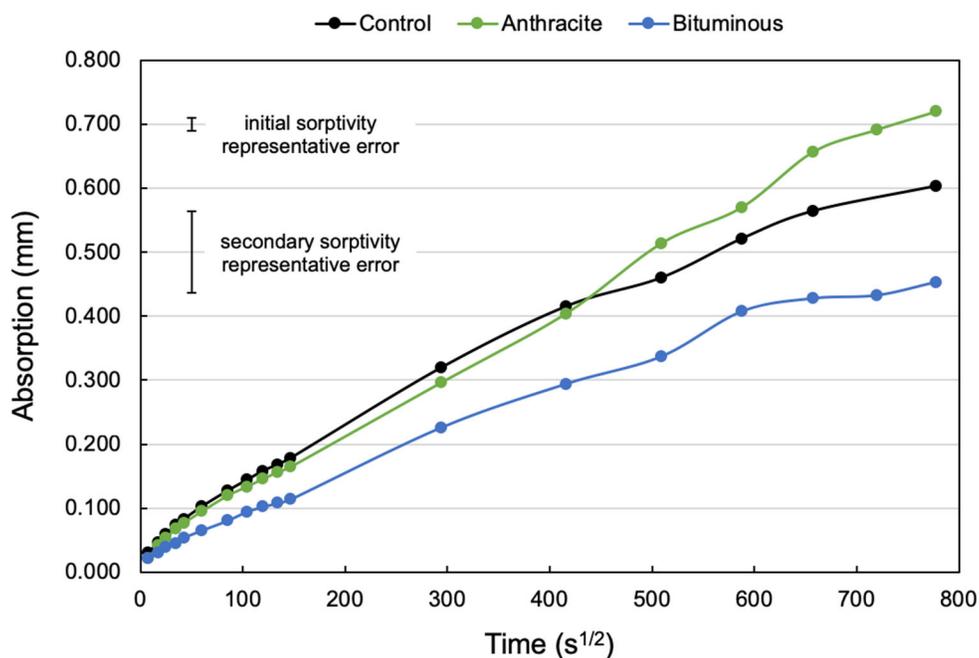
Figure 5-3. Rate of water absorption in concrete samples measured according to ASTM C1585

Table 5-7. Pore parameters obtained from MIP testing at the age of 56 days

Mixture	Porosity (%)	Critical pore diameter (nm)	Threshold pore diameter (nm)
Control (100% PC)	27.8	21.1	36.6
20% Ant. CFBC	27.3	11.0	22.0
20% Bit. CFBC	26.3	11.0	24.7

To evaluate the impact of the CFBC fly ashes on the volume stability of concrete, mortar mixtures were prepared and tested as described earlier. The potential for early expansion of mortars cured under water was evaluated using ASTM C1038 test. The average 14-day expansion of four mortar bars per mixture stored in saturated lime water was measured as 0.008%, 0.005%, and 0.024%, for the control, anthracite, and bituminous mixtures, respectively. While the control

mixture and the one containing 20% anthracite fly ash (whose SO_3 content was less than that of Portland cement) showed negligible expansion, the mortar containing the bituminous fly ash (having SO_3 content of 9.83%) expanded beyond ASTM C1157's suggested threshold of 0.020% but below 0.04% which is commonly assumed as the tensile strain capacity of concrete. It is safe to assume that this level of expansion is not deleterious by itself; however, it is advisable to monitor the volume stability of mortar or concrete containing high SO_3 FBC fly ash over a long term and in exposure to moisture, to more confidently rule out the risk of volume instability. Our earlier study [151] on this bituminous CFBC fly ash suggested that its anhydrite is highly soluble and results in elevated levels of SO_4 ions in the solution. This can combine with the dissolved alumina and calcium to form ettringite, which is likely responsible for the observed expansion of the bituminous fly ash mortars.

To evaluate the potential for deleterious expansion as a result of external sulfate attack, mortar mixtures were prepared and tested according to ASTM C1012. **Figure 5-4** shows the average expansion of six mortar bars per mixture as a function of time when stored in a 50 g/L (0.35 mol/lit) Na_2SO_4 solution. The control and the anthracite fly ash mortars met ASTM C618's optional expansion limit of 0.10% at 6 months for moderate sulfate exposure applications. Even ASTM's limit of 0.05% at 6 months for severe sulfate exposure applications was met. However, the mortar containing the bituminous fly ash far exceeded these limits. This performance is likely due to presence of slowly dissolvable alumina in this fly ash. The AFm phases (hydroxy-AFm and monosulfate) transform to ettringite in the presence of sulfate ions, while gypsum is formed in a reaction between portlandite and sodium sulfate [164][165][166]. The formation of ettringite is much more expansive than gypsum, resulting in increased capillary pressure and cracking in hardened samples [149]. It is interesting to note that the anthracite fly ash showed an acceptable sulfate-induced expansion despite having a significantly larger alumina content in comparison with the bituminous fly ash. Our earlier batch leaching study [151] showed that the alumina phase in the bituminous fly ash is slowly reacting, and may only become available after sustained exposure to the solution. Such slowly dissolving alumina can react with sulfates during ASTM C1012 test and form latent ettringite and cause expansion. Additionally, a higher concentration of portlandite is expected in the bituminous mortar due to its higher CaO content and the presence of free lime. It is also possible that the initial expansion of this mortar due to its higher SO_3 content, as discussed above in the context of ASTM C1038 results, reduced its residual tensile strain capacity and

accelerated the onset of cracking. Once cracked, the penteration of sulfates and the resulting expansion and deterioration of the mortar prisms are accelerated It is worth noting that after 8 weeks of exposure, the standard deviation of expansion readings for the bituminous mortar became significant and visible microcracking was observed in the samples. Overall, it can be concluded that while the anthracite fly ash can tolerate moderate or even severe sulfate attack, the use of bituminous fly ash should be avoided in concretes exposed to external sulfates. Further research on exploring and mitigating the potential deleterious expansion of FBC fly ashes in exposure to external sulfates is merited. It is important to determine whether the high SO_3 content or the kinetics of Al_2O_3 dissoltion, or both are dictating the sulfate resistance of FBC fly ashes.
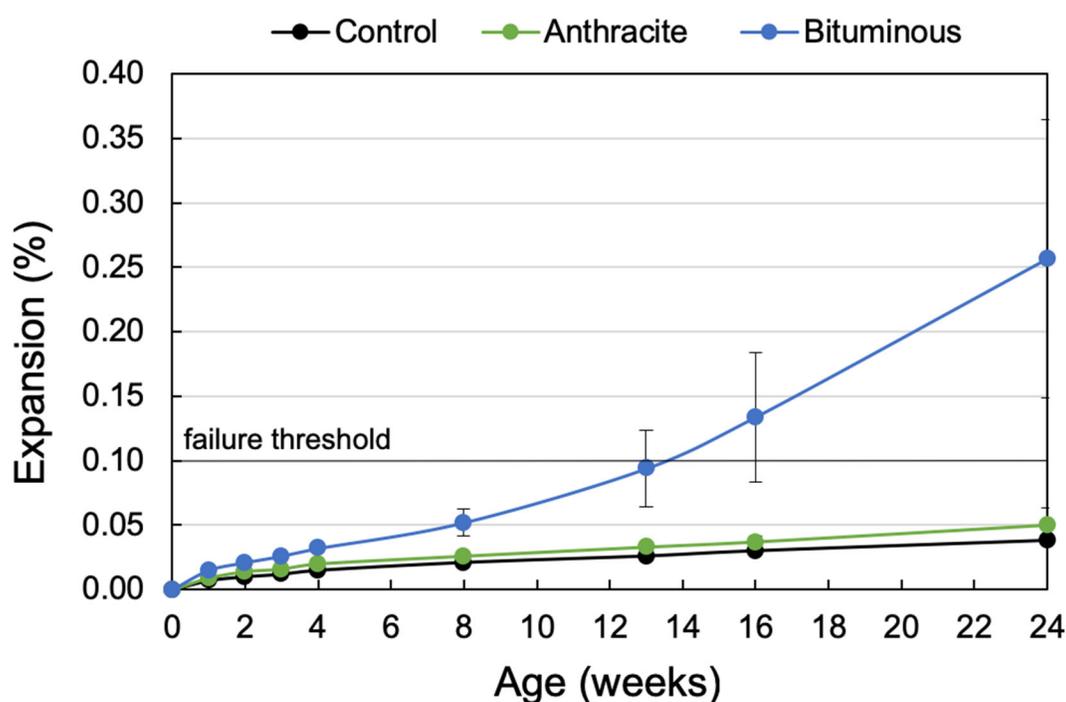
Figure 5-4. Expansion of mortar samples stored in Na_2SO_4 solution (ASTM C1012)

Finally, the results of drying shrinkage and mass loss of mortars containing the FBC fly ashes are provided in **Figure 5-5**. While the anthracite and control mortars showed similar drying shrinkage, samples containing the bituminous fly ash shrank more by approximately 15%. The higher rate of shrinkage in the bituminous samples during the initial two weeks of drying has mainly contributed to this difference. Meanwhile, the fly ash mortars had a slightly higher drying mass loss. The 28-day shrinkage of bituminous samples exceeds the control mixture by 0.017%, which is within ASTM C618-19 limits (max. 0.03%).

(a)
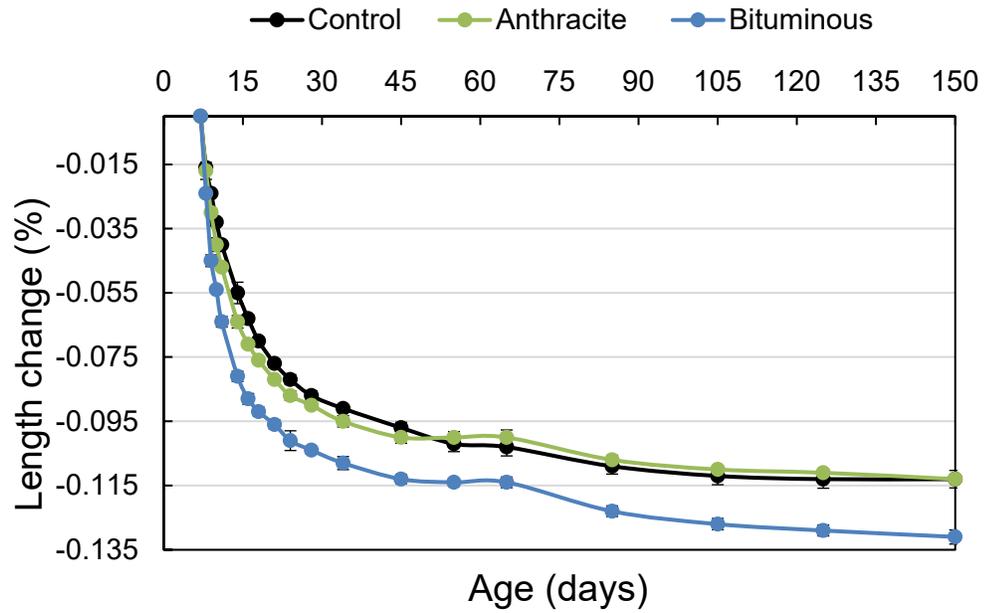
(b)
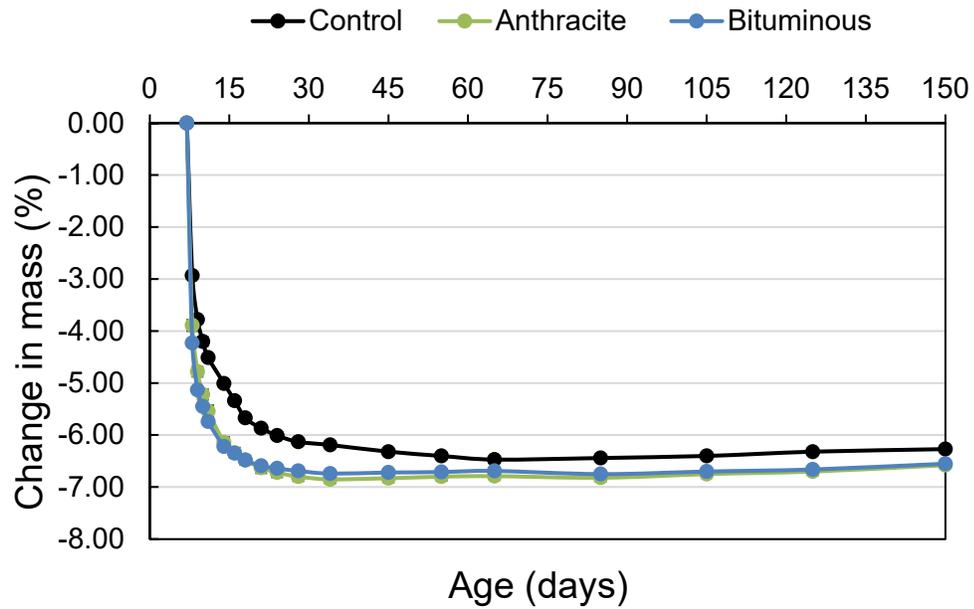
Figure 5-5. (a) drying shrinkage and (b) change in mass of mortar samples measured according to ASTM C157

5.4. Conclusions

The performance of two CFBC fly ashes in mortar and concrete mixtures were evaluated in this chapter. The fly ashes met ASTM C618 chemical and physical requirements except having

elevated LOI in both fly ashes and elevated SO_3 in one (the bituminous) fly ash. Based on the observations and analysis provided above, the following conclusions can be drawn:

- Concrete mixtures containing 20% CFBC fly ash and with proper dosing of water reducing and air entraining admixtures could achieve desirable slump, fresh and hardened air contents, and air spacing factor.

- These mixtures produced a similar compressive strength to that of the control mixture as early as 7 days of age, despite having a slightly higher (~1%) air content. The anthracite fly ash showed a potential for further strength improvement at later ages.

- Replacement of cement with CFBC fly ash delayed the setting time at all curing temperatures. Between the fly ashes, the bituminous fly ash showed further delays in setting, in agreement with its smaller strength activity index and higher anhydrate content, which can retard the hydration of C_3A.

- Use of CFBC fly ash improved concretes' electrical resistivity, formation factor, and resistance to chloride ion penetration. The anthracite fly ash was more effective in pore refinement and increasing the formation factor of concrete, and this was in agreement with reduction in the characteristic pore sizes, as evidenced from mercury porosimetry results. It is likely that CFBC fly ashes provide an added benefit of chemical binding of chlorides due to their high alumina content.

- Both CFBC fly ashes reduced the pH of concrete pore solution. This is in agreement with results in Chapter 4 suggesting the effectiveness of these fly ashes in mitigating the alkali-silica reaction.

- The mortar containing the bituminous fly ash exhibited an early-age expansion when cured under lime water. This is likely attributed to formation of ettringite as a result of elevated SO_3 content of this fly ash. Further, this mortar showed a poor resistance to external sulfates which may be attributed to the slow kinetics of Al_2O_3 dissolution. On the contrary, the anthracite fly ash showed desirable early age volume stability and long-term sulfate resistance despite having a high Al_2O_3 content.

- Both fly ashes showed acceptable performance with respect to drying shrinkage of mortar bars, meeting the relevant ASTM C618 limit.

Chapter 6

Sampling plan for Class F fly ash landfills and evaluation of an example landfill in Pennsylvania[2]

6.1. Introduction

A key challenge identified from the literature review on landfilled fly ash is the lack of a sampling plan and protocol for reliable evaluation of fly ash landfills and their degree of heterogeneity, and for determining the necessary beneficiations steps. This chapter addresses this research need. In addition to developing a statistical sampling approach for evaluating Class F fly ash landfills, the protocol has also been applied to characterize an example landfill in Pennsylvania. A generalized cost analysis was also performed as part of the study and is explained in this chapter.

6.2. Proposed sampling plan for class F fly ash landfills

The sampling plan for Class F fly ash landfills can be divided into two categories – initial sampling and quality control sampling. The purpose of the initial sampling is to assess the homogeneity of the landfill and to identify the beneficiations necessary to make the fly ash suitable for use as a concrete pozzolan. The quality control sampling is done during harvesting of the fly ash to ensure that good quality ash is supplied to concrete producers.

6.2.1. Initial Sampling

As mentioned in the literature review section, fly ash properties are affected by the changes in the power production process. Hence, the first step in successfully characterizing a fly ash landfill is to collect as much information about the landfill as possible from the power utility. The information available and its reliability significantly impact the number of samples required from the landfill. Important information includes the start and end dates of the landfilling operations, changes in the power production process, source of coal, or coal rank during the landfilling period, any co-mingling of fly ash and other materials, and the pattern in which the landfill was filled. Written records and permits are considered reliable, but information obtained through word-of-

mouth may or may not be reliable, and it is up to the judgement of the evaluating engineer whether to use such information. When reliable information on all of the above parameters is available, proceeding with the sampling plan in Method A is recommended to identify the necessary beneficiations. Otherwise, the plan in Method B should be followed to both identify the global heterogeneities within the landfill and to determine the beneficiation strategy. In general, Method B provides more extensive and reliable information about the landfill and would reduce the risk of uncertainties and unexpected heterogeneities during the fly ash reclamation/production phase. Method B comes at a higher cost but is the recommended method if sampling cost is not a significant constraint. It is also important to note that irrespective of the sampling method adopted, it may be necessary to discard the top and bottom layers of the fly ash from the landfill due to contamination with soil, vegetation, and liners as discussed in the literature review section.

Method A: Stratified Random Sampling Approach (based on ASTM D5956-15)

This method relies heavily on the historical utility data to identify any stratification that may exist within a landfill. It assumes the fly ash properties to be homogenous within each stratum but will allow verifying this assumption.

Step A.1: Based on the historical data and the pattern in which the fly ash was filled, the landfill is to be divided into various strata. Fly ash from before and after any change in the power production parameters listed above shall be considered as belonging to different strata. Boundaries should be drawn as accurate as possible using the available information. Each individual stratum is assumed to be homogeneous, but this will be verified through steps A.2 to A.4 below. Steps A.2 to A.4 shall be repeated for each stratum in the landfill.

Step A. 2: In the plan view of each stratum (e.g., A and B in **Figure 6-1a**), a 3×3 grid pattern shall be created such that the length and width of the stratum is divided into equal parts. The nine created grid blocks are numbered. Three (minimum) of the nine are chosen using a random number generator. Then a borehole sample is obtained from the X-Y centre of each of these three random grid blocks. For the boundary grid blocks, the X-Y centre may lie outside the landfill. In such cases, the approximate centre of the area within the landfill should be sampled. The boring sample is taken from the entire depth of the stratum. At every (maximum) 1.5 m, the boring shall be split to create separate segments. For example, if the stratum is 5 m deep at a given point, then 4 segments are to be made, one from each of the following depths: 0-1.5 m, 1.5-3 m,

3-4.5 m, and 4.5-5 m. A (minimum) of two segments in each boring are chosen at random (this can be done by numbering the segments and using a random number generator). Therefore, a total of (minimum) six random segments will be available ((minimum) three grid blocks × (minimum) two 1.5 m deep segments per grid block). The diameter of the boring must be large enough to obtain at least 2 kg of sample from each segment.

Step A.3: Each of the (minimum) six random segments shall be homogenized and tested according to the mandatory requirements of ASTM C618. The mean, range, standard deviation, and probability of exceeding or going below the ASTM C618 limit for each fly ash property must be determined by testing the six segments. **Eq. 6-1** and **Eq. 6-2** may be used to calculate the probability of true average value of any individual fly ash property exceeding an upper or lower specification limits.

$$P\{\text{Property} > \text{ASTM limit}\} = P\left\{T_{n-1} < \frac{\bar{X} - \text{USL}}{s/\sqrt{n}}\right\} \tag{Eq. 6-1}$$

$$P\{\text{Property} < \text{ASTM limit}\} = P\left\{T_{n-1} > \frac{\bar{X} - \text{LSL}}{s/\sqrt{n}}\right\} \tag{Eq. 6-2}$$

Where n is the sample size (for six segments, n=6), T_{n-1} is the statistical t-distribution with $n-1$ degrees of freedom, $\bar{X}$ is the sample average for every individual property, USL and LSL are the upper and lower specification limits, and s is the sample standard deviation.

Step A.4: A probability limit shall be selected based on the acceptable level of risk (say 5%). The properties for which the probability calculated in Step A.3 is below the acceptable risk value do not require beneficiation. The probability can exceed the acceptable risk value for certain properties due to two reasons – (1) the fly ash may have poor quality in general and thus requires beneficiation or (2) the historical information is not accurate and there are multiple strata within the stratum being tested (i.e., the assumption of homogenous stratum is violated; this will increase the standard deviation of the properties and thus the probability of not meeting the ASTM limits). For each property with a probability value higher than the acceptable risk limit, data from the individual samples must be compared. If certain samples have values significantly different from the other samples, then reason #2 is more likely. However, if all samples are equally poor in quality, then reason #1 is more likely. In cases where the likely reason cannot be qualitatively established or when reason #2 is likely, sampling according to Method B must be performed.

Sampling Method A can also be used as an initial feasibility study. If the fly ash from the landfill fails to meet the specification limits for several properties or if it is determined that the cost of beneficiation will be prohibitively high, then investing in the more rigorous sampling Method B can be avoided.
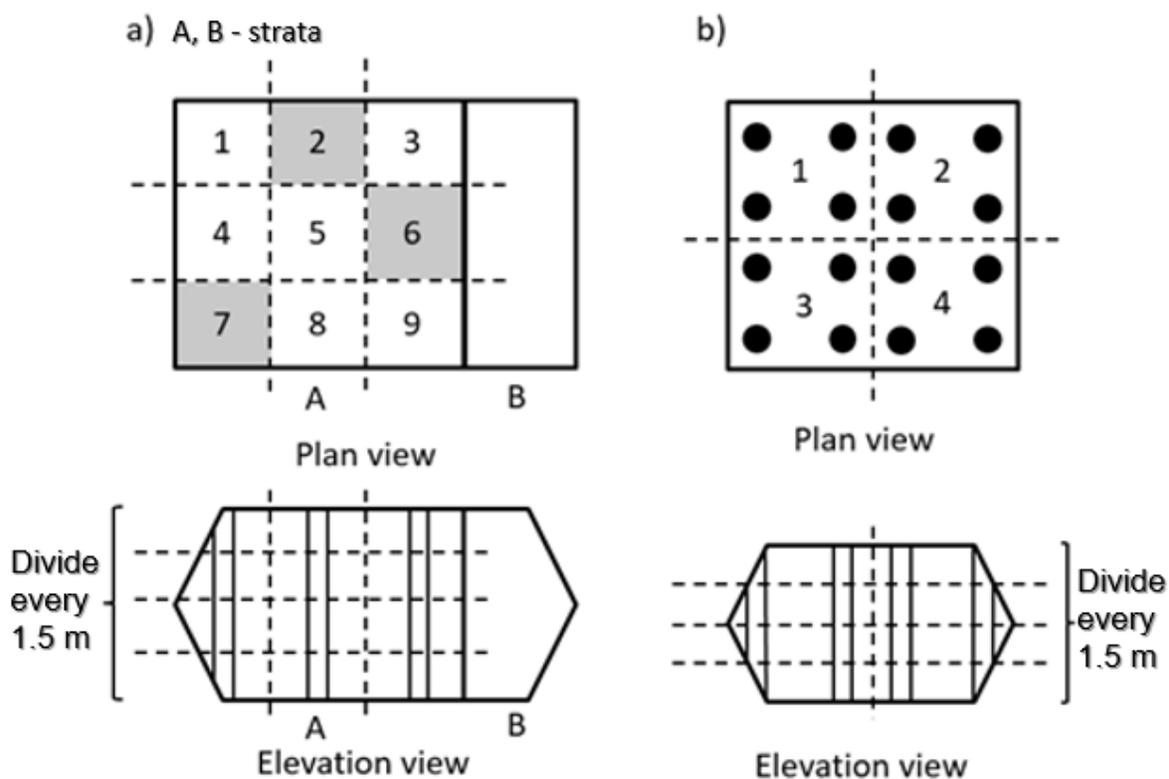
Figure 6-1. Schematic diagram for the initial sampling of a fly ash landfill with the location of boreholes shown: a) stratified random sampling (Method A), and b) regular grid-based sampling (Method B)

Method B: Regular Grid-based Sampling

This method makes a conservative assumption that the landfill is stratified, but the strata boundaries are unknown. It discretises the landfill horizontally into four grid blocks and vertically into 1.5 m deep segments, and samples each segment to capture the variability within the landfill. Subsequently, it determines the necessary fly ash beneficiations for each segment. The way that landfills are built (layer-by-layer or stockpiling materials in cells) ensures that the maximum heterogeneity will be across the depth.

Step B.1: In the plan view of the landfill (**Figure 6-1b**), a 2×2 grid pattern is created such that the length and width of the landfill is divided into equal parts. Within each grid block, (a

minimum of) 4 points are chosen such that they are as far as possible from each other and from the edges of the grid block. As such, the total number of points in the plan view will be (minimum) 16.

Step B.2: A boring sample is collected from each of the (minimum) 16 points in Step B.1 to sample the entire depth of the landfill. At every (maximum) 1.5 m, the boring is split to create separate segments. For example, if the landfill is 5 m deep at a given point, then 4 segments will be created: 0-1.5 m, 1.5-3 m, 3-4.5 m, and 4.5-5 m. The diameter of the boring must be large enough to obtain at least 2 kg of sample from each segment.

Step B.3: Each (minimum) 1.5 m deep segment within a grid block will be considered a homogeneous space. Each such space must be tested following steps A.3 and A.4 of Method A, but using four segment samples instead of six. The necessary beneficiations for each homogeneous space are determined accordingly. If the four samples within any homogeneous space have significantly different values when compared to each other, then stratification within the homogeneous space is possible. Such instances are to be noted and handled during the quality control sampling.

6.2.2. Quality Control (QC) Sampling

Although the initial sampling identifies the global heterogeneities within a landfill, it is not sufficient to handle localized heterogeneities (e.g., pockets of impurities) that may be present within a landfill. To make sure that fly ash with consistent quality and reliability is produced from the landfill, quality control sampling is needed during the excavation process. The QC sampling should comply with the requirements of ASTM C311/C311M-18, Table 1.

6.3. Experimental methods and materials
6.3.1. Characterization of the Fly Ash Landfill in Pennsylvania

The proposed initial sampling plan was applied to a fly ash landfill in Pennsylvania. A schematic of the landfill is shown in **Figure 6-2** along with the location of three borings and eleven 1.5m-deep, segment samples. The landfill is approximately 500×300×16m in dimensions and was constructed during the 1980s and 90s as a Class F fly ash mono-fill. It was constructed as a "dry stack" above the natural grade on a liner (mostly clay but one section has a synthetic membrane) and covered with a 0.6-meter-thick layer of top soil. The groundwater table is approximately 1.5

meters below the bottom lined surface of the landfill. The average annual precipitation in the area over the last 20 years was 1,053 mm. The landfill has a leachate collection and treatment facility. From the information collected from the power utility, it was concluded that the landfill is likely containing only one uniform stratum. As such, sampling Method A was chosen. It should be noted that when time and budget permits, sampling Method B is recommended to reliably identify the necessary beneficiation processes.

The three boring points (B1, B2 and B3) were chosen at random and divided into 1.5m-deep segments. From the available segments, the following were chosen randomly: 2 and 3 (from B1); 4 and 7 (from B2); and 8 and 10 (from B3). Materials from each segment (~2.0 kg) were placed inside large plastic bags and homogenized. Then, each sample was stored in re-sealable airtight bags to prevent moisture loss and tested for various properties as described below.

No.	Depth (m)	No.	Depth (m)	No.	Depth (m)
1	3-4.6	4	1.5-3	8	3-4.6
2	7.6-9.1	5	4.6-6.1	9	4.6-6.1
3	9.1-10.6	6	6.1-7.6	10	6.1-7.6
		7	12.2-13.7	11	7.6-9.1
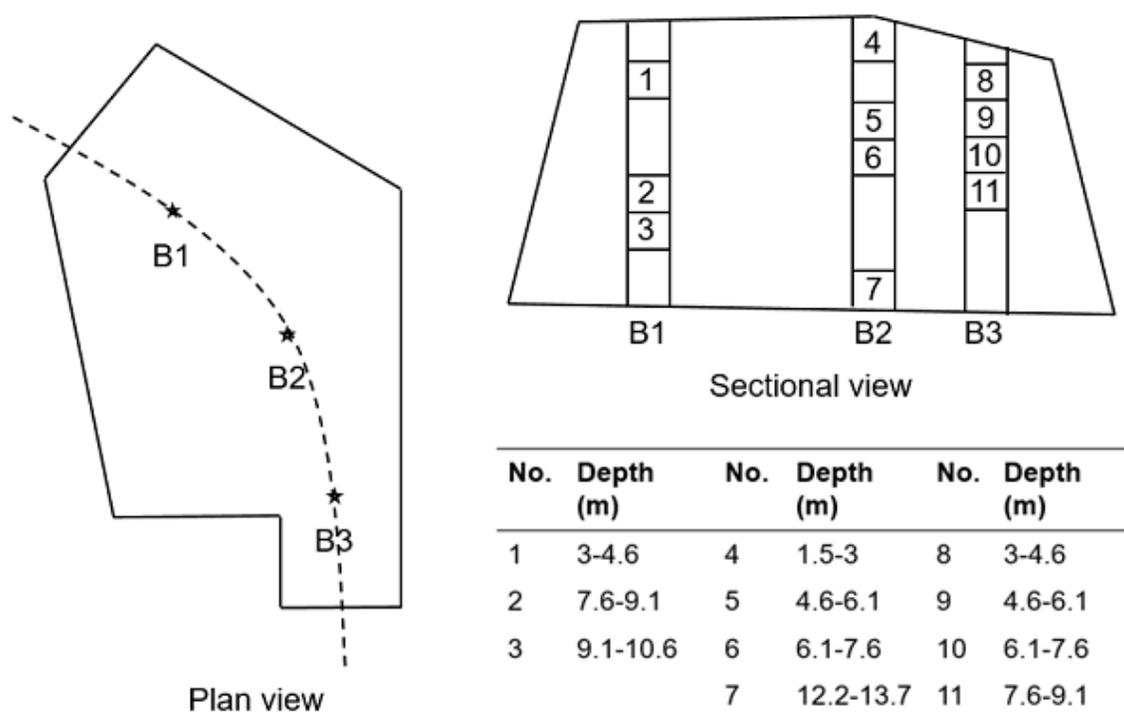
Figure 6-2. Schematics of the fly ash landfill in Pennsylvania and the boring locations

6.3.2. Other Materials

Type I/II portland cement with the following properties was used: specific gravity = 3.15, Blaine fineness = 400 m^2/kg, LOI = 2.69%, CaO = 60.78%, SiO$_2$ = 19.41%, Al$_2$O$_3$ = 4.61%, Fe$_2$O$_3$ = 3.82%, MgO = 2.91%, SO$_3$ = 4.0%, and Na$_2$O$_{eq}$ = 0.9%. Graded standard sand conforming to

ASTM C778-17 was used for strength activity index (SAI) experiments. For concrete mixtures, aggregates conforming to ASTM C33-18 were used. The coarse aggregates conformed to #56 grading with SSD specific gravity of 2.615 and absorption capacity of 1.32%. The fine aggregates had SSD specific gravity of 2.616 and an absorption of 1.66%.

6.3.3. Items of Investigation

The recovered fly ash segment samples were tested according to the mandatory requirements of ASTM C618-17a. All 11 segments were tested for moisture content, LOI, fineness, water requirement, SAI, density, and uniformity requirements. However, the statistical analysis was performed based on the results of the 6 segments chosen randomly as described above. The six random samples were also tested for the oxide composition, sulfur/carbon content via infrared analysis, and soundness tests.

Moisture content, loss on ignition, fineness, strength activity index at 7, 28, and 56 days, water requirement, soundness, and fineness uniformity tests were conducted according to ASTM C311-17 standard procedures. Oxide composition (by fused bead XRF), carbon/sulfur trioxide (by infrared LECO analyzer) and density (by helium pycnometer) were also tested. All 11 boring segment samples were also tested for particle size distribution using laser diffraction on the fraction passing sieve #20. Sieve analysis was also performed on 300 grams of a composite sample made by mixing equal parts from all 11 segments.

A bulk sample of the fly ash was also excavated from the landfill. This sample was dried and passed through sieve #100 to remove any large particles such as gravel or bottom ash that might be present. Quantitative XRD was performed on the beneficiated (i.e., sieved and dried) bulk sample. For XRD test, the sample was ground to less than #400 sieve size using a micronizing mill. 10% zincite (ZnO) was mixed with the fly ash as an internal standard. The diffraction pattern was obtained over 5-70º 2θ range using Cu Kα radiation, 0.02º step size, and a spinner stage. The pattern was analyzed using Rietveld refinement. The beneficiated bulk sample was also tested for ASR mitigation capacity (ASTM C1567-13) at 25% cement replacement by mass using a highly reactive (R2) aggregate[3]. The beneficiated bulk sample was used for making concrete mixtures at 25% cement replacement with fly ash. The properties of this concrete were compared to those of a control mixture containing pure portland cement. A w/cm = 0.48 was used in both mixtures. The mixture proportions for the control and the fly ash concrete mixtures are shown in **Table 6-1**.

The mixtures were tested for slump (ASTM C143/C143M-15a) and plastic air content (ASTM C231-17a). Cylinder samples (100×200 mm) were cast from each mixture and tested for hardened air analysis (ASTM C457-16, the linear traverse method) and strength development (ASTM C39-18). The slump and the plastic and hardened air contents of the mixtures are reported in **Table 6-1.**

Table 6-1. Proportions of concrete mixtures, as well as their slump, and plastic and hardened air contents

Material/Property	OPC mix	Fly ash blended mix
Cement (kg/m^3)	365	274
Water (kg/m^3)	175	175
Coarse aggregate (kg/m^3)	1020	1020
Fine aggregate (kg/m^3)	676	654
Fly ash (kg/m^3)	0	91
Air entraining admixture (ml/m^3)	475	475
Slump (mm)	165	171
Plastic air content (vol %)	6.12%	6.72%
Hardened air content (vol %)	5.98%	6.65%
Spacing factor (mm)	0.126	0.142

6.4. Experimental results and discussion
6.4.1. Tests on Segmented Boring Samples

Table 6-2 shows the summary of results obtained from the mandatory tests of ASTM C618. The table shows the mean, range, and standard deviation from testing the randomly selected six segment samples. It also shows the ASTM limit for each property and the probability of exceeding or going below the ASTM limit, calculated using **Eqs. (6-1)** and **(6-2)**. For fineness uniformity and density uniformity, the data from all 11 segments was used for calculating the mean value, and the results of any given sample was compared with the average of the other 10 samples, according to ASTM C618.

At an acceptable risk level of 5%, it can be seen from **Table 6-2** that all properties of the fly ash from the landfill, except the moisture content, were satisfactory. Based on the sampling plan, the consistently poor moisture content results for all samples tested validates the assumption regarding homogeneity of the landfill. The probability of 7-day strength activity index going below the ASTM limit was close to 5% (at 4.883%). But the 28-day strength activity index results were acceptable. The 56-day SAI data was also obtained and shown in **Figure 6-3**. For most samples,

SAI improved with age, suggesting pozzolanic reactivity. However, only 7 out of the 11 samples attained SAI greater than 100%, despite having a slight w/cm ratio advantage versus the control (w/cm= 0.484 vs. 0.471). This may suggest a slow pozzolanic reaction, which is in agreement with the concrete strength results discussed later. These results point to drying as the only required beneficiation for the fly ash from this landfill. As discussed below, dry sieving over #100 sieve is also recommended.

Table 6-2. Summary of ASTM C618 test results and probability analysis

Property	Mean	Std. Dev.	Minimum - Maximum	ASTM Limit for Class F	Probability of not meeting ASTM limit
Sum of SiO_2, Al_2O_3 & Fe_2O_3	87.28%	0.0161	85.42% - 89.40%	> 70%	<0.001%
Sulfur trioxide	0.81%	0.0013	0.70% - 1.05%	< 5%	<0.001%
Moisture content	15.93%	0.0091	14.3% - 16.8%	< 3%	~100%
Loss on Ignition	2.81%	0.0027	2.49% - 3.14%	< 6%	<0.001%
Carbon (LECO)	2.1%	0.0029	1.80% - 2.41%	N.A.	N.A.
Fineness (% retained on #325 sieve)	26.90%	0.0309	24.6% - 32.7%	< 34%	0.122%
Strength activity index 7-day	81.78%	0.0817	72% - 93%	> 75%	4.883%
Strength activity index 28-day	93.15%	0.0664	84% - 100%	>75%	0.056%
Water requirement	97.30%	0	97.3% - 97.3%	< 105%	N. A.
Soundness	-0.02%	0.0001	-0.03% - 0%	< ±0.8%	<0.001%
Fineness uniformity (max % variation from avg.)	2.49 %	0.0161	0.4% - 5.2%	< 5 %	0.610%
Density uniformity (max % variation from avg.)	0.87%	0.0054	0.4%-1.9%	< 5%	<0.001%

When the segment samples were removed from their containers, it was observed that some contained larger particles of sand, gravel, or bottom ash. Since the fineness test according ASTM C311 only uses 1 g of the sample, the test sample is not representative of this contamination. To better characterize the fineness of fly ash in this landfill, a combination of sieving and laser diffraction was used. 25 g of each segment sample was sieved through a #20 sieve and the passing fraction was tested using laser diffraction to determine its particle size distribution. The combination of the two tests was used to determine the fineness of the fly ash as the mass fraction larger than 45µm (#325 sieve). The two fineness test results for all eleven segment samples are shown in **Figure 6-4**. The average D10, D50 and D90 (the corresponding range of these values are reported in parentheses) of the particle size distribution of the fly ash samples were found to be 2.06 µm (1.86 to 2.32 µm), 20.04 µm (17.26 to 24.26 µm), and 121.55 µm (107.66 to 144.06 µm)

respectively. Data from boring #5 was excluded from these calculations due to significant contamination with sand as seen in **Figure 6-4**. For reference, D10, D50, and D90 of the OPC used in the study was 2.63 μm, 11.85 μm, and 36.98 μm. The recovered fly ash was considerably coarser that the cement, although the fly ash met ASTM C618 fineness requirements.
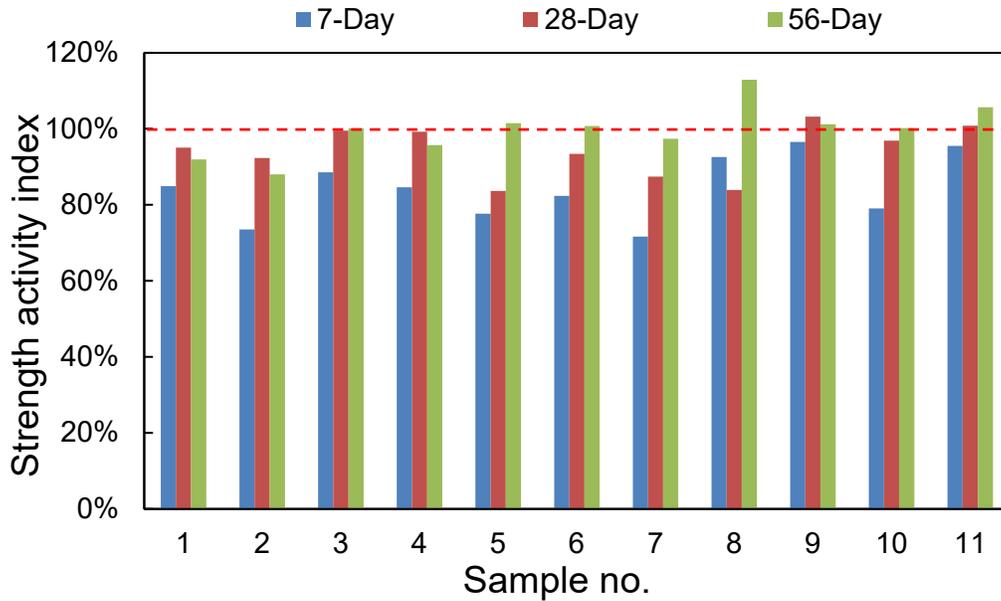
Figure 6-3. Strength activity index values at 7, 28 and 56 days for the eleven segment samples
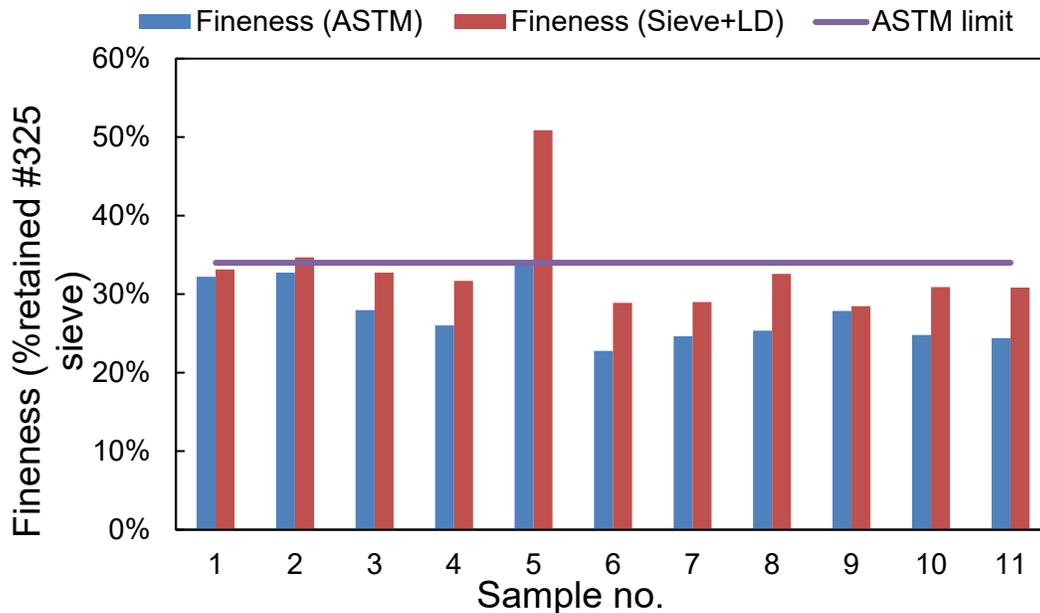
Figure 6-4. Comparison of the fly ash fineness measured using ASTM C311 protocol and using sieving (#20) plus laser diffraction (sieve+LD)

Two conclusions can be drawn from the results in **Figure 6-4**. First, the initial sampling plan does not accurately reflect localized heterogeneity, as was predicted and discussed previously. When fly ash fineness was measured using a larger sample size (25 g as opposed to 1 g), sample #5 had a fineness higher than the ASTM limit. The sampling plan enables an estimation of the cost of beneficiation, but the quality of the fly ash supplied needs to be controlled through QC sampling and testing during the harvesting period. Second, the sole fineness criteria given in ASTM C618 might not be sufficient for fly ash recovered from landfills. All samples showed a higher fineness value when a large sample size was used to allow capturing any contamination (large particles) that may be present. Therefore, increasing the sample size for the fineness test of recovered fly ash to 25 g is recommended. Therefore, and based on the results in **Figure 6-4** for the Pennsylvania landfill tested here, sieving was also added as a required beneficiation strategy. Sieve analysis conducted on the composite sample showed that 94.7% and 90.9% of the material is finer than No. 50 and No. 100 sieves, respectively. Either sieve could be used for beneficiation, but No. 100 was chosen since it had a good throughput (>90%) and provided finer fly ash. The combination of drying and sieving through No. 100 sieve was used for beneficiating the bulk fly ash sample obtained from the landfill.
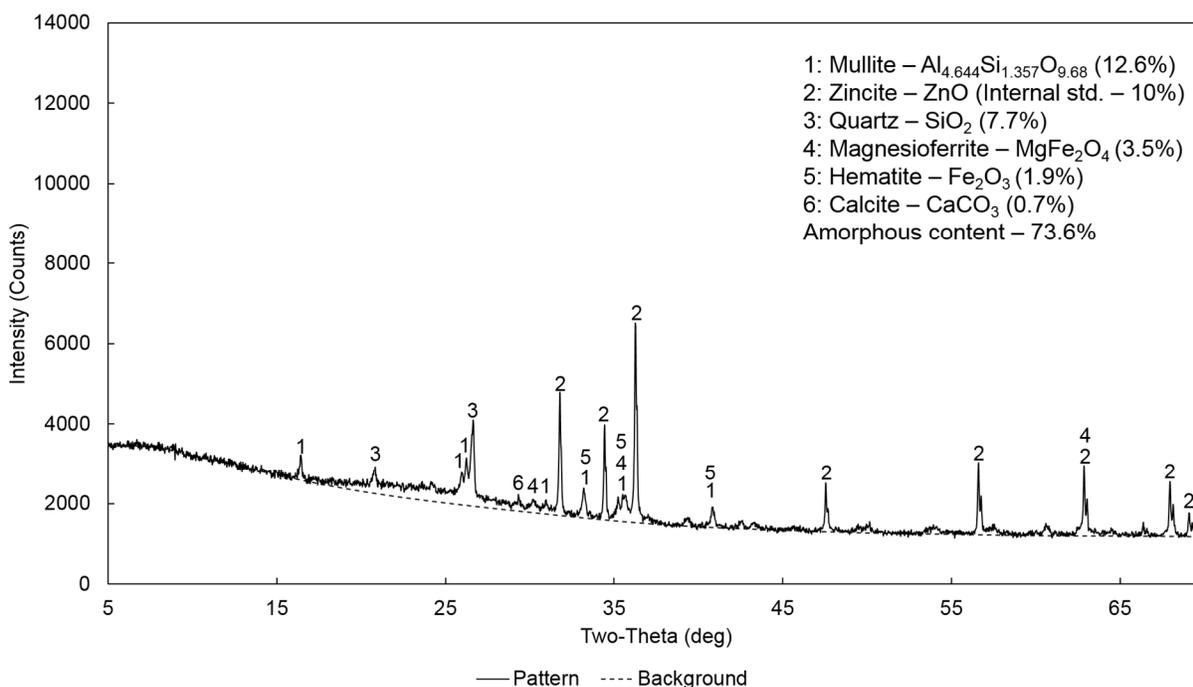
Figure 6-5. Quantitative X-ray diffraction pattern of the beneficiated bulk fly ash sample

6.4.2. Tests on the Beneficiated Bulk Sample

The quantitative XRD pattern of the beneficiated bulk fly ash sample is shown in **Figure 6-5**. The amorphous content of the sample was found to be 73.6%. The major crystalline phases were mullite, quartz, iron-bearing phases, and calcite. No hydrated mineral phase was observed. The accelerated mortar bar test results for the control (100%OPC) and test mixtures (25% cement replacement by fly ash) are shown in **Figure 6-6**. From the test results, it is clear that the fly ash from this landfill is suitable for ASR mitigation of a highly reactive aggregate. The slump, plastic air, and hardened air content of the control OPC and the fly ash blended mixtures are reported in **Table 6-1** along with their mixture proportions. It can be observed that the unburned carbon in the fly ash did not affect the performance of the air entraining admixture. The slump of the concrete was also improved slightly when 25% by mass of OPC was replaced with fly ash. **Figure 6-7** shows the compressive strength development of the OPC and fly ash blended concrete mixtures. The fly ash blended concrete had 61%, 70% and 80% of the strength of the control concrete at 7, 28, and 56 days, respectively. This indicates a slow pozzolanic reaction which is consistent with the strength activity index results. Concrete proportions may be adjusted (e.g., by reducing the w/cm) to compensate for the loss of strength.
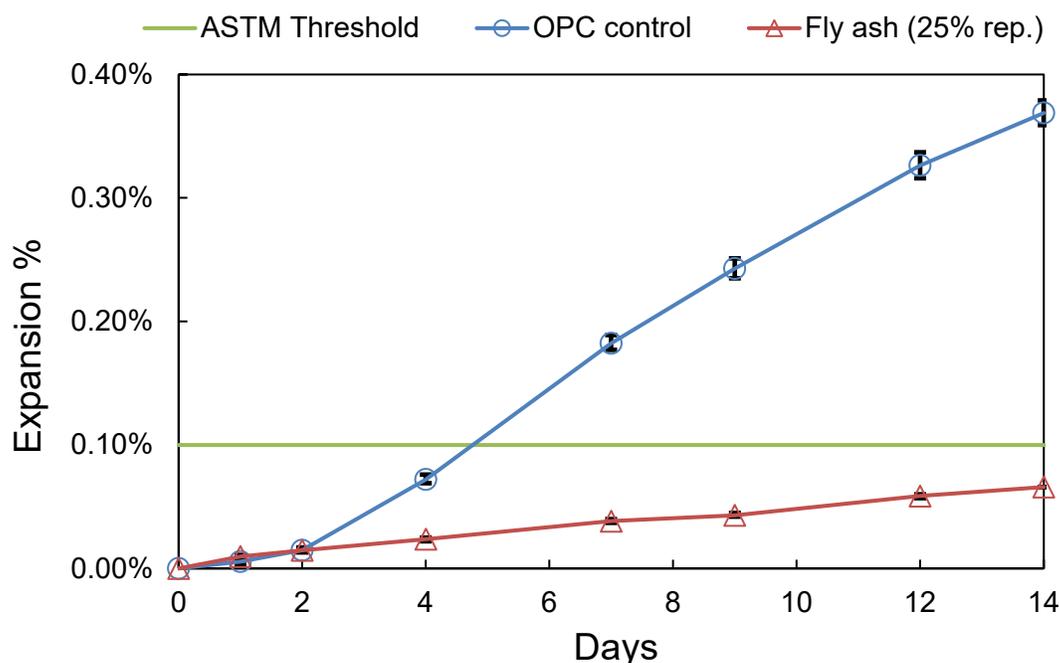
Figure 6-6. ASTM C1260 and C1567 results for mortars containing a highly reactive aggregate: 100%OPC (control) and 25% cement replacement with fly ash (test) mixtures
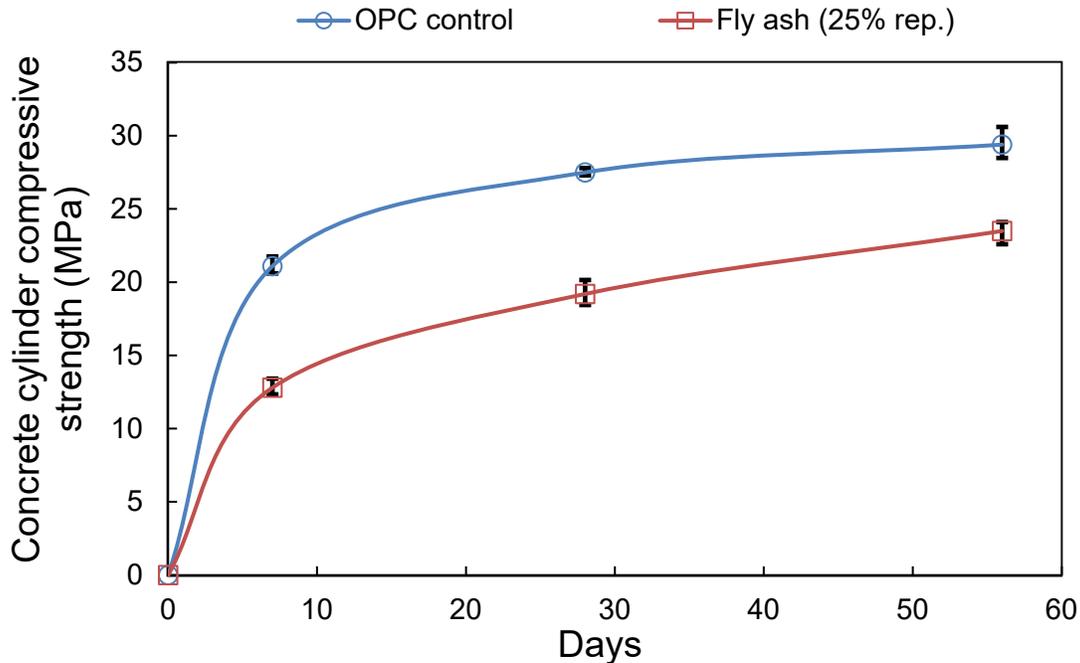
Figure 6-7. Concrete cylinder compressive strength test results for 100%OPC and fly ash blended mixtures

6.5. Cost analysis

The cost of recovering good quality fly ash from the landfill in Pennsylvania was also estimated as part of the research work. This cost analysis can serve as an example for evaluation of other landfills in the future. The additional costs involved in using recovered fly ash when compared to fresh fly ash includes 1) Sampling and characterization cost, 2) excavation cost (cover and fly ash), 3) beneficiation cost (in this case drying and sieving), and 4) cost of permits and other regulatory requirements. While the cost of excavation and drying could be calculated on the basis the data available, the remaining costs were assumed to be a percentage of the total cost.

6.5.1. Excavation cost

The landfill in Pennsylvania had a top soil cover of roughly 0.6 meters. In order to estimate the volume of the top soil cover, it was essential to calculate the surface area. The projected flat area of the landfill could be found using online mapping tools [167] and the elevation data for the landfill was obtained from a separate mapping tool [167]. The mapping tool used for finding the flat projected area was also capable of providing lengths and perimeters. Using the above two tools, the slope of the landfill was calculated as shown in **Figure 6-8.**

Rise = 20 feet (from elevation data)
Run = 66.3 feet (from above)
Tan A = Rise/Run = (20/66.3)
A = 16.8 degrees

Figure 6-8. Calculation of slope of the landfill using online mapping tools

Area of the topmost flat surface of the landfill	$= 32191\ m^2$
Projected flat area of the entire landfill	$= 97993\ m^2$
Total surface area of the landfill	$= 32191 + (97993\text{-}32191)/\text{Cos A}$
	$= 32191 + 65802/\text{Cos } 16.8°$
Total surface area of the landfill	$= 100926.7\ m^2$
Total volume of cover soil	$= 0.6 * 100926.7\ m^2$
	$= \mathbf{60556\ m^3 \sim 79205\ Cu.\ Y.}$

The cost of excavation was estimated using the data available in RSmeans [167] – assembly number G10301201000 (Excavate common earth, ½ C.Y. Backhoe, two 8 C.Y. dump trucks, 1 MRT). The cost per cubic yard for this operation is $8.28.

Therefore, total cost of excavating topsoil cover   = $8.28*79205   = **$655,818**

It is known from the utility that the landfill contains roughly 2,000,000 C.Y. (also roughly equal to 2,000,000 tons) of fly ash. Once again, the cost of excavation of fly ash was estimated using RSmeans – assembly number G10301601000 (Excavate sandy clay/loam, ½ C.Y. backhoe, two 8 C.Y. dump trucks, 1 MRT). The cost per cubic yard for this operation is $11.43.

Total cost of excavating fly ash from landfill   = $11.43*2,000,000   = **$22,860,000**

Therefore, the total cost of excavation operations   **= $23,515,818 ~ $24,000,000**

6.5.2. Beneficiation cost

For estimating the cost of drying, the data provided in "Handbook of Industrial Drying" [133] textbook was used. For steam tube indirect rotary dryer, with ~2.6 tons/h throughput capacity, cost including auxiliary subsystems such as finned air heaters, transition piece, drive, product collector, fan and duct is approximately $320,000 for a moisture content of 25%. The lower moisture content of the fly ash in the Pennsylvania landfill will primarily reduce only the fuel cost and may increase throughput due to shorter residence time. Installation costs are typically 300% of the equipment cost for this type of dryer. It is assumed that 5 dryers will be working in parallel to produce the necessary throughput.

Total fixed cost   = 5* (320,000 + 960,000 (this is 300% of 320,000)) = **$6,400,000**

At 2.6 tons/h, assuming 24 hours by 365 days of operation, for 5 dryers in parallel:

Time required to fully process the fly ash in landfill = 2,000,000/ (2.6*5*365*24) = 17.5 years

From the textbook, the total maintenance and operating cost per year can be assumed to be 10 percent of the installation cost. Therefore:

Total maintenance + operating cost   = 10% (5*960,000)   = $480,000/year

Total variable cost for the entire operation   = $480,000*17.5   = **$8,400,000**

Total drying cost   = 8,400,000+6,400,000   = **$14,800,000**

                                  ~ $15,000,000

6.5.3. Total cost of producing recovered fly ash

The cost of sieving, permits, sampling, testing (characterization), and other activities could not be estimated and hence were assumed to add 20% to the existing costs.

Total cost   = 1.2*(24,000,000+15,000,000) = $46,800,000 ~ **$47,000,000**

Cost per ton of fly ash   = $47,000,000/2,000,000   = **$23.5/ton**

Cost per year of operation   = $47,000,000/17.5   = **$2,685,714.3 ~ $2,700,000/year**

6.6. Conclusions

Fly ash recovered from mono-fills can be a valuable pozzolan source, subject to a methodical sampling, evaluation against ASTM C618 requirements, and beneficiation. Initial and quality control (QC) sampling of the fly ash in the landfill are both required. The initial sampling identifies any global heterogeneities within a landfill and determines the necessary beneficiations. QC sampling ensures that good quality fly ash is produced on a daily basis from a landfill. Two methods for the initial sampling were proposed herein: the cheaper and simpler approach was based on stratified random sampling and the costlier and more reliable approach was based on regular grid-based sampling. Both methods use ASTM C618 requirements and a probabilistic analysis to determine if fly ash from a given landfill is suitable for use in concrete.

Beneficiation of landfilled Class F fly ash, at a minimum, includes drying and sieving (to remove larger particles that may be present). Other beneficiations that may be necessary include LOI reduction and grinding to breakdown agglomerated particles and improve fly ash reactivity. A review of these beneficiation methods was provided. The stratified random sampling approach was applied to a fly ash landfill in Pennsylvania. Fly ash retrieved from the Pennsylvania landfill had good quality across a wide range of properties and was found to be in compliance with ASTM C618 requirements. It only needed drying and sieving over No. 100 sieve. It showed excellent ASR mitigation and produced a concrete with desirable workability and air content. The strength development was slower than the control mixture, which can be remedied by a *w*/*cm* adjustment.

Chapter 7

Conclusions

As the supply of conventional pozzolans fall further behind concrete industry's demand, interest in non-traditional pozzolanic materials continues to grow. One such material is fluidized bed combustion fly ash, with an annual U.S. production exceeding 15 million tons. In this study, two compositionally different fly ashes from circulating FBC power plants were evaluated for their compliance with ASTM C618-19 standard and their impact on the fresh and hardened properties of pavement-grade concrete mixtures. The pozzolanic reactivity of the fly ashes was also quantified based on the new RILEM test method. These fly ashes met the chemical and physical requirements of ASTM, except for elevated LOI (in both fly ashes) and elevated SO_3 (in one fly ash). Despite this, it was observed that desirable slump, air content, air structure, and strength development can be achieved in concrete with FBC fly ash (with 20% mass replacement of portland cement). FBC fly ashes improved concrete's electrical resistivity, formation factor, and resistance to chloride penetration. Both fly ashes mitigated ASR, with the anthracite fly ash being more effective due to its lower CaO and higher Al_2O_3 and SiO_2 contents. Drying shrinkage and autogenous shrinkage performance were also acceptable. While the SO_3 content of the fly ashes did not cause a deleterious expansion by itself, concretes containing the high-sulfur fly ash were more prone to sulfate attack. Lack of specifications is a significant impediment against the use of FBC fly ashes in concrete. For the time being, it is proposed that the definition of fly ash within ASTM C618 is expanded to also include coal-based FBC fly ashes. This way, FBC fly ashes that meet the physical and chemical requirements of ASTM C618 can be used by themselves or blended with other pozzolans for use in concrete. Further research results can be used to revise the FBC fly ash specifications where it may be needed.

Another non-traditional pozzolan that was explored in this work is landfilled fly ash. A comprehensive review of the available literature on this resource was provided in this report. The possible technical challenges with landfilled fly ash and the beneficiation options that can be employed to mitigate these problems were discussed. Most commonly, landfilled fly ash must be dried and sieved and/or ground to a proper particle size. Some landfills may require more extensive beneficiation such as carbon/LOI management, while others may not be usable due to presence of

deleterious impurities such as FGD materials. A significant step toward use of landfilled fly ash is employing a reliable statistical sampling plan to quantify the heterogeneity and properties of the fly ash within a given landfill. Another challenge is development and deployment of economically viable options for beneficiation and treatment of the fly ash on site to bring its quality to concrete use standards. In the present study, a sampling plan was developed for evaluating the heterogeneity of fly ash and its properties across a landfill. This sampling plan was successfully applied to a landfill in Pennsylvania. It was observed that in most cases, drying and sieving will necessarily have to be a part of the beneficiation strategy. The cost of recovering and beneficiating the fly ash from the landfills was also discussed. This sampling plan can be transformed into specifications for evaluation and use of landfilled fly ash as concrete pozzolan.

References

[1] B. Lothenbach, K. Scrivener, R.D. Hooton, Supplementary cementitious materials, Cem. Concr. Res. 41 (2011) 1244–1256. doi:10.1016/j.cemconres.2010.12.001.

[2] ACI 232.2R, Report on the Use of Fly Ash in Concrete, Am. Concr. Inst. (2016).

[3] AASHTO R80-17 Standard Practice for Determining the Reactivity of Concrete Aggregates and Selecting Appropriate Measures for Preventing Deleterious Expansion in New Concrete Construction (2017), Am. Assoc. State Highw. Transp. Off. 444 North Cap. Str. NW, Washington, DC 20001, USA. https://www-astm-org.ezaccess.libraries.psu.edu/cgi-bin/resolver.cgi?3PC+AASHTO+AASHTO R80-17+en-US.

[4] AASHTO Subcommittee on Materials (SOM) fly ash task force report, (2016).

[5] American Coal Ash Association (ACAA), coal combustion products production and use survey report, (2017). Available at: https://www.acaa-usa.org/Portals/9/Files/PDFs/2018-Survey-Results.pdf. Accessed: February 2020.

[6] S. Seraj, R. Cano, S. Liu, D. Whitney, D. Fowler, R. Ferron, J. Zhu, M. Juenger, Evaluating the performance of alternative supplementary cementing material in concrete, FHWA Report No. FHWA/TX-14/0-6717-1, 2014.

[7] ACI 232.2R-18, Report on the use of fly ash in concrete, ACI Comm. 232. (2018).

[8] Production and use of coal combustion products in the U.S., Market Forecast through 2033, Am. Road Transp. Build. Assoc. (2015).

[9] U.S. electricity generation by energy source, U.S. Energy Inf. Adm. Available at: https://www.eia.gov/tools/faqs/faq.php?id=427&t=3. Accessed: February 2020.

[10] Annual Energy Outlook 2018 (AEO), U.S. Energy Inf. Adm. Available at: https://www.eia.gov/pressroom/presentations/Capuano_02052018.pdf. Accessed: February 2020.

[11] B.G. Miller, Clean Coal Engineering Technology, Elsevier Inc. (2011).

[12] I. Barnes, L. Sear, Ash utilization from coal-based power plants, DTI, 2004.

[13] Electricity, U.S Energy Inf. Adm. (Eia)-Independent Statics Anal. Available at: https://www.eia.gov/electricity/. Accessed: February 2020.

[14] The story of coal, Available at: https://byjus.com/chemistry/coal-story/ Accessed: February 2020.

[15] Coal, West. Oregon Univ. Available at: https://www.wou.edu/las/physci/GS361/Fossil%20fuels/Coal.htm. Accessed: February 2020.

[16] X. Shen, Coal combustion and combustion products, Coal, Oil Shale, Nat. Bitumen, Heavy Oil Peat. I (2009).

[17]   Types   of   coal,   U.S.   Energy   Inf.   Adm.   Available   at:
        https://www.eia.gov/energyexplained/print.php?page=coal_home. Accessed: February 2020.

[18]   USGS,   Assessing   U.S.   coal   resources   and   reserves,   Available   at:
        https://pubs.usgs.gov/fs/2017/3067/fs20173067.pdf. Accessed: February 2020.

[19]   Abandoned   coal   mine   drainage   projects   in   Pennsylvania,   Available   at:
        http://www.ei.lehigh.edu/envirosci/enviroissue/amd/links/Pa_projects.html. Accessed: February
        2020.

[20]   S. Rajaram, Next generation CFBC, Chem. Eng. Sci. 54 (1999) 5565–5571.

[21]   J. Havlica, J. Brandstetr, I. Odler, Possibilities of utilizing solid residues from pressured fluidized
        bed coal combustion (PSBC) for the production of blended cements, Cem. Concr. Res. 28 (1998)
        299–307.

[22]   S.N. Oka, Fluidized bed combustion, Marcel Dekker, Inc, (2004). Available at:
        http://sv.20file.org/up1/887_0.pdf. Accessed: February 2020.

[23]   ARIPPA, Available at: http://arippa.org/. Accessed: February 2020.

[24]   Available and emerging technologies for reducing greenhouse gas emissions from coal-fired electric
        generating   units,   (2010),   Available   at: https://www.epa.gov/sites/production/files/2015-
        12/documents/electricgeneration.pdf. Accessed: February 2020.

[25]   A. Minchener, Fluidized bed combustion systems for power generation and other industrial
        applications, J. Power Energy. 217 (2003) 9–18.

[26]   PARTHA DAS SHARMA's Weblog on "Keeping World Environment Safer and Greener,"
        Available at: https://saferenvironment.wordpress.com/posts/page/5/. Accessed: February 2020.

[27]   N. Noda, H. Makino, Influence of operating temperature on performance of electrostatic precipitator
        for pulverized coal combustion boiler, Adv. Powder Technol. 21 (2010) 495–499.
        doi:10.1016/j.apt.2010.04.012.

[28]   Air pollution control, Encycl. Br. Available at: https://www.britannica.com/technology/air-
        pollution-control. Accessed: February 2020.

[29]   X.S. Shi, F.G. Collins, X.L. Zhao, Q.Y. Wang, Mechanical properties and microstructure analysis
        of fly ash geopolymeric recycled concrete, J. Hazard. Mater. 237–238 (2012) 20–29.
        doi:10.1016/j.jhazmat.2012.07.070.

[30]   User guidelines for waste and byproduct materials in pavement construction-coal fly ash, Fed.
        Highw.   Adm.   Res.   Technol.   Available   at:
        https://www.fhwa.dot.gov/publications/research/infrastructure/structures/97148/intro.cfm.
        Accessed: February 2020.

[31]   W.D.A. Rickard, R. Williams, J. Temuujin, A. Van Riessen, Assessing the suitability of three
        Australian fly ashes as an aluminosilicate source for geopolymers in high temperature applications,

Mater. Sci. Eng. A. 528 (2011) 3390–3397. doi:10.1016/j.msea.2011.01.005.

[32] C. V Ly, D.C. Southam, Determining the reactivity of a fly ash for production of geopolymer, J. Am. Ceram. Soc. 92 (2009) 881–887. doi:10.1111/j.1551-2916.2009.02948.x.

[33] T. Robl, K. Mahboub, W. Stevens, R. Rathbone, Fluidized bed combustion ash utilization: CFBC fly ash as a pozzolanic additive to Portland cement concrete, in: Second Int. Conf. Sustain. Constr. Mater. Technol., Ancona, Italy, 2010.

[34] G.J. Mccarthy, K.D. Swanson, L.P. Keller, W.C. Blatter, Mineralogy of western fly ash, Cem. Concr. Res. 14 (1984) 471–478.

[35] 232.2R-03: Use of fly Ash in concrete, Am. Concr. Inst, (2003).

[36] H. Feuerborn, E. Coal, C. Products, Coal ash utilisation over the world and in Europe, in: Work. Environ. Heal. Asp. Coal Ash Util., Tel-Aviv, Israel, 2005.

[37] B. Will, S. Thomas, K. Mahboub, The cementitious and pozzolanic properties of fluidized bed combustion fly ash, in: 2009 World Coal Ash Conf., Lexington, KY, USA, (2009).

[38] K.S. Sajwan, I. Twardowska, T. Punshon, A.K. Alva, Coal combustion byproducts and environmental issues, Springer, New York, 2006.

[39] What are CCP?, Am. Coal Ash Assoc. Available at: https://www.acaa-usa.org/AboutCoalAsh/WhatareCCPs/BoilerSlag.aspx. Accessed: February 2020.

[40] Boiler slag, Am. Coal Ash Assoc, Available at: https://www.acaa-usa.org/aboutcoalash/whatareccps/boilerslag.aspx. Accessed: February 2020.

[41] K.J. Ladwig, G.M. Blythe, Flue-gas desulfurization products and other air emissions controls, Coal Combust. Prod. (2017) 67–95.

[42] X. Li, Q. Chen, B. Ma, J. Huang, S. Jian, B. Wu, Utilization of modified CFBC desulfurization ash as an admixture in blended cements: Physico-mechanical and hydration characteristics, Fuel. 102 (2012) 674–680. doi:10.1016/j.fuel.2012.07.010.

[43] C. Yin, 5 - Biomass co-firing, in: Biomass Combust. Sci. Technol. Eng., 2013: pp. 84–105.

[44] E.J. Anthony, L. Jia, M. Caris, F. Preto, S. Burwell, An examination of the exothermic nature of fluidized bed combustion (FBC) residues, Waste Manag. 19 (1999) 293–305.

[45] W. Roszczynialski, W. Nocuń-Wczelik, Studies of cementitious systems with new generation by-products from fluidized bed combustion, J. Therm. Anal. Calorim. 77 (2004) 151–158.

[46] J. Brandštetr, J. Havlica, Phase composition of solid residues of fluidized bed coal combustion, quality tests, and application possibilities, Chem. Pap. 50 (1996) 188–194.

[47] I. Barnes, Application of circulating fluidized bed combustion with low-rank Asian coals, Cornerstone, Off. J. World Coal Ind, Available at: http://cornerstonemag.net/application-of-circulating-fluidized-bed-combustion-with-low-rank-asian-coals/. Accessed: February 2020.

[48]   Fluidized bed combustion technology, Available at: http://www.cfbworks.com/service/. Accessed: February 2020.

[49]   L. Ruhi, G.S. Dwyer, G. Schwartz, A. Romanski, S.D. Smith, N. Carolina, U. States, The impact of coal combustion residue effluent on water resources: A North Carolina example, Environ. Sci. Technol. 46 (2012) 12226–12233.

[50]   American Coal Ash Association (ACAA), coal combustion products production and use survey report, (2018). Available at: https://www.acaa-usa.org/Portals/9/Files/PDFs/2018-Survey-Results.pdf. Accessed: February 2020.

[51]   D. Gazdič, M. Fridrichová, K. Kulísek, L. Vehovská, The potential use of the FBC ash for the preparation of blended cements, Procedia Eng. 180 (2017) 1298–1305. doi:10.1016/j.proeng.2017.04.292.

[52]   X. Li, Q. Chen, K. Huang, B. Ma, B. Wu, Cementitious properties and hydration mechanism of circulating fluidized bed combustion (CFBC) desulfurization ashes, Constr. Build. Mater. 36 (2012) 182–187. doi:10.1016/j.conbuildmat.2012.05.017.

[53]   N.T. Plaks, A.M. Palomino, A.M. Asce, B.E. Scheetz, G.D. Braun, A.M. Asce, Testing framework for analysis of time-dependent behavior of coal combustion products, J. Mater. Civ. Eng. 28 (2016) 1–9. doi:10.1061/(ASCE)MT.1943-5533.0001326.

[54]   Y. Jung, D. Park, Fluidized bed combustion of high ash anthracite analysis of combustion efficiency and particle size distribution, Korean J. Chem. Eng. 5 (1988) 109–115.

[55]   P. Sulovsk, Mineralogy and chemistry of conventional and fluidized bed coal ashes, Bull. Czech Geol. Surv. 77 (2002) 1–11.

[56]   R.B. Jewell, R.F. Rathbone, T.L. Robl, K.S. Cement, C. Phases, F.B.C. Ash, The Fabrication of value added cement products from circulating fluidized bed combustion ash, in: 2007 World Coal Ash Conf., May 7-10, Northern Kentucky, USA, 2007.

[57]   ASTM C618-19, Standard specification for coal fly ash and raw or calcined natural pozzolan for use in concrete. ASTM Int. (2019).

[58]   X. Fu, Q. Li, J. Zhai, G. Sheng, F. Li, The physical – chemical characterization of mechanically-treated CFBC fly ash, Cem. Concr. Compos. 30 (2008) 220–226.

[59]   R. Kobylecki, Unburned carbon in the circulating fluidized bed boiler fly ash, Chem. Process Eng. 32 (2011) 255–266. doi:10.2478/v10176-011-0020-8.

[60]   R.L. Hill, R.F. Rathbone, J.C. Hower, An examination of fly ash carbon and its interactions with air entraining agent, Cem. Concr. Res. 27 (1997) 193–204.

[61]   Y. Gao, H. Shim, R.H. Hurt, E.M. Suuberg, N.Y.C. Yang, Effects of carbon on air entrainment in fly ash concrete : The role of soot and carbon black, Energy & Fuels. 11 (1997) 457–462. doi:10.1021/ef960113x.

[62] J. Paya, J. Monzo, M. V. Borrachero, E. Perris, F. Amahjour, Thermogravimetric methods for determining carbon content in fly ashes, Cem. Concr. Res. 28 (1998) 675–686.

[63] H. Nguyen, T. Chang, J. Shih, C. Chen, T. Nguyen, Influence of circulating fluidized bed combustion (CFBC) fly ash on properties of modified high volume low calcium fly ash (HVFA) cement paste, Constr. Build. Mater. 91 (2015) 208–215. doi:10.1016/j.conbuildmat.2015.05.075.

[64] M.A. Glinicki, M. Zieliński, The influence of CFBC fly ash addition on phase composition of air-entrained concrete, Bull. POLISH Acad. Sci. 56 (2008).

[65] T. Wu, M. Chi, R. Huang, Characteristics of CFBC fly ash and properties of cement-based composites with CFBC fly ash and coal-fired fly ash, Constr. Build. Mater. 66 (2014) 172–180. doi:10.1016/j.conbuildmat.2014.05.057.

[66] T. Robl, A. Oberlink, J. Brien, J. Pagnotti, The utilization potential of anthracite CFBC spent bed fly ash as a concrete additive, in: World Pf Coal Ash Conf., Denver, USA, 2011.

[67] M. Chi, R. Huang, Durability performance of concrete containing CFBC fly ash and coal-fired fly ash, Appl. Mech. Mater. 627 (2014) 283–287. doi:10.4028/www.scientific.net/AMM.627.283.

[68] D. Jóźwiak-Niedźwiedzka, Effect of fluidized bed combustion fly ash on the chloride resistance and scaling resistance of concrete, Concr. Aggress. Aqueous Environ. Performance, Test. Model. 2. 5 (2009).

[69] M.A. Glinicki, M. Zielinski, Frost salt scaling resistance of concrete containing CFBC fly ash, Mater. Struct. 42 (2009) 993–1002. doi:10.1617/s11527-008-9438-y.

[70] M.J. McCarthy, M.R. Jones, L. Zheng, T.L. Robl, J.G. Groppo, Characterising long-term wet-stored fly ash following carbon and particle size separation, Fuel. 111 (2013) 430–441. doi:10.1016/j.fuel.2013.02.048.

[71] R.A. Carroll, Coal Combustion Products in the United Kingdom and the Potential of Stockpile Ash, 2015 World Coal Ash Conf. (2015). http://www.flyash.info/2015/140-carroll-edit-2015.pdf.

[72] J.C. Hower, J.G. Groppo, U.M. Graham, C.R. Ward, I.J. Kostova, M.M. Maroto-Valer, S. Dai, Coal-derived unburned carbons in fly ash: A review, Int. J. Coal Geol. 179 (2017) 11–27. doi:10.1016/j.coal.2017.05.007.

[73] M.J. Mccarthy, P.A.J. Tittle, R.K. Dhir, Characterization of conditioned pulverized fuel ash for use as a cement component in concrete, Mag. Concr. Res. 51 (1999) 191–206. doi:http://dx.doi.org/10.1680/macr.1999.51.3.191.

[74] X. Wirth, C.R. Shearer, S.E. Burns, E. Kimberly, Evolution of the Properties of Organic Matter and Mineral Phases of Reclaimed Coal Fly Ash, 2017 World Coal Ash Conf. (2017). http://www.flyash.info/2017/066-Wirth-woca2017p.pdf

[75] S.A. Akinyemi, A. Akinlua, W.M. Gitari, N. Khuse, P. Eze, R.O. Akinyeye, L.F. Petrik, Natural weathering in dry disposed ash dump: Insight from chemical, mineralogical and geochemical analysis of fresh and unsaturated drilled cores, J. Environ. Manage. 102 (2012) 96–107.

doi:10.1016/j.jenvman.2011.11.018.

[76]   M. Ahmaruzzaman, A review on the utilization of fly ash, Prog. Energy Combust. Sci. 36 (2010) 327–363. doi:10.1016/j.pecs.2009.11.003.

[77]   W.C. Turner, S. Doty, Energy management handbook, 6th Ed., Fairmont press, GA, USA, 2004.

[78]   A. Bahadori, H.B. Vuthaluru, Estimation of potential savings from reducing unburned combustible losses in coal-fired systems, Appl. Energy. 87 (2010) 3792–3799. doi:10.1016/j.apenergy.2010.06.009.

[79]   W. Yan, J. Li, Modeling of the Unburned Carbon in Fly Ash, Energy Power Eng. 1 (2009) 90–93. doi:10.4236/epe.2009.12014.

[80]   S. Dinarloo, J. Hower, Prediction of the Unburned Carbon Content of Fly Ash in Coal-Fired Power Plants, Coal Combust. Gasif. Prod. 7 (2015) 19–29. doi:10.4177/CCGP-D-14-00009.1.

[81]   L. Bartoňová, Unburned carbon from coal combustion ash: An overview, Fuel Process. Technol. 134 (2015) 136–158. doi:10.1016/j.fuproc.2015.01.028.

[82]   M. Bilen, S. Kizgut, Modeling of unburned carbon in fly ash and importance of size parameters, Fuel Process. Technol. 143 (2016) 7–17. doi:10.1016/j.fuproc.2015.10.039.

[83]   J.C. Hower, T.L. Robl, R.F. Rathbone, W.H. Schram, G.A. Thomas, Characterization of pre- and post-NOx conversion fly ash from the Tennessee Valley Authority's John Sevier fossil plant, in: 12th Int. Symp. Coal Combust. By-Product Manag. Use, Electric Power Research Institute, Orlando, FL, pp. 39-1-39–13.

[84]   M. Mohebbi, F. Rajabipour, B. Scheetz, Evaluation of Two-Atmosphere Thermogravimetric Analysis for Determining the Unburned Carbon Content in Fly Ash, ASTM J. Adv. Civ. Eng. Mater. 6 (2017) 258–279.

[85]   R. Hill, R. Rathbone, J.C. Hower, Investigation of fly ash carbon by thermal analysis and optical microscopy, Cem. Concr. Res. 28 (1998) 1479–1488. doi: https://doi.org/10.1016/S0008-8846(98)00122-7.

[86]   Z.T. Ahmed, D.W. Hand, L.L. Sutter, M.K. Watkins, Fly ash iodine number for measuring adsorption capacity of coal fly ash, ACI Mater. J. 111 (2014) 383–390. doi:10.14359/51686582.

[87]   M.K. Watkins, Z. Ahmed, L. Sutter, D. Hand, Characterization of coal fly ash by absolute foam index, ACI Mater. J. 112 (2015) 393–398. doi:10.14359/51686792.

[88]   L. Sutter, R.D. Hooton, S. Schlorholtz, Methods for Evaluating Fly Ash for Use in Highway Concrete, National Academies Press, 2013. doi:10.17226/22483.

[89]   Y. Soong, M.R. Schoffstall, M.L. Gray, J.P. Knoer, K.J. Champagne, R.J. Jones, D.J. Fauth, Dry beneficiation of high loss-on-ignition fly ash, Sep. Purif. Technol. 26 (2002) 177–184. doi:10.1016/S1383-5866(01)00162-9.

[90]   J.G. Groppo, Selective beneficiation for high loss-of-ignition fly ash, Min. Eng. 48 (1996) 51–53.

[91]   R. Gupta, Dry Electrostatic Beneficiation of Illinois Coal and Eastern Oil Shales, Ph.D. Dissertation, Illinois Institute of Technology, 1990.

[92]   J. Kim, H. Cho, S. Kim, H. Chun, Electrostatic beneficiation of fly ash using an ejector-tribocharger, J. Environ. Sci. Heal. Part A. 35 (2000) 357–377. doi:10.1080/10934520009376976.

[93]   A.D. Moore, Electrostatics and its applications, Wiley, New York, 1973.

[94]   S. Masuda, M. Toraguchi, T. Takahashi, K. Haga, Electrostatic Beneficiation of Coal Using a Cyclone-Tribocharger, IEEE Trans. Ind. Appl. IA-19 (1983) 789–793. doi:10.1109/TIA.1983.4504289.

[95]   H. Ban, T.X. Li, J.C. Hower, J.L. Schaefer, J.M. Stencel, Dry triboelectrostatic beneficiation of fly ash, Fuel. 76 (1997) 801–805. doi:10.1016/s0016-2361(97)00045-8.

[96]   Y. Soong, M.R. Schoffstall, T.A. Link, Triboelectrostatic beneficiation of fly ash, Fuel. 80 (2001) 879–884. doi:10.1016/S0016-2361(00)00150-2.

[97]   M.M. Maroto-valer, D.N. Taulbee, J.C. Hower, Novel separation of the differing forms of unburned carbon present in fly ash using density gradient centrifugation, Energy & Fuels. 13 (1999) 947–953.

[98]   J. Groppo, T. Robl, J.C. Hower, The beneficiation of coal combustion ash, Geol. Soc. London, Spec. Publ. 236 (2004) 247–262. doi:10.1144/GSL.SP.2004.236.01.15.

[99]   F. Cangialosi, M. Notarnicola, L. Liberti, J. Stencel, The role of weathering on fly ash charge distribution during triboelectrostatic beneficiation, J. Hazard. Mater. 164 (2009) 683–688. doi:10.1016/j.jhazmat.2008.08.050.

[100]   L. Baker, A. Gupta, S. Gasiorowski, Triboelectrostatic Beneficiation of Land Filled Fly Ash, 2015 World of Coal Ash Conf. (2015).

[101]   J.P. Baltrus, J.R. Diehl, Y. Soong, W. Sands, Triboelectrostatic separation of fly ash and charge reversal, Fuel. 81 (2002) 757–762. doi:10.1016/S0016-2361(01)00196-X.

[102]   J.K. Kim, H.C. Cho, S.C. Kim, Removal of unburned carbon from coal fly ash using a pneumatic triboelectrostatic separator, J. Environ. Sci. Heal. - Part A Toxic/Hazardous Subst. Environ. Eng. 36 (2001) 1709–1724. doi:10.1081/ESE-100106253.

[103]   J.D. Bittner, S.A. Gasiorowski, STI' s Six Years of Commercial Experience in Electrostatic Benefication of Fly Ash, (2001), https://p2infohouse.org/ref/45/44689.pdf.

[104]   J.Y. Hwang, X. Sun, Z. Li, Unburned Carbon from Fly Ash for Mercury Adsorption : I . Separation and Characterization of Unburned Carbon, J. Miner. Mater. Charact. Eng. 1 (2002) 39–60. doi:10.4236/jmmce.2002.11004.

[105]   H. Sung, K. Yoo, S. Lee, The removal of unburned carbon from fly ash by kerosene extraction, Geosystem Eng. 19 (2016) 96–99. doi:10.1080/12269328.2015.1096841.

[106]   U. Demir, A. Yamik, S. Kelebek, B. Oteyaka, A. Ucar, O. Sahbaz, Characterization and column flotation of bottom ashes from Tuncbilek power plant, Fuel. 87 (2008) 666–672.

doi:10.1016/j.fuel.2007.05.040.

[107] M. Uçurum, O.̈ Y. Toraman, T. Depci, E. Yoğurtçuoğlu, A study on characterization and use of flotation to separate unburned carbon in bottom ash from Çayirhan power plant, Energy Sources, Part A Recover. Util. Environ. Eff. 33 (2011) 562–574. doi:10.1080/15567030903117638.

[108] 911 Metallurgist, https://www.911metallurgist.com/blog/froth-flotation-process, Accessed: 25th Feb 2020

[109] M.R. Jones, M.J. Mccarthy, L. Zheng, T.L. Robl, J. Groppo, Experiences of processing fly ashes recovered from United Kingdom stockpiles and lagoons, their characteristics and potential end uses, in: 2009 World Coal Ash Conf., Lexington, KY, USA, n.d.: pp. 1–24.

[110] G. Li, L. Deng, J. Liu, Y. Cao, H. Zhang, J. Ran, A New Technique for Removing Unburned Carbon from Coal Fly Ash at an Industrial Scale, Int. J. Coal Prep. Util. 35 (2015) 273–279. doi:10.1080/19392699.2015.1008098.

[111] V.P. Mehrotra, K.V.S. Sastry, B.W. Morey, Review of oil agglomeration techniques for processing of fine coals, Int. J. Miner. Process. 11 (1983) 175–201. doi:10.1016/0301-7516(83)90025-X.

[112] J. Castleman, Thermal processing, in: Coal Combust. Prod. Charact. Util. Benef., Elsevier Ltd., 2017: pp. 309–326. doi:10.1016/B978-0-08-100945-1.00012-5.

[113] J.G. Keppeler, Carbon Burn-out and update on commercial applications, in: Int. Ash Util. Symp., 2001.

[114] PMI Ash Technologies, FAQ – acquired by another company, website inaccessible.

[115] N.A. Blissett, R.S., Rowson, A review of the multi- component utilisation of coal fly ash, Fuel. 97 (2012) 1–23. doi:http://dx.doi.org/10.1016/j.fuel.2012.03.024.

[116] W. Fedorka, J. Knowles, J. Castleman, Staged Turbulent Air Reactor (STAR TM) Beneficiation Process – Commercial Update, (2013), http://www.flyash.info/2013/157-Fedorka-2013.pdf, Accessed: 25th Feb 2020.

[117] R. Minkara, Chemical passivation, in: Coal Combust. Prod. Charact. Util. Benef., Elsevier Ltd., 2017: pp. 327–342. doi:10.1016/B978-0-08-100945-1.00013-7.

[118] RestoreAir Passivation of Activated Carbon in Ash, Headwaters – original webpage removed. Alternate: https://flyash.com/wp-content/uploads/2019/07/Boral-TB36-RestoreAir-7-1-19.pdf, Accessed: 25th Feb 2020.

[119] G.C. Plunk, How PACT was used to avoid 5 million tons of landfilled fly ash, Ash Work. 69 (2015).

[120] R. Minkara, J.M. Kelley, Second generation carbon passivation agent with tamed dosing response for treatment of carbon containing fly ash, in: World Coal Ash 24(2), 2015.

[121] M. Maroto-Valer, D. Taulbee, J. Hower, Characterization of differing forms of unburned carbon present in fly ash separated by density gradient centrifugation, Fuel. 80 (2001) 795–800.

[122]   H. Hurt, K. a Davis, N.Y.C. Yang, D. Mitchell, J. Headley, Residual boilers carbon from pulverized-coal-fired, Science (80). 74 (1995) 1297–1306.

[123]   R. Hela, D. Orsáková, The Mechanical Activation of Fly Ash, Procedia Eng. 65 (2013) 87–93. doi:10.1016/j.proeng.2013.09.016.

[124]   N. Bouzoubaa, M. Zhang, A. Bilodeau, V. Malhotra, The effect of grinding on the physical properties of fly ashes and a Portland cement clinker, Cem. Concr. Res. 27 (1997) 1861–1874.

[125]   R. Cheerarot, C. Jaturapitakkul, A study of disposed fly ash from landfill to replace Portland cement, Waste Manag. 24 (2004) 701–709. doi:10.1016/j.wasman.2004.02.003.

[126]   D.F. Velandia, C.J. Lynsdale, J.L. Provis, F. Ramirez, A.C. Gomez, Evaluation of activated high volume fly ash systems using Na2SO4, lime and quicklime in mortars with high loss on ignition fly ashes, Constr. Build. Mater. 128 (2016) 248–255. doi:10.1016/j.conbuildmat.2016.10.076.

[127]   C. Shi, R.L. Day, Acceleration of the reactivity of fly ash by chemical activation, Cem. Concr. Res. 25 (1995) 15–21. doi:https://doi.org/10.1016/0008-8846(94)00107-A.

[128]   J.L. Provis, J.S.J. Van Deventer, Geopolymers: structures, processing, properties and industrial applications, Elsevier, 2009.

[129]   C. Shi, D. Roy, P. Krivenko, Alkali-activated cements and concretes, CRC press, 2003.

[130]   M.J. McCarthy, L. Zheng, R.K. Dhir, G. Tella, Dry-processing of long-term wet-stored fly ash for use as an addition in concrete, Cem. Concr. Compos. (2017). doi:https://doi.org/10.1016/j.cemconcomp.2017.10.004.

[131]   J. Knowles, New Commercial Beneficiation Process Staged Turbulent Air Reactor (STAR), 2009 World of Coal Ash Conf. (2009), 1–21.

[132]   J. Knowles, W. Fedorka, A New Solution for a Long-standing Dilemma, Ash Work (Issue 2). (2015) 6–9.

[133]   A.S. Mujumdar, Handbook of industrial drying, Fourth, CRC press, 2014.

[134]   I. Diaz-Loya, M. Juenger, S. Seraj, R. Minkara, Extending supplementary cementitious material resources: Reclaimed and remediated fly ash and natural pozzolans, Cem. Concr. Compos. (2017) 4–11. doi:10.1016/j.cemconcomp.2017.06.011.

[135]   S. Al-Shmaisani, Evaluation of Reclaimed and Remediated Fly Ashes as a Substitute for Class F Fly Ash in Concrete, M.S.Thesis, University of Texas at Austin, 2017.

[136]   M.D.A. Thomas, E.G. Moffatt, The Durability of Concrete Produced with Reclaimed Fly Ash, in: 14th Int. Conf. Durab. Build. Mater. Components, Ghent, Belgium, 2017: pp. 155–167.

[137]   M.J. McCarthy, T. Robl, L.J. Csetenyi, Recovery, processing, and usage of wet-stored fly ash, in: Coal Combust. Prod. Charact. Util. Benef., Elsevier Ltd., 2017: pp. 343–367. doi:10.1016/B978-0-08-100945-1.00014-9.

[138] M.J. McCarthy, P.A.J. Tittle, R.K. Dhir, Influences of conditioned pulverized-fuel ash as a cement component on the properties of concrete, Mag. Concr. Res. 52 (2000) 329–343. doi:10.1680/macr.2000.52.5.329.

[139] M. McCarthy, P.A. Tittle, K. Kii, R. Dhir, Mix proportioning and engineering properties of conditioned PFA concrete, Cem. Concr. Res. 31 (2001) 321–326. doi:10.1016/S0008-8846(00)00469-5.

[140] R. Dhir, J. Halliday, M. McCarthy, A. Wibowo, Roles of PFA quality and conditioning in minimizing alkali-silica reaction in concrete, (2006) 49–61. doi:10.1680/macr.2006.58.1.49.

[141] AASHTO Subcommittee on Materials (SOM) fly ash task force report. Available at:http://sp.materials.transportation.org/Documents/Announcements/AASHTO_SOM_FA_Report_11_04_2016-under%20announcement.pdf. Accessed: February 2020.

[142] American Road and Transportation Building Association, Production and use of coal combustion products in the U.S. - Market forecast through 2033, (2015), Available at: https://www.acaa-usa.org/Portals/9/Files/PDFs/ReferenceLibrary/ARTBA-final-forecast.compressed.pdf Accessed: February 2020.

[143] R.T. Chancey, P. Stutzman, M.C.G. Juenger, D.W. Fowler, Comprehensive phase characterization of crystalline and amorphous phases of a Class F fly ash, Cem. Concr. Res. 40 (2010) 146–156. doi:10.1016/j.cemconres.2009.08.029.

[144] R.B. Jewell, Optical properties of coal combustion byproducts for particle-size analysis by laser diffraction, Coal Combust. Gasif. Prod. 1 (2009) 1–7. doi:10.4177/CCGP-D-09-00001.

[145] T. Kim, J. Olek, Effects of sample preparation and interpretation of thermogravimetric curves on calcium hydroxide in hydrated pastes and mortars, J. Transp. Res. Board. 2290 (2012) 10–18. doi:10.3141/2290-02.

[146] A.A. Ramezanianpour, Fly ash. Cement replacement materials, Springer, Berlin, Heidelberg, 2014. doi:10.1007/978-3-642-36721-2.

[147] J. Iribarne, A. Iribarne, J. Blondin, E.J. Anthony, Hydration of combustion ashes - A chemical and physical study, Fuel. 80 (2001) 773–784.

[148] G. Sheng, Q. Li, J. Zhai, Investigation on the hydration of CFBC fly ash, Fuel. 98 (2012) 61–66.

[149] T. Szeles, J. Wright, F. Rajabipour, S. Stoffels, Mitigation of alkali – silica reaction by hydrated alumina, J. Transp. Res. Board. 2629 (2017) 15–23.

[150] A.M. Neville, Properties of concrete, Fourth, Prentice Hall, 2006.

[151] P.J.F. Wright, Entrained air in concrete, Proc. Inst. Civ. Eng. Part 1, 2 (1953) 337–358.

[152] M. Zahedi, F. Rajabipour, Fluidized Bed Combustion (FBC) fly ash and its performance in concrete, ACI Mater. Journal, Pozzolans Spec. Eddition. 116 (2019).

[153] M.T. Chang, L. Montanari, P. Suraneni, W.J. Weiss, Expression of cementitious pore solution and

the analysis of its chemical composition and resistivity using X-ray fluorescence, J. Vis. Exp. (2018) 1–9. doi:10.3791/58432.

[154] K. Scrivener, R. Snellings, B. Lothenbach, A practical guide to microstructural analysis of cementitious materials, Crc Press, 2018.

[155] K.A. Snyder, X. Feng, B.D. Keen, T.O. Mason, Estimating the electrical conductivity of cement paste pore solutions from OH⁻, K+ and Na+ concentrations, Cem. Concr. Res. 33 (2003) 793–798. doi:10.1016/S0008-8846(02)01068-2.

[156] Design and control of concrete mixtures, 16th Edition, Portl. Cem. Assoc (2016).

[157] P.K. Mehta, P.J. Monteiro, Concrete microstructure, properties and materials, 2017.

[158] Y. Shen, J. Qian, Z. Zhang, Investigations of anhydrite in CFBC fly ash as cement retarders, Constr. Build. Mater. 40 (2013) 672–678. doi:10.1016/j.conbuildmat.2012.11.056.

[159] P.K. Mehta, D. Pirtz, M. Polivka, Properties of alite cements, Cem. Concr. Res. 9 (1979) 439–450.

[160] F. Rajabipour, J. Weiss, Electrical conductivity of drying cement paste, Mater. Struct. 40 (2007) 1143–1160. doi:10.1617/s11527-006-9211-z.

[161] E.J. Garboczi, Permeability, diffusivity, and microstructural parameters: a critical review, Cem. Concr. Res. 20 (1990) 591–601.

[162] K.K. Aligizaki, Pore structure of cement-based materials: testing, interpretation and requirements, CRC Press, 2005.

[163] Q. Yuan, C. Shi, G. De Schutter, K. Audenaert, D. Deng, Chloride binding of cement-based materials subjected to external chloride environment – A review, Constr. Build. Mater. 23 (2009) 1–13. doi:10.1016/j.conbuildmat.2008.02.004.

[164] D.K. Panesar, J. Francis, Influence of limestone and slag on the pore structure of cement paste based on mercury intrusion porosimetry and water vapour sorption measurements, Constr. Build. Mater. 52 (2014) 52–58. doi:10.1016/j.conbuildmat.2013.11.022.

[165] C. Xiong, L. Jiang, Y. Xu, Z. Song, H. Chu, Q. Guo, Influences of exposure condition and sulfate salt type on deterioration of paste with and without fly ash, Constr. Build. Mater. 113 (2016) 951–963. doi:10.1016/j.conbuildmat.2016.03.154.

[166] J. Sun, Z. Chen, Influences of limestone powder on the resistance of concretes to the chloride ion penetration and sulfate attack, Powder Technol. 338 (2018) 725–733. doi:10.1016/j.powtec.2018.07.041.

[167] T. Schmidt, B. Lothenbach, M. Romer, J. Neuenschwander, K. Scrivener, Physical and microstructural aspects of sulfate attack on ordinary and limestone blended Portland cements, Cem. Concr. Res. 39 (2009) 1111–1121. doi:10.1016/j.cemconres.2009.08.005.

[168] AASHTO R80-17 Standard Practice for Determining the Reactivity of Concrete Aggregates and Selecting Appropriate Measures for Preventing Deleterious Expansion in New Concrete

Construction (2017). Am Assoc State Highw Transp Off 444 North Cap Str NW, Washington, DC 20001, USA

[169]   Zonum Solutions, http://www.zonums.com/gmaps/terrain.php, Accessed: 25th Feb 2020